ARC SEMINAR: SIMULATING ASTROPHYSICAL PLASMAS IN LABORATORY EXPERIMENTS

PRESENTER: JOSHUA 'QUINN' MORGAN

BELLAN PLASMA LAB, WATSON 124

NOVEMBER 27TH, 2023

jqmorgan@caltech.edu

INTRODUCTIONS

- 3rd Year Graduate Student working with Dr. Paul Bellan on astrophysical/fusion related laboratory plasmas
- Relevant Previous Experience:
  - Electrical Engineer at Second Order Effects, Inc. 2020-2021
- Hobbies & Interests:
  - Reading and writing—secretary of Caltech's fiction writing club, Techlit!
  - Guitar, from heavy metal to jazz
  - Woodworking, especially instruments

Fig.1: A student pretending to know what he is doing

OUTLINE

- Background: MHD & Scalability
- Experiment: What is it?
  - Experimental Pedagogy
  - Experimental Design
- Caltech's Astrophysical Plasma Experiments
  - Astrophysical Jets: Similarities, Differences, & Models
  - Solar-coronal Loops: Similarities, Differences, & Models
  - Ice dusty plasmas: Scale, depth, & Saturn's Rings
- Other Relevant Experiments
- Summary & Questions

BACKGROUND: MAGNETOHYDRODYNAMICS & SCALE

BACKGROUND

- Many plasmas are governed by magnetohydrodynamics (MHD)
  - MHD is the simplest method for describing plasmas
    - Assumes plasma is fluid, i.e. distribution function is Maxwellian
      - Pressure & temperature are (typically) not tensorial
    - Assumes gas is sufficiently ionized/magnetized

BACKGROUND

- MHD has 6 principal equations:

Momentum Equation $\rho(\frac{\partial \boldsymbol{u}}{\partial t} + \boldsymbol{u} \cdot \nabla \boldsymbol{u}) = \boldsymbol{J} \times \boldsymbol{B} - \nabla P$, $P(\boldsymbol{x}, t) \propto [\rho(\boldsymbol{x}, t)]^\gamma$

Where $\boldsymbol{u}$ = avg. fluid velocity, $\boldsymbol{B}$ = magnetic field, $\boldsymbol{E}$ = magnetic field, $\boldsymbol{J}$ = current density, ρ = density, P = pressure
$\gamma = 1$ if the plasma is isothermal, $\gamma = 5/3$ if it is adiabatic

BACKGROUND

- MHD has 6 principal equations:

Momentum Equation

Where $\boldsymbol{u}$ = avg. fluid velocity, $\boldsymbol{B}$ = magnetic field, $\boldsymbol{E}$ = magnetic field, $\boldsymbol{J}$ = current density, ρ = density, P = pressure ,

$\gamma = 1$ if the plasma is isothermal, $\gamma = 5/3$ if it is adiabatic

$$P(\boldsymbol{x}, t) \propto [\rho(\boldsymbol{x}, t)]^{\gamma}$$

Continuity Equation

Where $\boldsymbol{u} =$ avg. fluid velocity, $\boldsymbol{B} =$ magnetic field, $\boldsymbol{E} =$ magnetic field, $\boldsymbol{J} =$ current density, $\rho =$ density, $P =$ pressure
$\gamma = 1$ if the plasma is isothermal, $\gamma = 5/3$ if it is adiabatic

BACKGROUND

- MHD has 6 principal equations:

Momentum Equation

Where $\boldsymbol{u}$ = avg. fluid velocity, $\boldsymbol{B}$ = magnetic field, $\boldsymbol{E}$ = magnetic field, $\boldsymbol{J}$ = current density, ρ = density, P = pressure ,
$\gamma = 1$ if the plasma is isothermal, $\gamma = 5/3$ if it is adiabatic

$$P(\boldsymbol{x}, t) \propto [\rho(\boldsymbol{x}, t)]^\gamma$$

Continuity Equation

Induction Equation $$\frac{\partial \boldsymbol{B}}{\partial t} - \nabla \times (\boldsymbol{u} \times \boldsymbol{B}) = \nabla \times (\eta \boldsymbol{J})$$

Where $\boldsymbol{u}$ = avg. fluid velocity, $\boldsymbol{B}$ = magnetic field, $\boldsymbol{E}$ = magnetic field, $\boldsymbol{J}$ = current density, ρ = density, P = pressure
$\gamma = 1$ if the plasma is isothermal, $\gamma = 5/3$ if it is adiabatic

BACKGROUND

- MHD has 6 principal equations:

Momentum Equation $$\rho(\frac{\partial \boldsymbol{u}}{\partial t} + \boldsymbol{u} \cdot \nabla \boldsymbol{u}) = \boldsymbol{J} \times \boldsymbol{B} - \nabla P \quad , \quad P(\boldsymbol{x}, t) \propto [\rho(\boldsymbol{x}, t)]^\gamma$$

Continuity Equation $$\frac{\partial \rho}{\partial t} + \nabla \cdot (\rho \boldsymbol{u}) = 0$$

Induction Equation $$\frac{\partial \boldsymbol{B}}{\partial t} - \nabla \times (\boldsymbol{u} \times \boldsymbol{B}) = \nabla \times (\eta \boldsymbol{J})$$

Remaining Maxwell's Equations
$$\begin{cases} \nabla \cdot \boldsymbol{B} = 0 & \nabla \cdot \boldsymbol{E} = \frac{\rho_{\text{charge}}}{\epsilon_0} \xrightarrow[\text{quasi-neutrality}]{\text{assume}} 0 \\ \nabla \times \boldsymbol{B} = \mu_0 \boldsymbol{J} + \mu_0 \epsilon_0 \frac{\partial \boldsymbol{E}}{\partial t} & \end{cases}$$

Where $\boldsymbol{u}$ = avg. fluid velocity, $\boldsymbol{B}$ = magnetic field, $\boldsymbol{E}$ = magnetic field, $\boldsymbol{J}$ = current density, ρ = density, P = pressure
$\gamma = 1$ if the plasma is isothermal, $\gamma = 5/3$ if it is adiabatic

BACKGROUND

- Magnetohydrodynamics (MHD) is scale-independent
  - Lab experiments provide insights into much larger systems via scaling laws

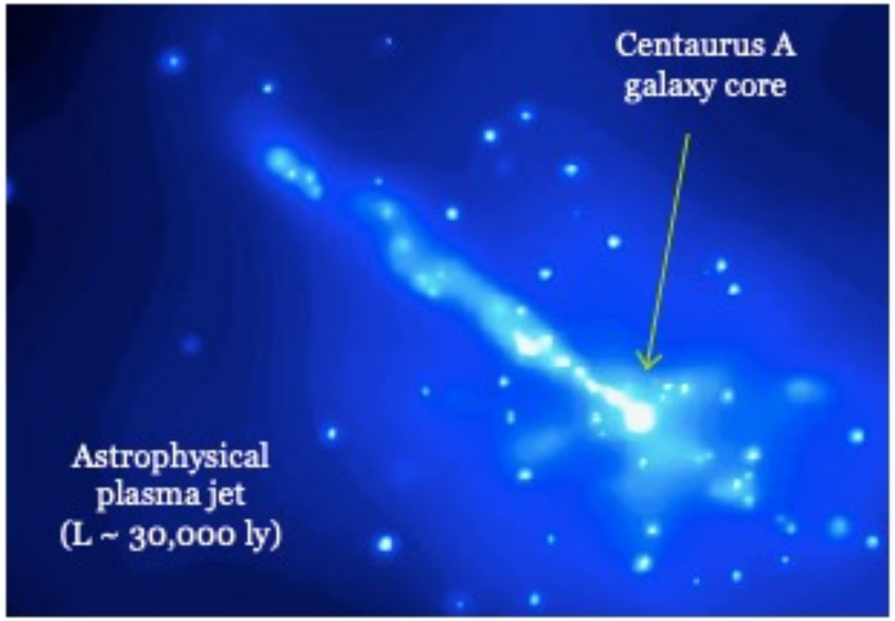

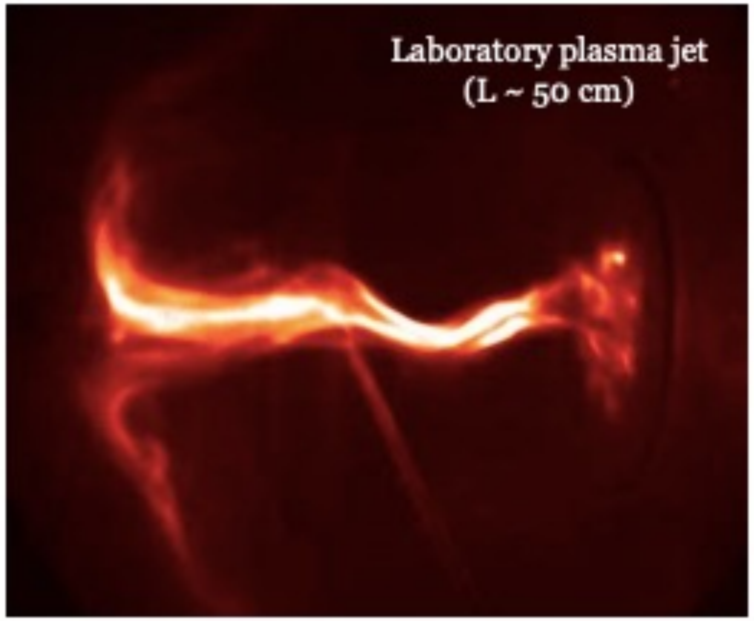

Yun, 2008

BACKGROUND

- Magnetohydrodynamics (MHD) is scale-independent
  - Lab experiments provide insights into much larger systems via scaling laws

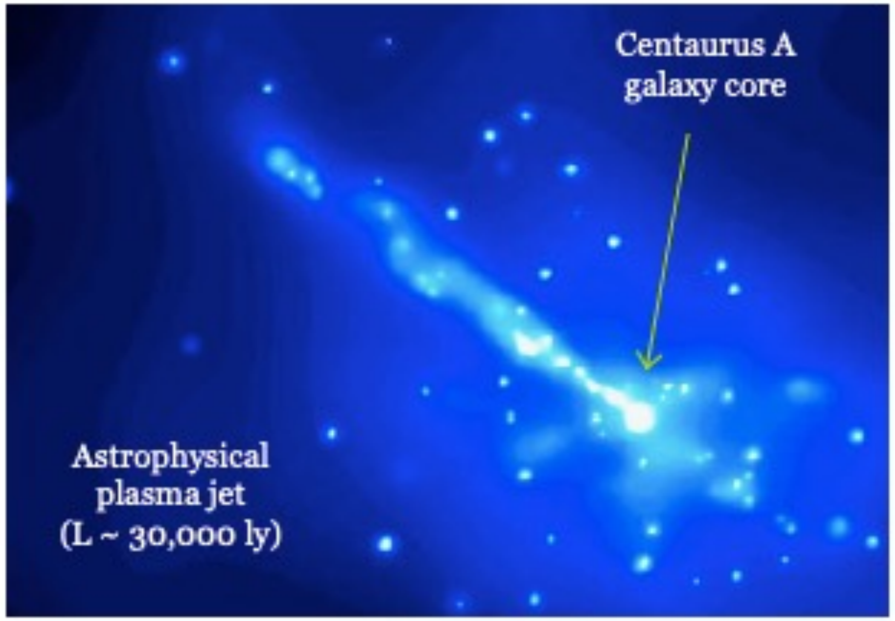

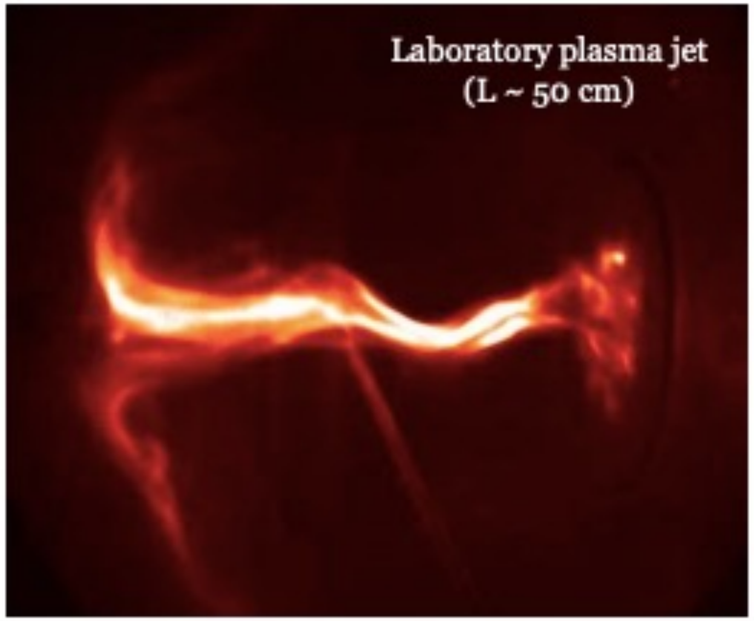

$$\beta \equiv \frac{2\mu_0 P_0}{B_0^2}$$ Beta

$$S \equiv \frac{\mu_0 L v_A}{\eta}$$ Lundquist number

$$\gamma \equiv \begin{cases} 1 & \text{if isothermal} \\ 5/3 & \text{if adiabatic} \end{cases}$$

Yun, 2008

Where B_0 = nominal field, P_0 = nominal pressure, L = characteristic length, v_a = alfvén velocity, and η = resistivity

BACKGROUND

- Magnetohydrodynamics (MHD) is scale-independent
  - Lab experiments provide insights into much larger systems via scaling laws

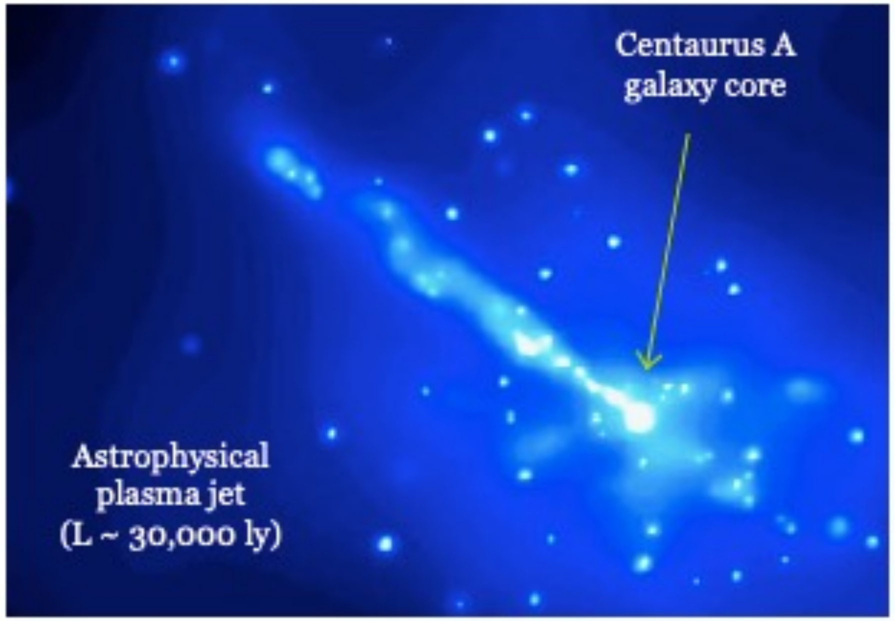

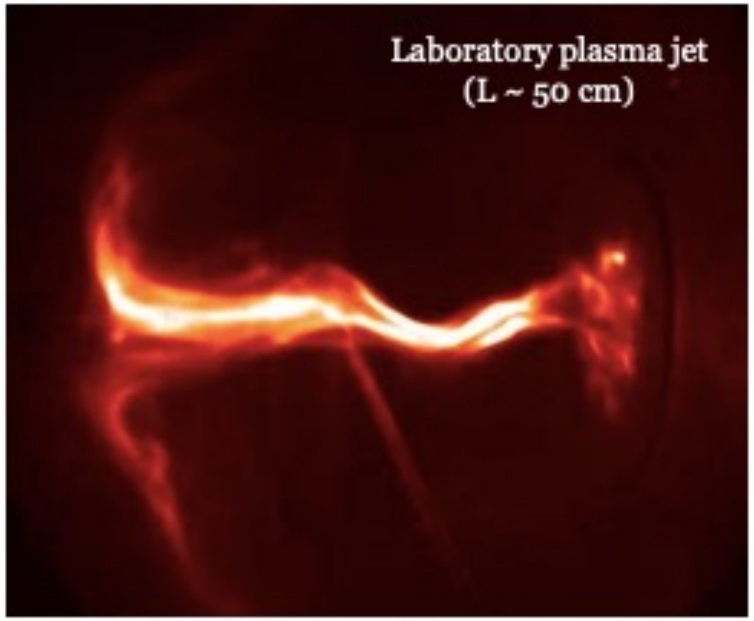

Yun, 2008

$$\beta \equiv \frac{2\mu_0 P_0}{B_0^2}$$ Beta

$$S \equiv \frac{\mu_0 L v_A}{\eta}$$ Lundquist number

$$\gamma \equiv \begin{cases} 1 & \text{if isothermal} \\ 5/3 & \text{if adiabatic} \end{cases}$$

Systems with identical β, S, γ have the same physics!

Where B_0 = nominal field, P_0 = nominal pressure, L = characteristic length, v_a = alfvén velocity, and η = resistivity

BACKGROUND

- Made non-dimensional with β, γ, and S:

Momentum Equation $$\overline{\rho}(\frac{\partial \overline{\boldsymbol{u}}}{\partial \tau} + \overline{\boldsymbol{u}} \cdot \overline{\nabla}\, \overline{\boldsymbol{u}}) = (\overline{\nabla} \times \overline{\boldsymbol{B}}) \times \overline{\boldsymbol{B}} - \beta \overline{\nabla}\, \overline{P} \qquad P(\boldsymbol{x}, t) \propto [\rho(\boldsymbol{x}, t)]^{\gamma}$$

Continuity Equation $$\frac{\partial \overline{\rho}}{\partial \tau} + \overline{\nabla} \cdot (\overline{\rho \boldsymbol{u}}) = 0$$

Induction Equation $$\frac{\partial \overline{\boldsymbol{B}}}{\partial \tau} - \overline{\nabla} \times (\overline{\boldsymbol{u}} \times \overline{\boldsymbol{B}}) = \frac{1}{S} \overline{\nabla} \times (\overline{\nabla} \times \overline{\boldsymbol{B}})$$

Remaining Maxwell's Equations $$\begin{cases} \overline{\nabla} \cdot \overline{\boldsymbol{B}} = 0 \\ \overline{\nabla} \cdot \overline{\boldsymbol{E}} \xrightarrow[\text{quasi-neutrality}]{\text{assume}} 0 \end{cases}$$

Where all overbarred quantities are normalized to a peak value, overbarred nabla is normalized to a characteristic length, and tau is normalized to a characteristic time

EXPERIMENT: WHAT IS IT?

EXPERIMENTAL PEDAGOGY

- What does an experiment even look like?
- What do you want to get from an experiment?
- How do you run an experiment?

EXPERIMENTAL PEDAGOGY – WHAT DOES AN EXPERIMENT LOOK LIKE?

- Small!
  - Compared to the original system…

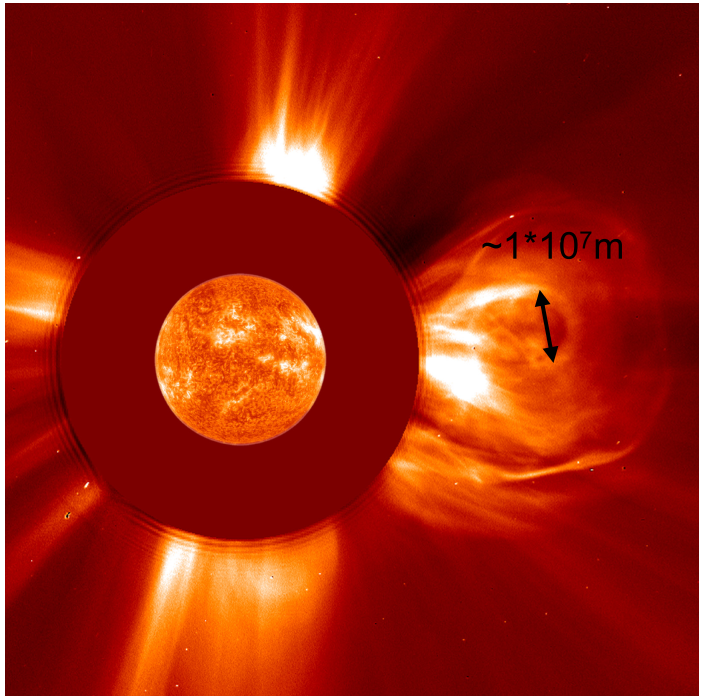

NASA, 2001
Largest solar flare on record, 04/22/2001

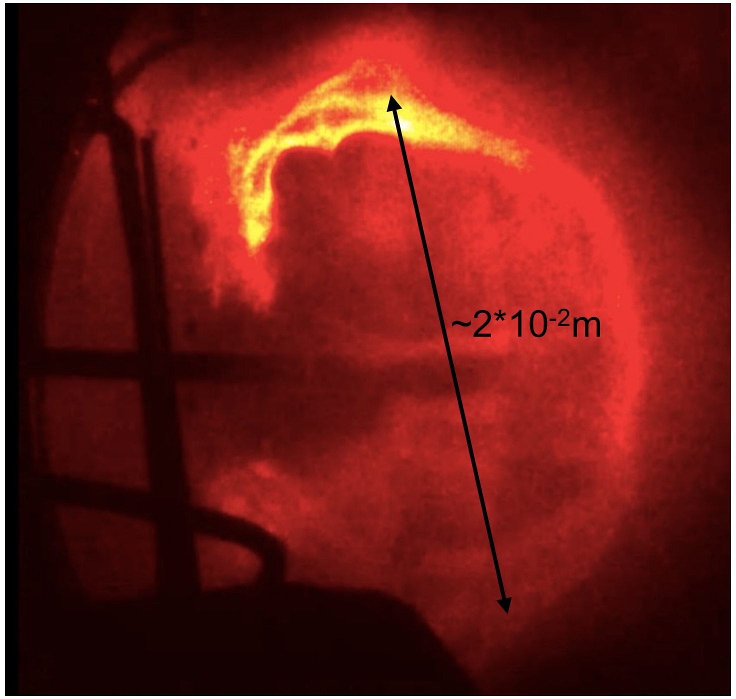

EXPERIMENTAL PEDAGOGY – WHAT DOES AN EXPERIMENT LOOK LIKE?

- How we model various real-world forces in an experiment?

Goal		Laboratory Analogue
Simulate gravity	→	Acoustic pressure, RF electric fields
Simulate electric field	→	Charged electrodes
Simulate magnetic field	→	Background field coils
Achieve specific current configuration	→	Strategic magnetic reconnection, wire arrays (creates heavier plasmas)

EXPERIMENTAL PEDAGOGY – WHAT DO YOU WANT FROM AN EXPERIMENT?

- Hope to map in-lab results to real-world results
  - Seek insights into observed phenomena
  - Help predict unexpected or unseen emergent phenomena

EXPERIMENTAL PEDAGOGY – HOW DO YOU RUN AN EXPERIMENT?

- Experimental physics is typically extremely high dimensional
  - Lots of knobs to turn → Lots of grad students needed!
- An example with Buckingham's Pi theorem:

$$Q = G(A, L, J) \xrightarrow{\text{Implies}} f(A, L, I, Q) = 0,$$

$$\begin{aligned} A &\propto [\text{length}]^2 \\ L &\propto [\text{length}] \\ I &\propto [\text{current}] \\ Q &\propto [\text{temperature}] * [\text{mass}]^2 * [\text{time}]^{-2} \end{aligned}$$

EXPERIMENTAL PEDAGOGY – HOW DO YOU RUN AN EXPERIMENT?

- Experimental physics is typically extremely high dimensional
  - Lots of knobs to turn → Lots of grad students needed!
- An example with Buckingham's Pi theorem:

$Q = G(A, L, J)$ —Implies→ $f(A, L, I, Q) = 0,$

$$A \propto [\text{length}]^2$$
$$L \propto [\text{length}]$$
$$I \propto [\text{current}]$$
$$Q \propto [\text{temperature}] * [\text{mass}]^2 * [\text{time}]^{-2}$$

↓ $p = n - k = 4 - 2,$ dimless params given by all dims minus dimensionally independent dims

$F(\pi_1, \pi_2) = 0$

EXPERIMENTAL PEDAGOGY – HOW DO YOU RUN AN EXPERIMENT?

- Experimental physics is typically extremely high dimensional
  - Lots of knobs to turn → Lots of grad students needed!
- An example with Buckingham's Pi theorem:

$$Q = G(A, L, J)$$

Implies

$$f(A, L, I, Q) = 0,$$

$$A \propto [\text{length}]^2$$
$$L \propto [\text{length}]$$
$$I \propto [\text{current}]$$
$$Q \propto [\text{temperature}] * [\text{mass}]^2 * [\text{time}]^{-2}$$

To scan parameter space with 8pts per dim requires 512 measurements!

$p = n - k = 4 - 2$, dimless params given by all dims minus dimensionally independent dims

Just 64pts per dimensionless param in reduced space!

$$F(\pi_1, \pi_2) = 0$$

EXPERIMENTAL PEDAGOGY – HOW DO YOU RUN AN EXPERIMENT?

- For our plasma experiments…

$$\boldsymbol{u} = G(T, P, \boldsymbol{B}, \boldsymbol{J}, \rho) \quad \xrightarrow{\text{Implies}} \quad f(T, P, \boldsymbol{B}, \boldsymbol{J}, \boldsymbol{u}, \rho) = 0,$$

$$T \propto [\text{temperature}]$$
$$P \propto [\text{mass}] * [\text{length}]^{-1} * [\text{time}]^{-2}$$
$$\boldsymbol{B} \propto [\text{mass}] * [\text{current}]^{-1} * [\text{time}]^{-2}$$
$$\boldsymbol{J} \propto [\text{current}] * [\text{length}]^{-2}$$
$$\boldsymbol{u} \propto [\text{length}] * [\text{time}]^{-2}$$
$$\rho \propto [\text{mass}] * [\text{length}]^{-3}$$

To scan parameter space with 8pts per dim <u>requires 32,768 measurements</u>…

EXPERIMENTAL PEDAGOGY – HOW DO YOU RUN AN EXPERIMENT?

- For our plasma experiments…

$$\boldsymbol{u} = G(T, P, \boldsymbol{B}, \boldsymbol{J}, \rho)$$

Implies

$$f(T, P, \boldsymbol{B}, \boldsymbol{J}, \boldsymbol{u}, \rho) = 0,$$

$$T \propto [\text{temperature}]$$
$$P \propto [\text{mass}] * [\text{length}]^{-1} * [\text{time}]^{-2}$$
$$\boldsymbol{B} \propto [\text{mass}] * [\text{current}]^{-1} * [\text{time}]^{-2}$$
$$\boldsymbol{J} \propto [\text{current}] * [\text{length}]^{-2}$$
$$\boldsymbol{u} \propto [\text{length}] * [\text{time}]^{-2}$$
$$\rho \propto [\text{mass}] * [\text{length}]^{-3}$$

$$p = n - k = 6 - 1$$

$$F(\pi_1, \pi_2, \pi_3, \pi_4, \pi_5) = 0$$

To scan parameter space with 8pts per dim <u>requires 32,768 measurements</u>…
And so does scanning our 'reduced' parameter space

EXPERIMENTAL PEDAGOGY – HOW DO YOU RUN AN EXPERIMENT?

- For our plasma experiments…

$$\boldsymbol{u} = G(T, P, \boldsymbol{B}, \boldsymbol{J}, \rho) \xrightarrow{\text{Implies}} f(T, P, \boldsymbol{B}, \boldsymbol{J}, \boldsymbol{u}, \rho) = 0,$$

$$T \propto [\text{temperature}]$$
$$P \propto [\text{mass}] * [\text{length}]^{-1} * [\text{time}]^{-2}$$
$$\boldsymbol{B} \propto [\text{mass}] * [\text{current}]^{-1} * [\text{time}]^{-2}$$
$$\boldsymbol{J} \propto [\text{current}] * [\text{length}]^{-2}$$
$$\boldsymbol{u} \propto [\text{length}] * [\text{time}]^{-2}$$
$$\rho \propto [\text{mass}] * [\text{length}]^{-3}$$

$$p = n - k = 6 - 1$$

$$F(\pi_1, \pi_2, \pi_3, \pi_4, \pi_5) = 0$$

To scan parameter space with 8pts per dim requires 32,768 measurements…
And so does scanning our 'reduced' parameter space

- No matter what, probing an experimental parameter space takes a lot of time!
  - You'll need a lot of grad students…

EXPERIMENTAL DESIGN

- How do you make a versatile experiment?
- How do you measure an experiment?
- How do you run an experiment???

EXPERIMENTAL DESIGN - VERSATILITY

- Plasma systems are *highly* interdisciplinary
  - Require electrical engineering/power engineering expertise
  - Require mechanical engineering/vacuum systems expertise
  - Requires physics knowledge and expertise!

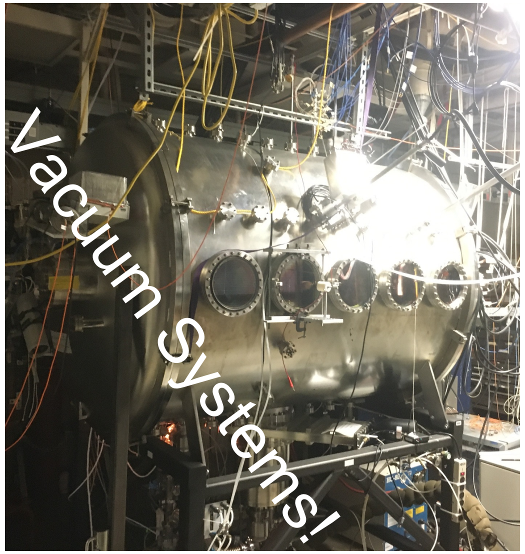

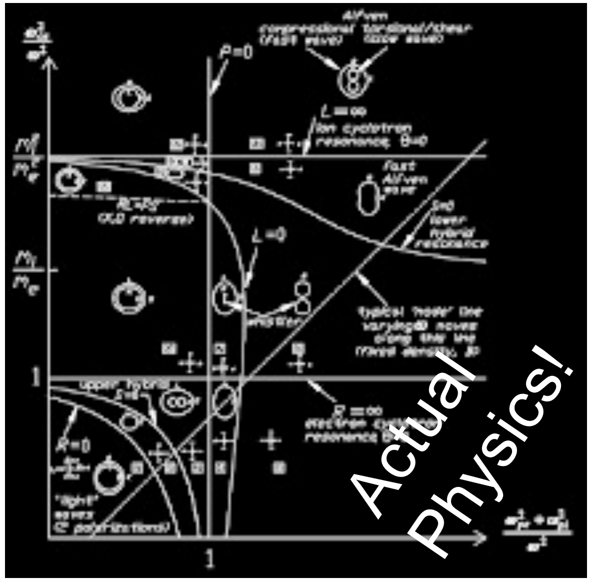

details

EXPERIMENTAL DESIGN - MEASUREMENT

- Measurements require diagnostics & diagnostic access

A multitude of vacuum ports allows for many probes

Design experiment chambers with large viewports for optical diagnostic access

EXPERIMENTAL DESIGN - MEASUREMENT

- Huge arsenal of diagnostic tools may be required:

Physical Probes	Pros	Cons	Use
Langmuir probes	Simple!	Can destroy plasma features, not very accurate	Detect plasma frequency, density
B-dot probes	Simple!	Difficult to construct, perturb magnetic fields	Detect plasma magnetic field, extract current density
Impedance probes	Accurate!	Difficult to construct	
Faraday cups	Simple!	Not very accurate	Capture particles, analyze energy spectra
Optical Probes	**Pros**	**Cons**	**Use**
Spectrometers	Info-dense!	Can be hard to acquire and use	Detect emission spectra of neutrals
EUV/X-ray diodes	Simple!	Difficult to construct	Capture high-energy emissions
Cameras	Easy to use!	Expensive	Capture optical emissions

EXPERIMENTAL DESIGN – HOW DO YOU RUN AN EXPERIMENT???

- Carefully!!!

LABORATORY ASTROPHYSICS AT CALTECH

LABORATORY ASTROPHYSICS AT CALTECH

- The Caltech Jet Experiment
  - Simulates astrophysical jets from stars & nebulae

LABORATORY ASTROPHYSICS AT CALTECH

- The Caltech Jet Experiment
  - Simulates astrophysical jets from stars & nebulae
- The Single Loop Experiment & Double Loop Experiments
  - Simulates solar-coronal loops and merging flux-ropes

LABORATORY ASTROPHYSICS AT CALTECH

- The Caltech Jet Experiment
  - Simulates astrophysical jets from stars & nebulae
- The Single Loop Experiment & Double Loop Experiments
  - Simulates solar-coronal loops and merging flux-ropes
- The Ice Dusty Plasma Experiment
  - Simulates low ionization-fraction plasmas with embedded water ice

CALTECH JET EXPERIMENT

- The Caltech Jet Experiment produces an MHD-driven plasma jet
  - Configuration varies with bias magnetic field strength, gas volume, etc.

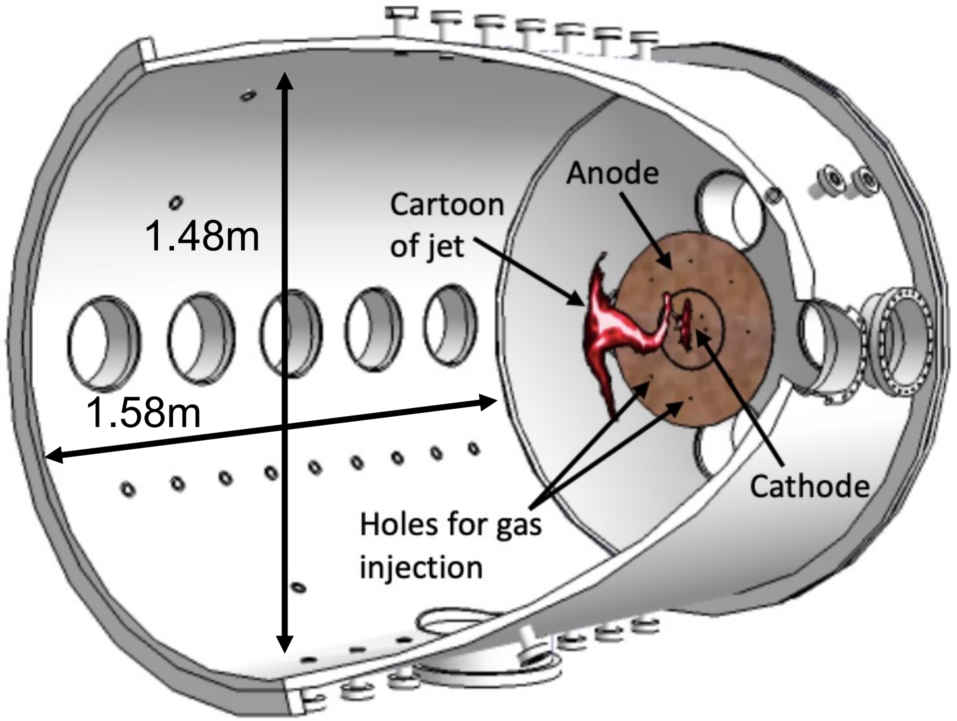

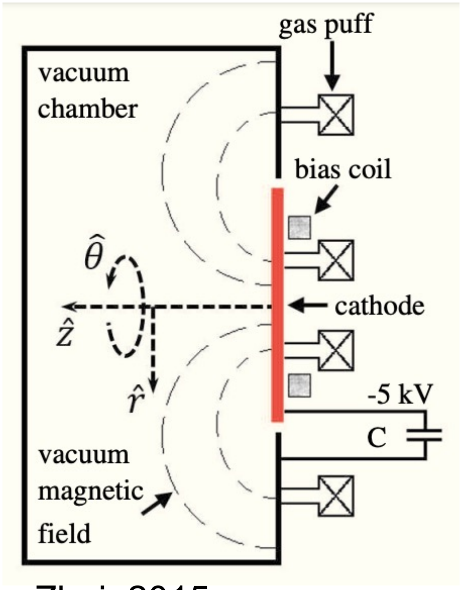

Zhai, 2015

details

Primary point of contact: me!
jqmorgan@caltech.edu

CALTECH JET EXPERIMENT

- The Caltech Jet Experiment produces an MHD-driven plasma jet
  - Configuration varies with bias magnetic field strength, gas volume, etc.
- Typical plasma parameters:
  - Plasma temperature, T ~ 2eV
  - Particle density, n ~ 10^{21} - 10^{22}m^{-3}

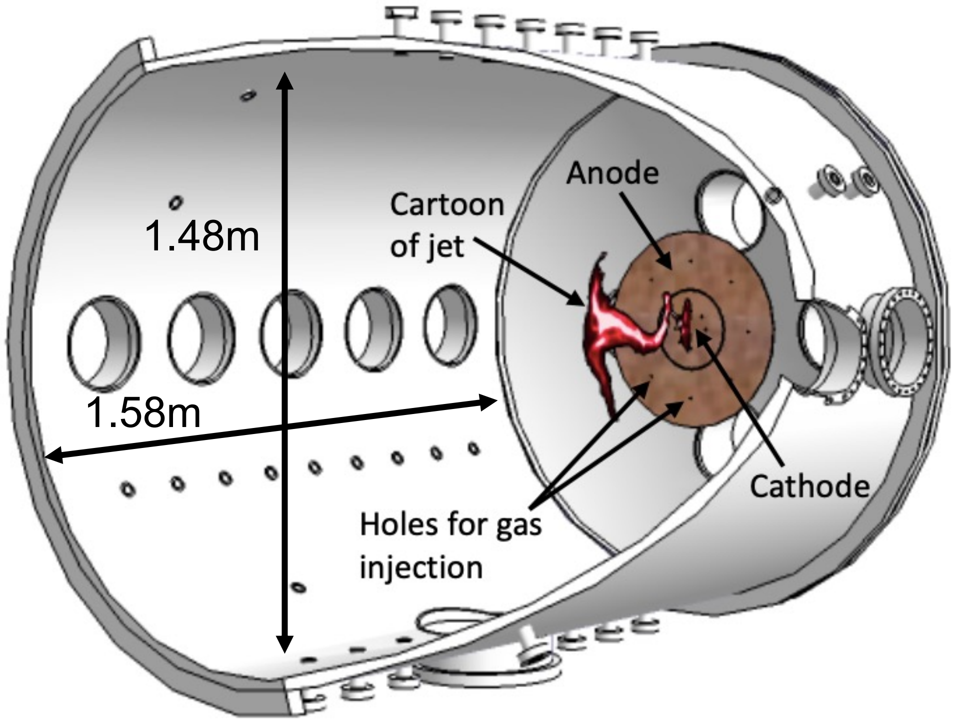

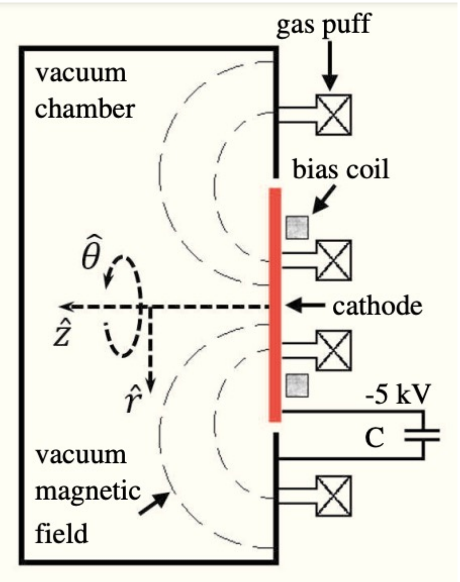

Zhai, 2015

details

Primary point of contact: me!
jqmorgan@caltech.edu

CALTECH JET EXPERIMENT

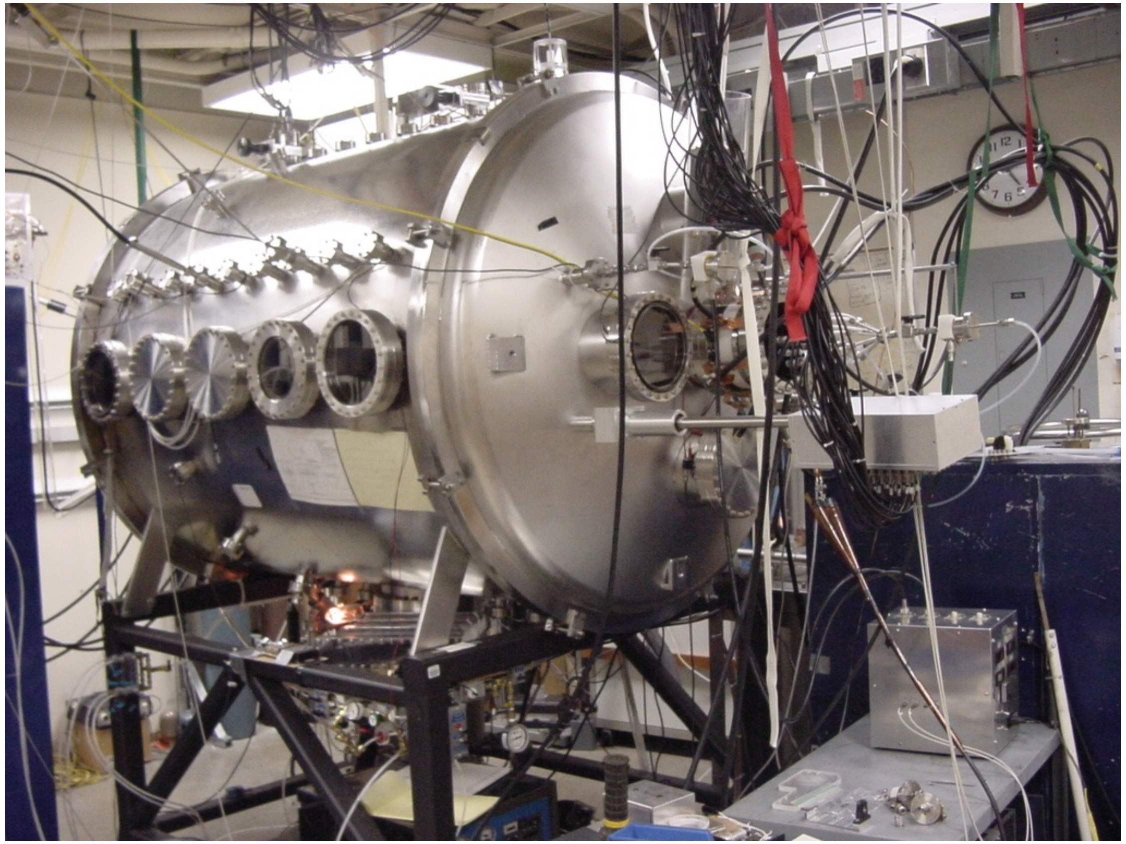

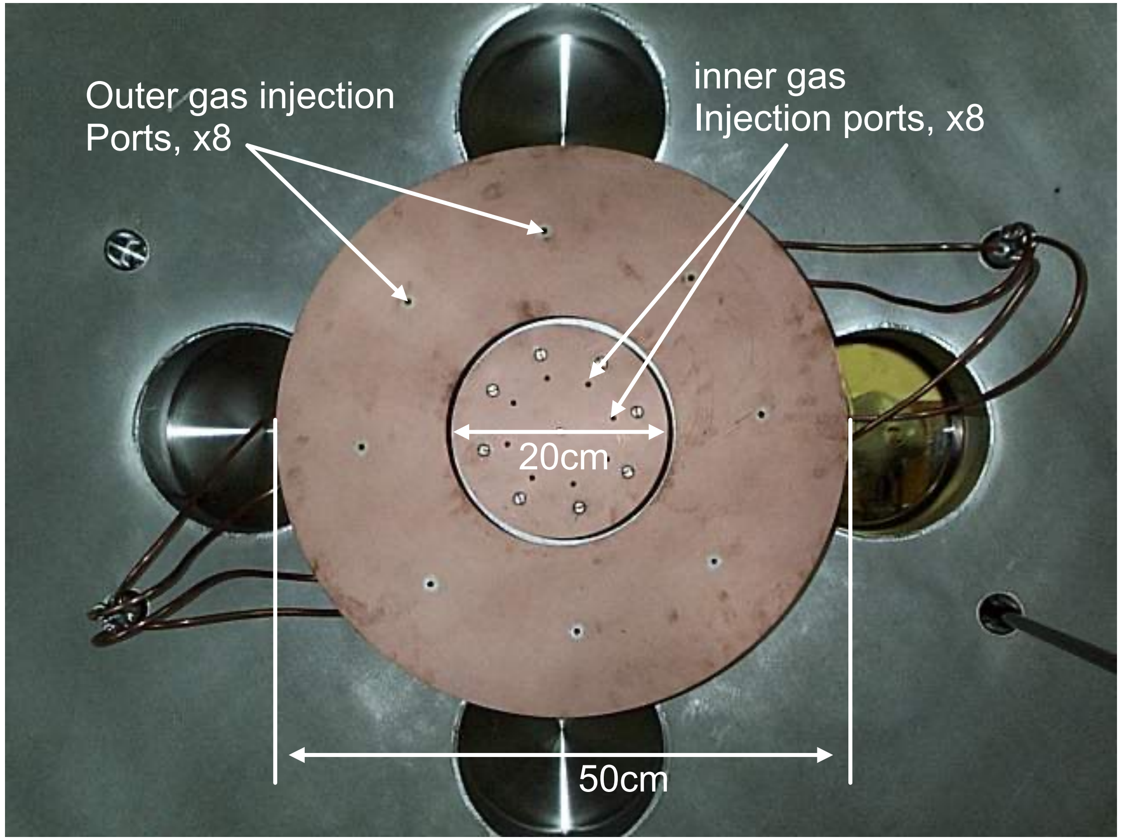

details

CALTECH JET EXPERIMENT

- Generates long jet which undergoes a series of instabilities
  - Kink instability, Rayleigh-Taylor Instability (RTI)

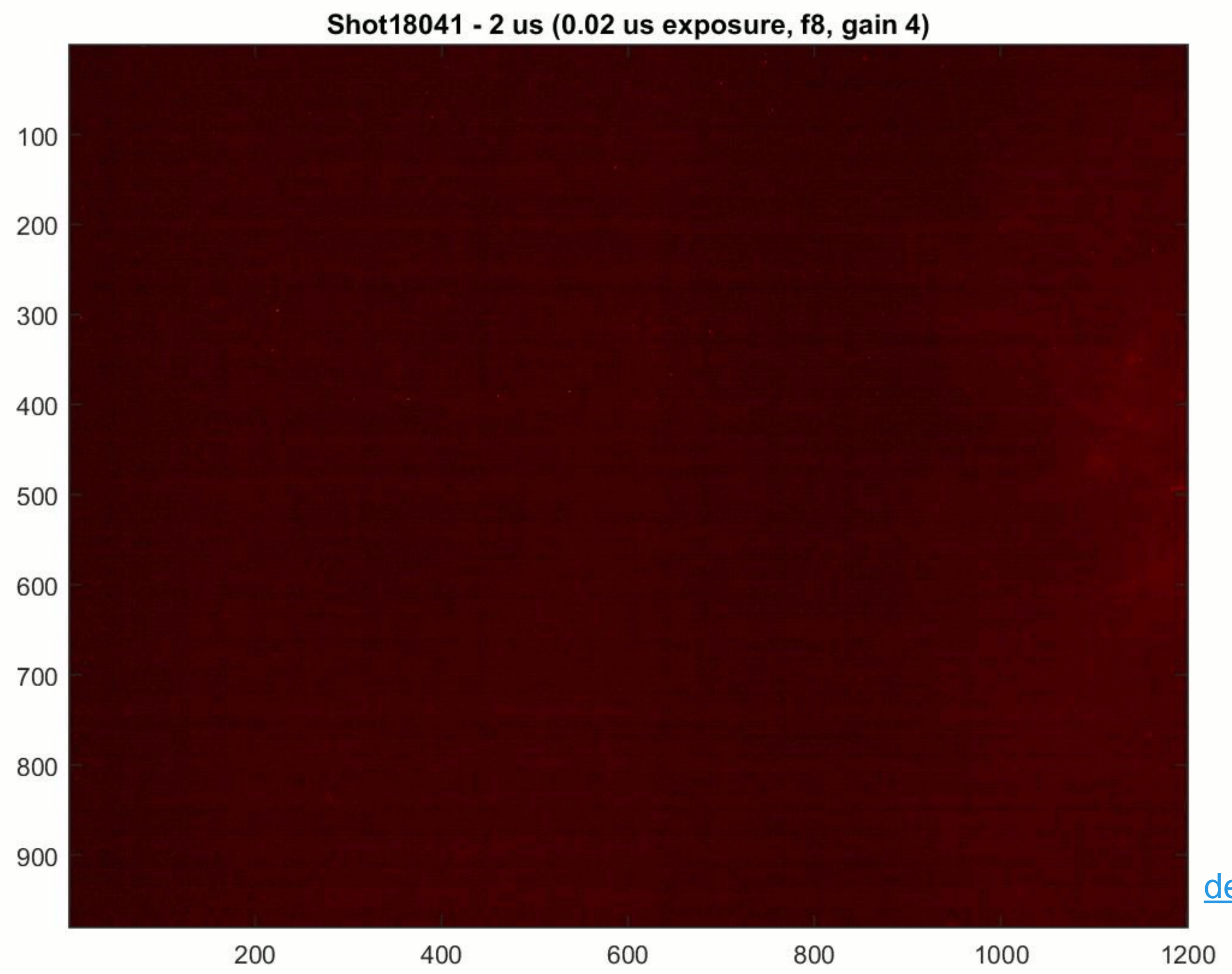

details

CALTECH JET EXPERIMENT

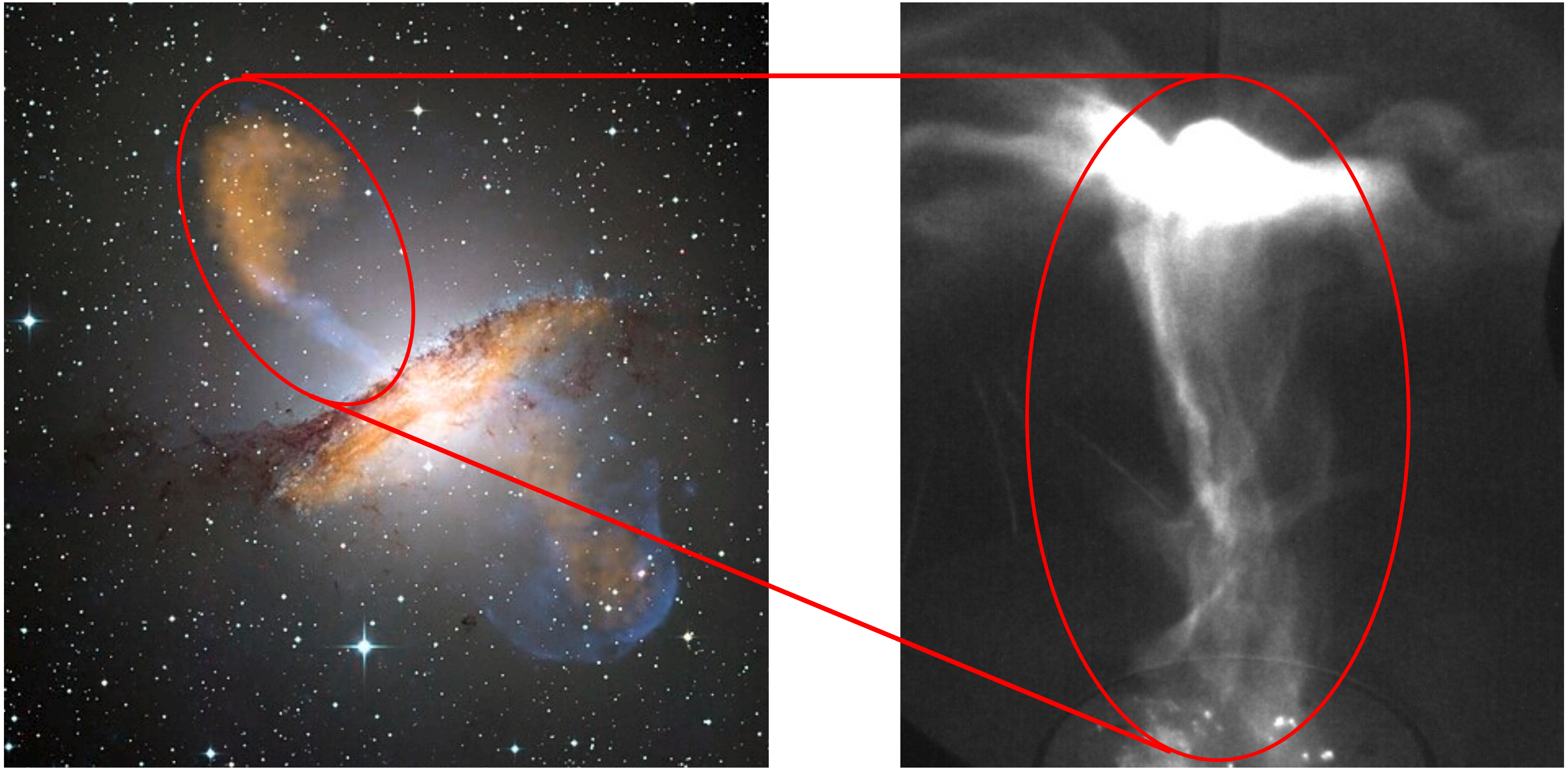

ESO/WFI, 2009

CALTECH JET EXPERIMENT

- This experiment assumes YSO/AGN jets charge like a radial dynamo to drive the jet

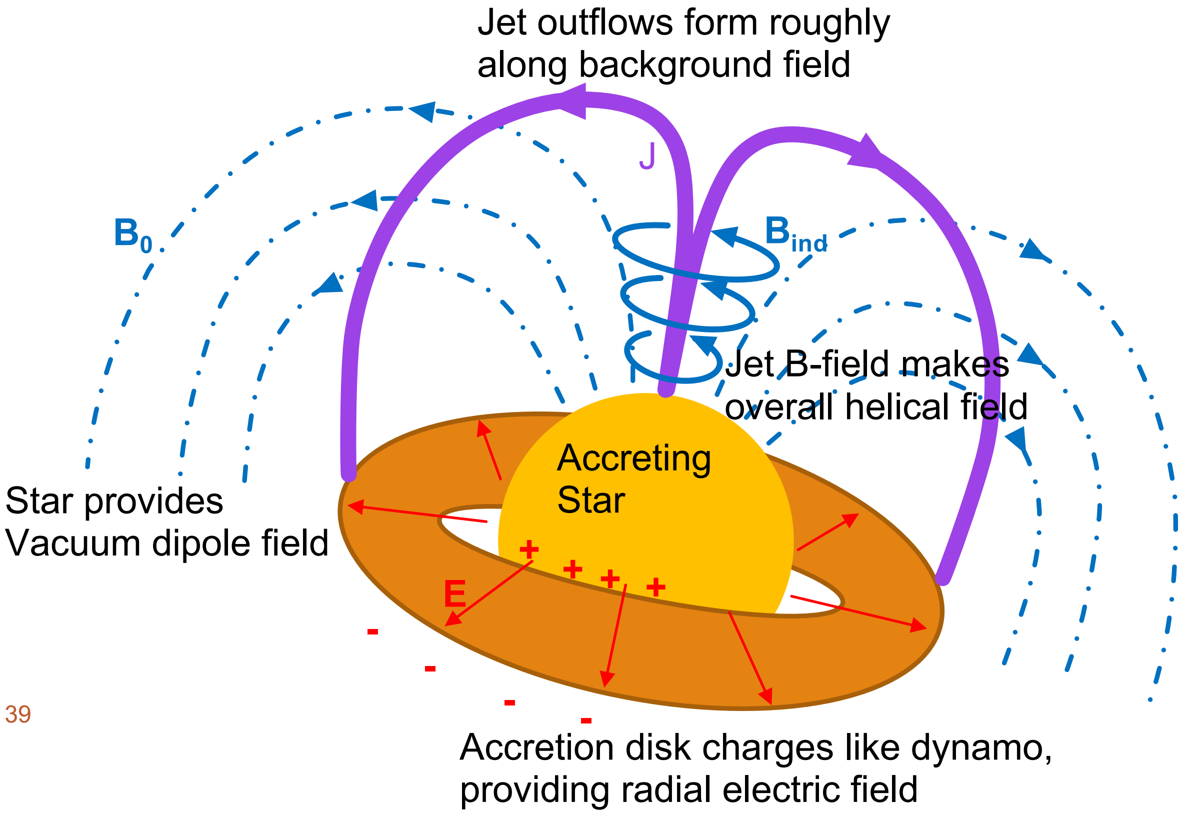

CALTECH JET EXPERIMENT

- This experiment assumes YSO/AGN jets charge like a radial dynamo to drive the jet

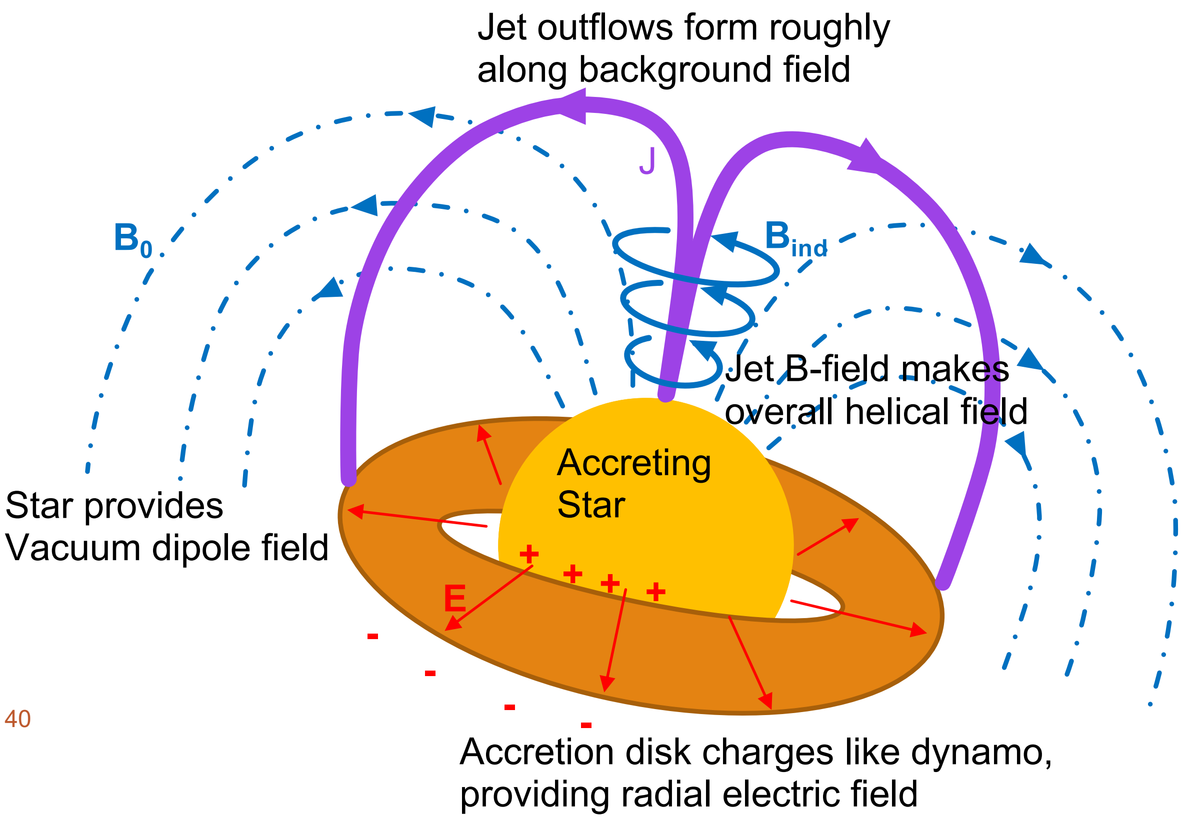

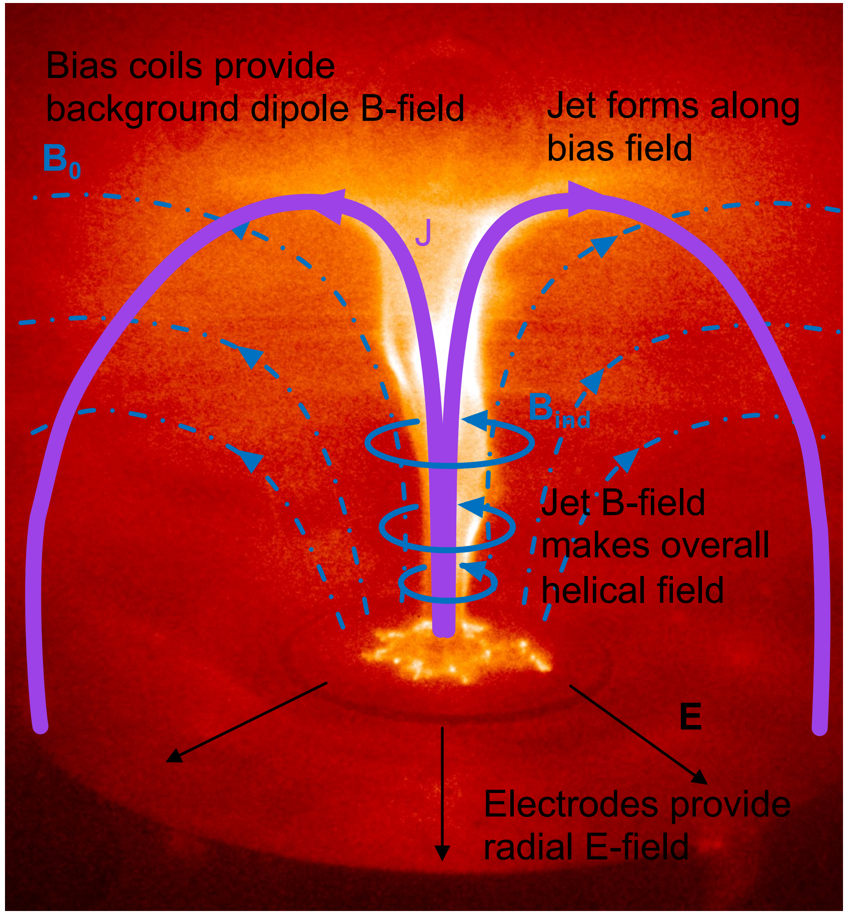

CALTECH JET EXPERIMENT

- Scaling laws indicate good agreement between laboratory and astrophysical systems
  - Evolution expected to be similar when MHD applies

Quantity	Lab Jet (hydrogen)
L	0.3 m
n	10^{22} m^{-3}
B	0.1 T
v_A	20 km/s
β	0.1–1
S	10–100

$$\mathbf{r}_a = c_1\,\mathbf{r}_l \qquad \rho_a = c_2\,\rho_l \qquad P_a = c_3\,P_l$$

$$\mathbf{B}_a = \sqrt{c_3}\,\mathbf{B}_l \qquad \mathbf{v}_a = \sqrt{\frac{c_3}{c_2}}\,\mathbf{v}_l \qquad t_a = c_1\sqrt{\frac{c_2}{c_3}}\,t_l.$$

Quantity	YSO Jet
L	10^{14} m
n	10^{10} m^{-3}
B	10^{-7} T
v_A	20 km/s
β	0.4
S	10^{15}

Chaplin, 2015

CALTECH JET EXPERIMENT

- Scaling laws indicate good agreement between laboratory and astrophysical systems
  - Evolution expected to be similar when MHD applies

Quantity	Lab Jet (hydrogen)
L	0.3 m
n	10^{22} m^{-3}
B	0.1 T
v_A	20 km/s
β	0.1–1
S	10–100

$$\mathbf{r}_a = c_1\,\mathbf{r}_l \qquad \rho_a = c_2\,\rho_l \qquad P_a = c_3\,P_l$$

$$\mathbf{B}_a = \sqrt{c_3}\,\mathbf{B}_l \qquad \mathbf{v}_a = \sqrt{\frac{c_3}{c_2}}\,\mathbf{v}_l \qquad t_a = c_1\sqrt{\frac{c_2}{c_3}}\,t_l.$$

Quantity	YSO Jet
L	10^{14} m
n	10^{10} m^{-3}
B	10^{-7} T
v_A	20 km/s
β	0.4
S	10^{15}

Chaplin, 2015

S>>1 in both cases; ideal MHD applies

CALTECH SOLAR LOOP EXPERIMENT(S)

- The Caltech Single-loop Experiment produces a half-loop of plasma simulating a solar prominence
  - Background field supplied by two bias coils

Primary point of contact: Yang Zhang (& me!)
yangzhan@caltech.edu

CALTECH SOLAR LOOP EXPERIMENT(S)

- The Caltech Single-loop Experiment produces a half-loop of plasma simulating a solar prominence
  - Background field supplied by two bias coils
- Similar plasma parameters:
  - Plasma temperature, T ~ 2eV
  - Particle density, n ~ 10^{21} - $10^{22} m^{-3}$

Primary point of contact: Yang Zhang (& me!)
yangzhan@caltech.edu

CALTECH SOLAR LOOP EXPERIMENT(S)

- Two bias coils create complex field which promotes a loop-like formation

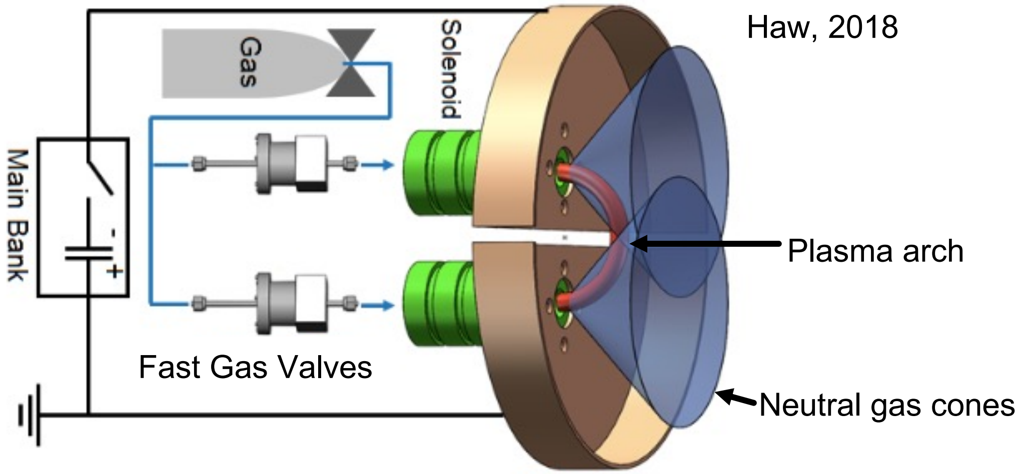

Haw, 2018

Double Solenoid
Vacuum field

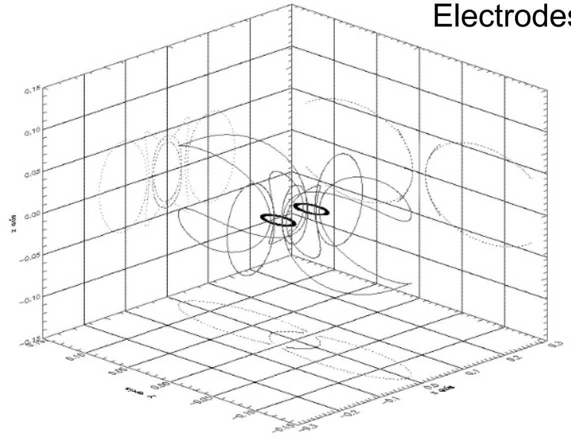

Stensen, 2012

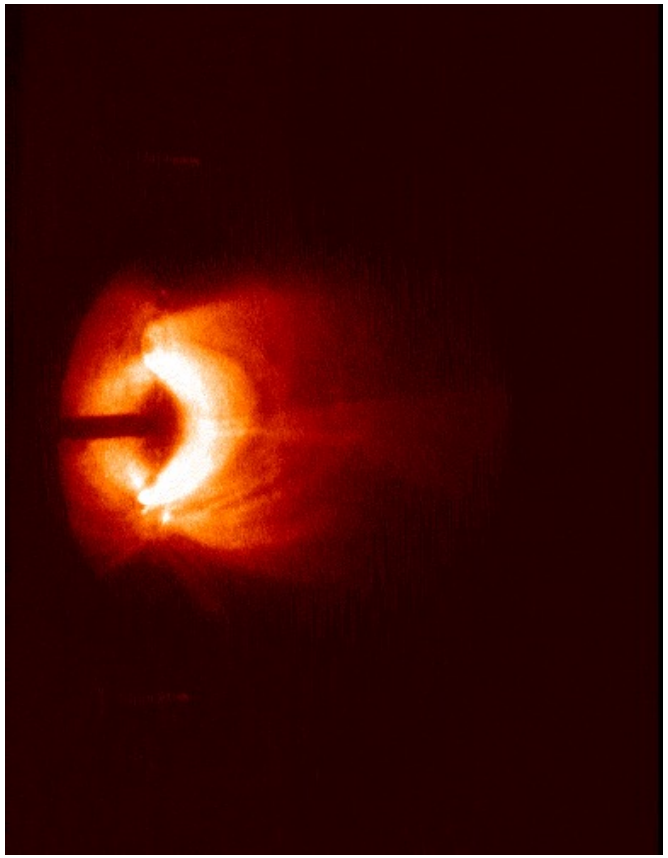

CALTECH SOLAR LOOP EXPERIMENT(S)

- Loop dynamics readily replicate observed solar phenomena…

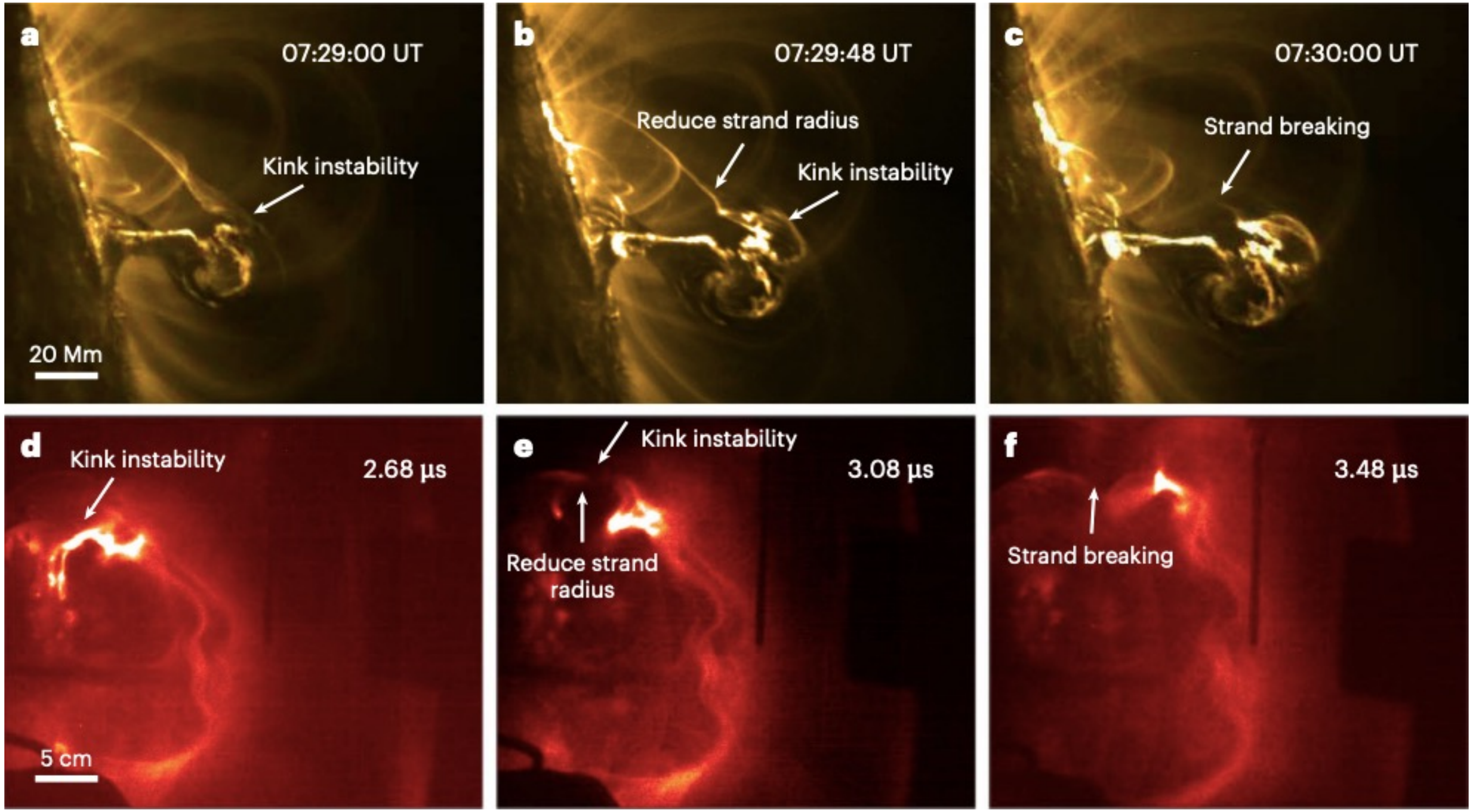

Zhang, 2022

CALTECH SOLAR LOOP EXPERIMENT(S)

- Despite missing critical topological feature assumed by most models of solar prominences!
  - Experiment may better represent a simpler arcade model

Huge X-point our magnetic field topology doesn't include!

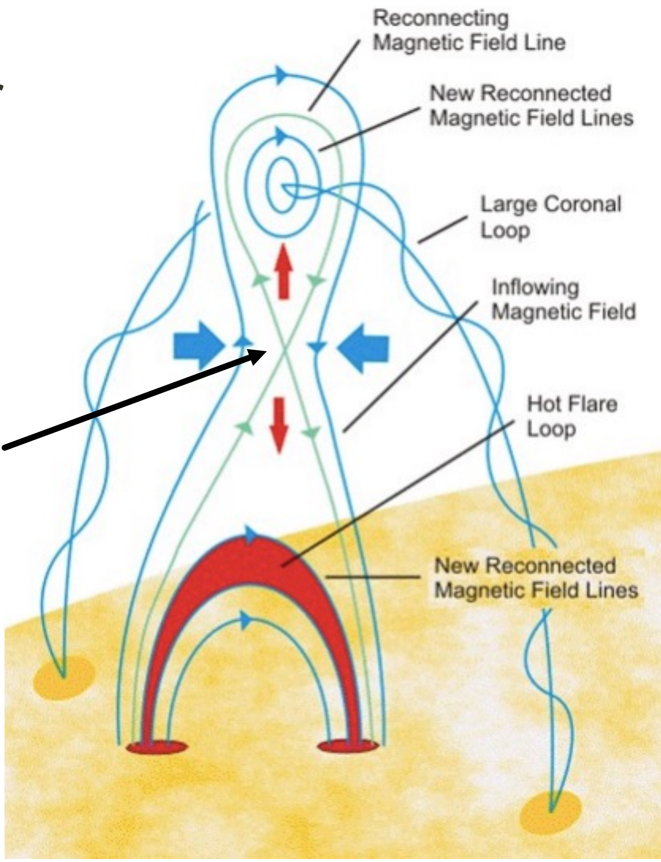

Max-Planck Institute, 2014

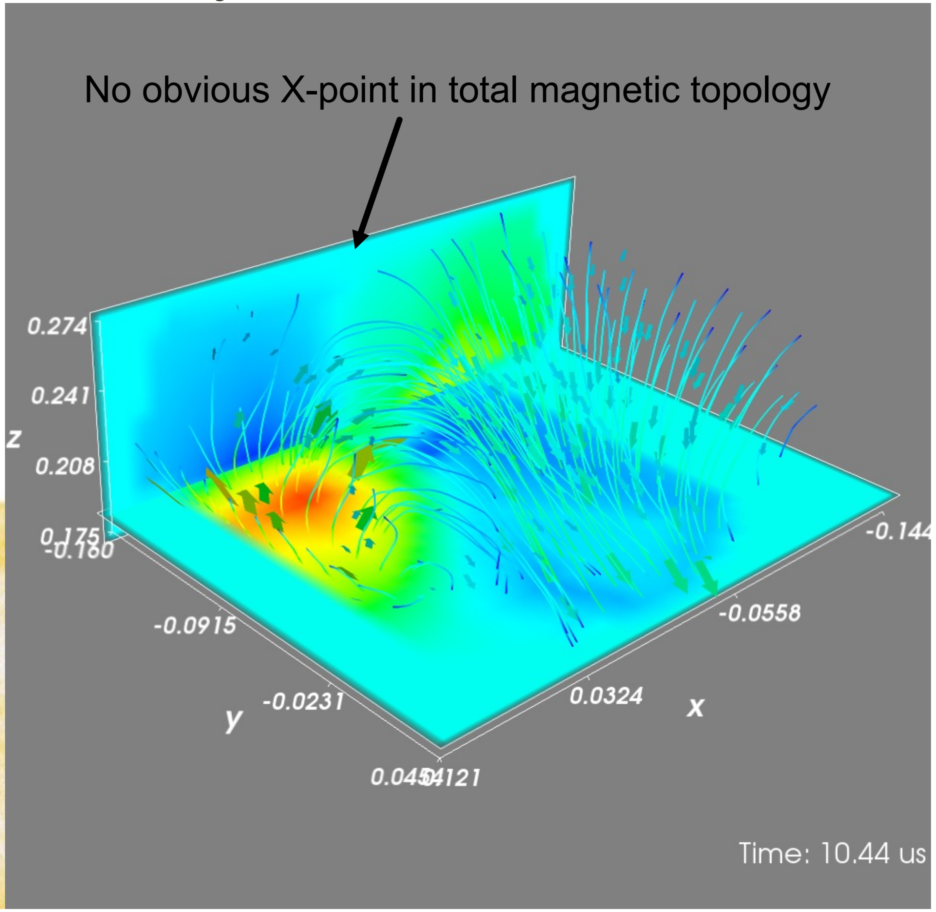

CALTECH SOLAR LOOP EXPERIMENT(S)

- Existing experiment also scales well
  - Worst point of agreement is the force of gravity

Experimental Parameters	$B = 3000$ G	$L = 0.5$ m	$\rho = 10^{-4} \frac{kg}{m^3}$	$\tau_A = 20\ \mu s$
	$g = 10 \frac{m}{s^2}$	$P = 300$ Pa	$v_A = 3 \cdot 10^4 \frac{m}{s}$	$\beta = 0.01$

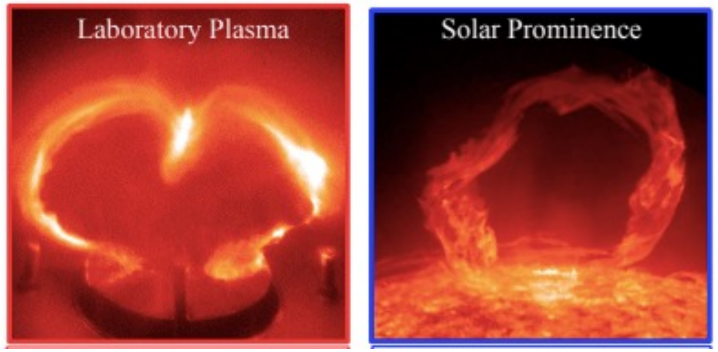

Haw, 2018

CALTECH SOLAR LOOP EXPERIMENT(S)

- Existing experiment also scales well
  - Worst point of agreement is the force of gravity

Experimental Parameters	$B = 3000$ G $g = 10\ \frac{\text{m}}{\text{s}^2}$	$L = 0.5$ m $P = 300$ Pa	$\rho = 10^{-4}\frac{\text{kg}}{\text{m}^3}$ $v_A{=}3{\cdot}10^4\frac{\text{m}}{\text{s}}$	$\tau_A = 20\ \mu$s $\beta = 0.01$

$$\mathbf{r}_a = c_1\,\mathbf{r}_l \qquad \rho_a = c_2\,\rho_l \qquad P_a = c_3\,P_l$$

$$\mathbf{B}_a = \sqrt{c_3}\,\mathbf{B}_l \qquad \mathbf{v}_a = \sqrt{\frac{c_3}{c_2}}\,\mathbf{v}_l \qquad t_a = c_1\sqrt{\frac{c_2}{c_3}}\,t_l.$$

Scaled Exp. Parameters	$B = 30$ G $g = 3\cdot10^{-3}\ \frac{\text{m}}{\text{s}^2}$	$L = 2{\cdot}10^7$ m $P = 3\cdot10^{-2}$ Pa	$\rho = 10^{-12}\frac{\text{kg}}{\text{m}^3}$ $v_A{=}3{\cdot}10^6\frac{\text{m}}{\text{s}}$	$\tau_A = 7$ s $\beta = 0.01$
Typical Coronal Loop T= 1.5 MK	$B = 50$ G $g = 300\ \frac{\text{m}}{\text{s}^2}$	$L = 2{\cdot}10^7$ m $P = 1\cdot10^{-2}$ Pa	$\rho = 10^{-12}\frac{\text{kg}}{\text{m}^3}$ $v_A{=}4{\cdot}10^6\frac{\text{m}}{\text{s}}$	$\tau_A = 5$ s $\beta = 0.002$

Haw, 2018

CALTECH SOLAR LOOP EXPERIMENT(S)

- Single-loop experiment is extended by crossed flux tube (CroFT) experiment
  - Designed to examine role of magnetic reconnection in solar prominence formation

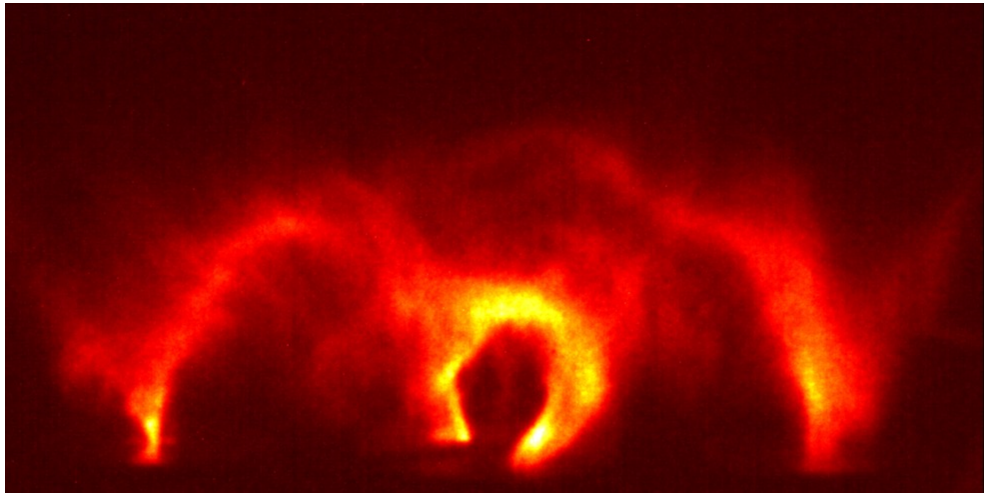

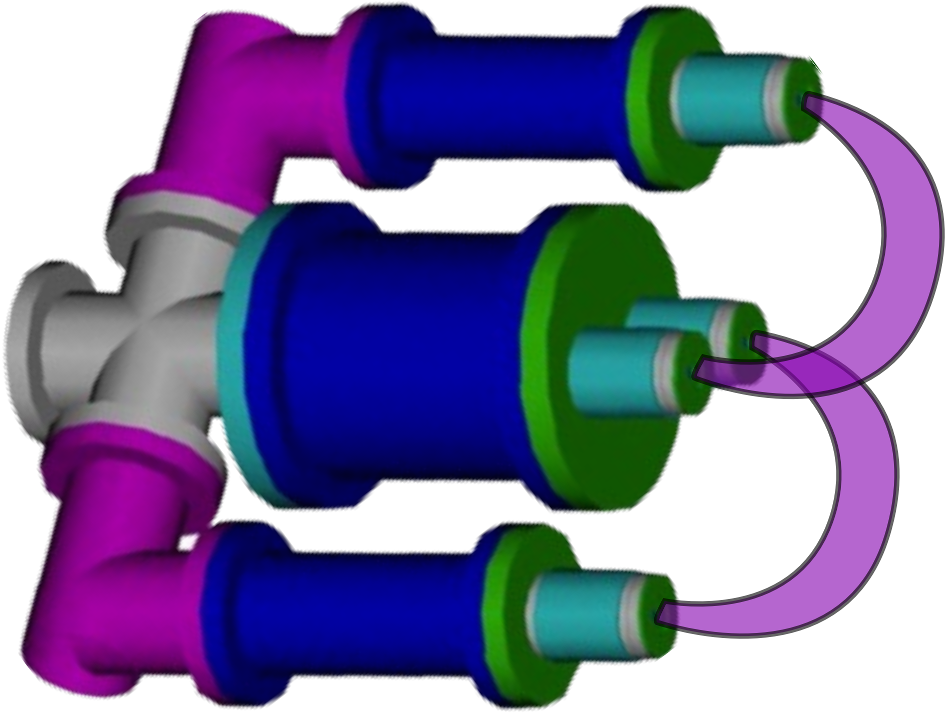

Tobin, 2013

CALTECH ICE DUSTY PLASMA EXPERIMENT

- The Caltech Ice Dusty Plasma experiment is designed to simulate a wide variety of space (& terrestrial) plasmas

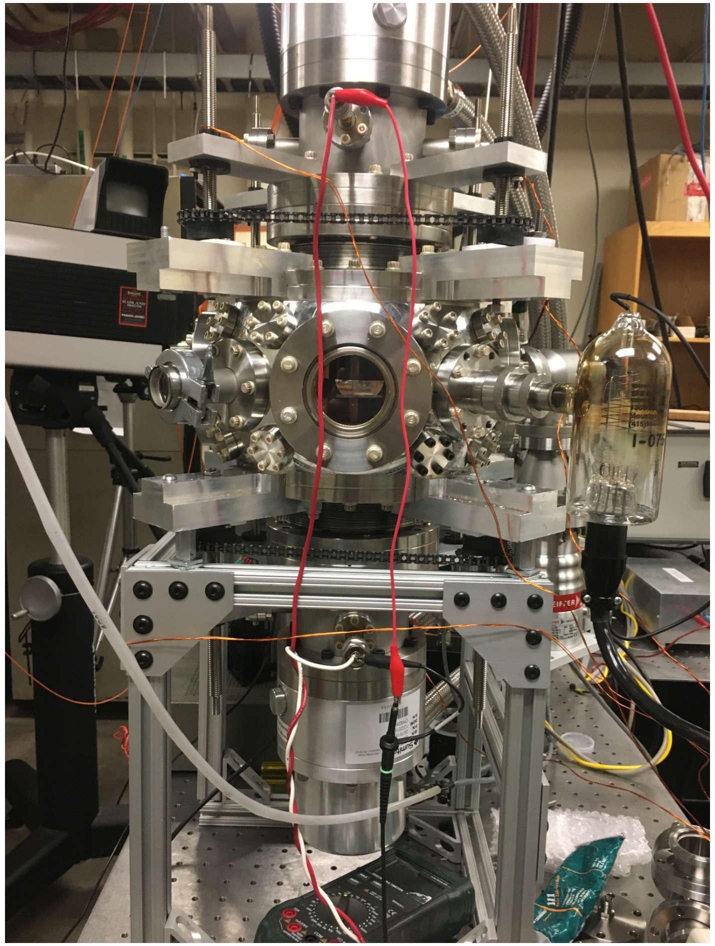

Primary point of contact: André Nicolov
anicolov@caltech.edu

CALTECH ICE DUSTY PLASMA EXPERIMENT

- The Caltech Ice Dusty Plasma experiment is designed to simulate a wide variety of space (& terrestrial) plasmas

Noctilucent clouds

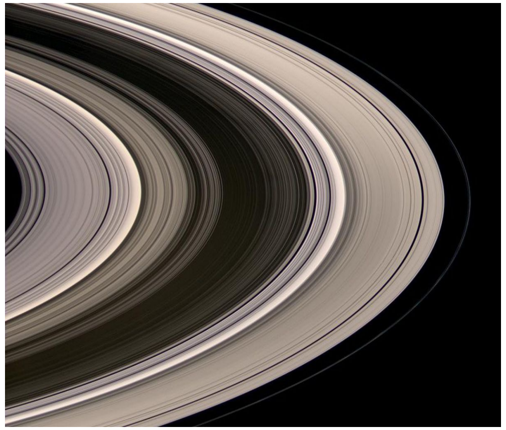

Saturn's Rings

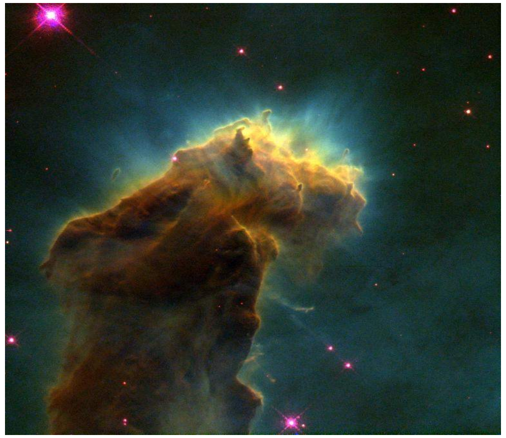

Molecular clouds

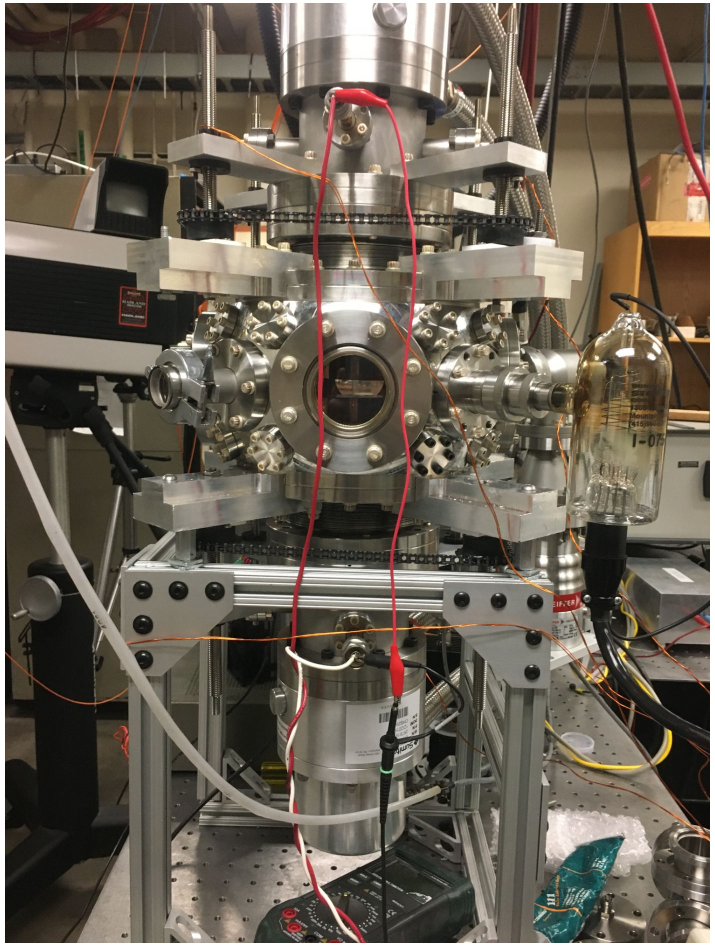

Primary point of contact: André Nicolov
anicolov@caltech.edu

CALTECH ICE DUSTY PLASMA EXPERIMENT

- Small, steady state plasma volume w/ significant diagnostic access
  - Injecting water permits formation of ice grains
  - Unmagnetized, RF-coupled plasma (negates gravity)

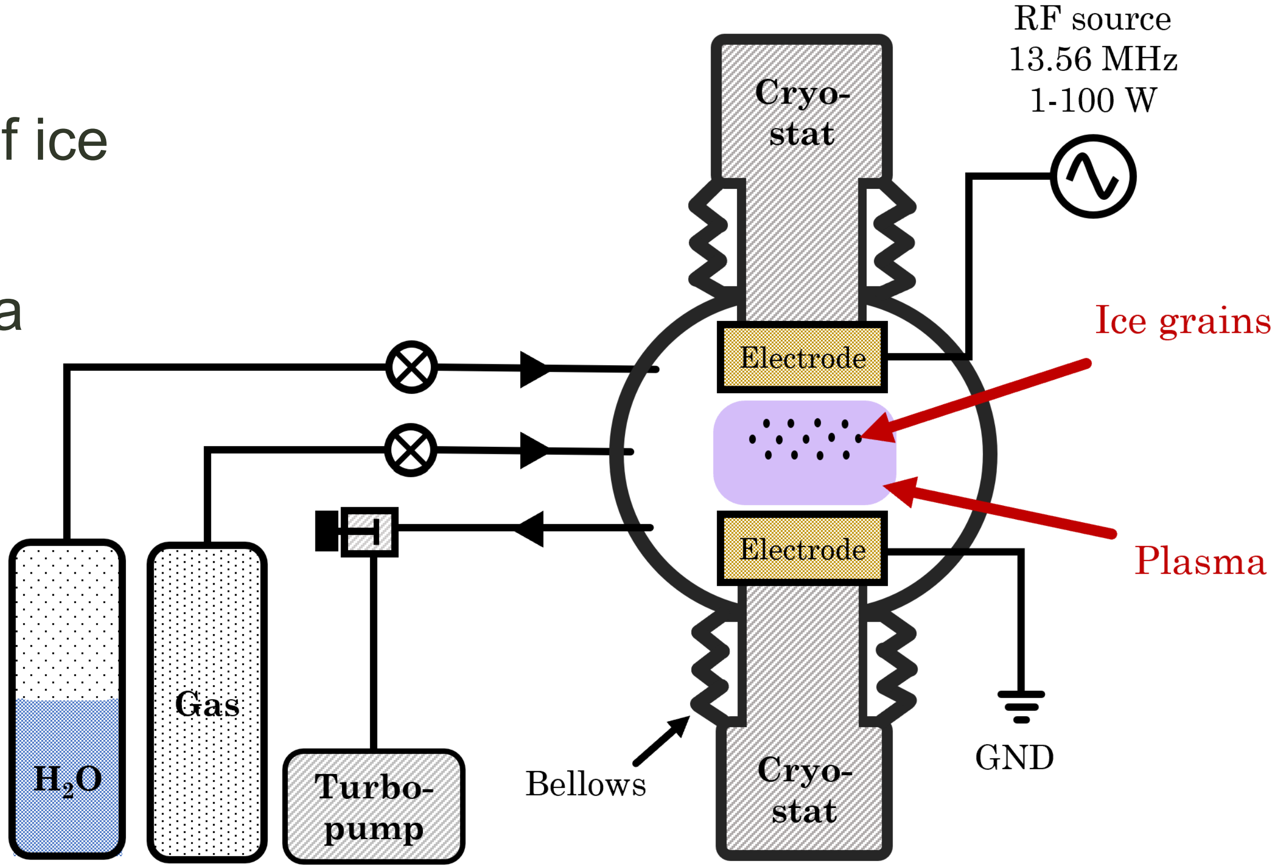

Nicolov, 2023

CALTECH ICE DUSTY PLASMA EXPERIMENT

- Ice grains form spontaneously
  - Microscope camera allows for imaging
  - FTIR spectroscopy can be used to examine ice phase

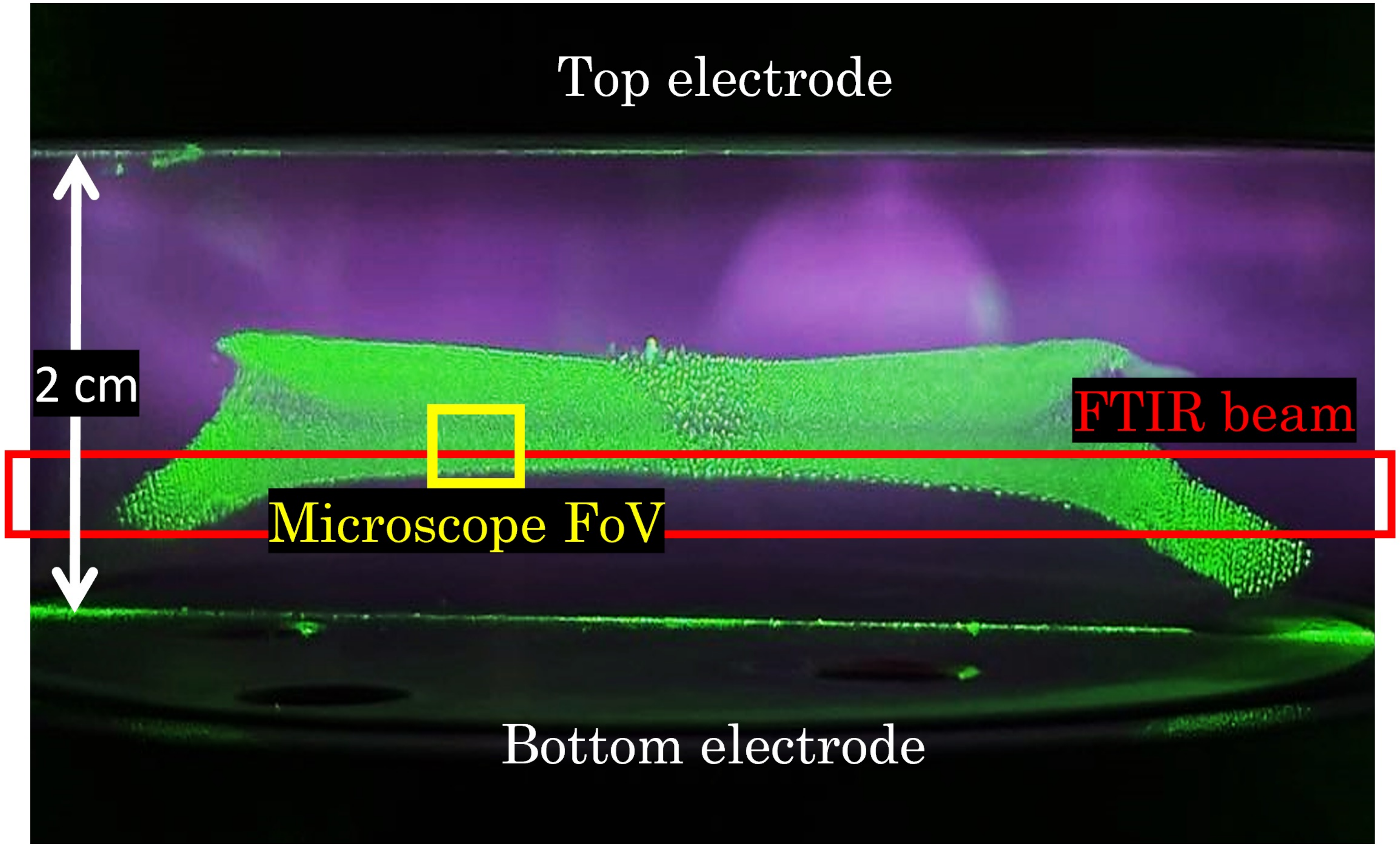

Nicolov, 2023

CALTECH ICE DUSTY PLASMA EXPERIMENT

- Ice grains are elongated & fractal-like
- Multiple theories on nucleation mechanism
- Ice grains exhibit interesting wave-like behavior

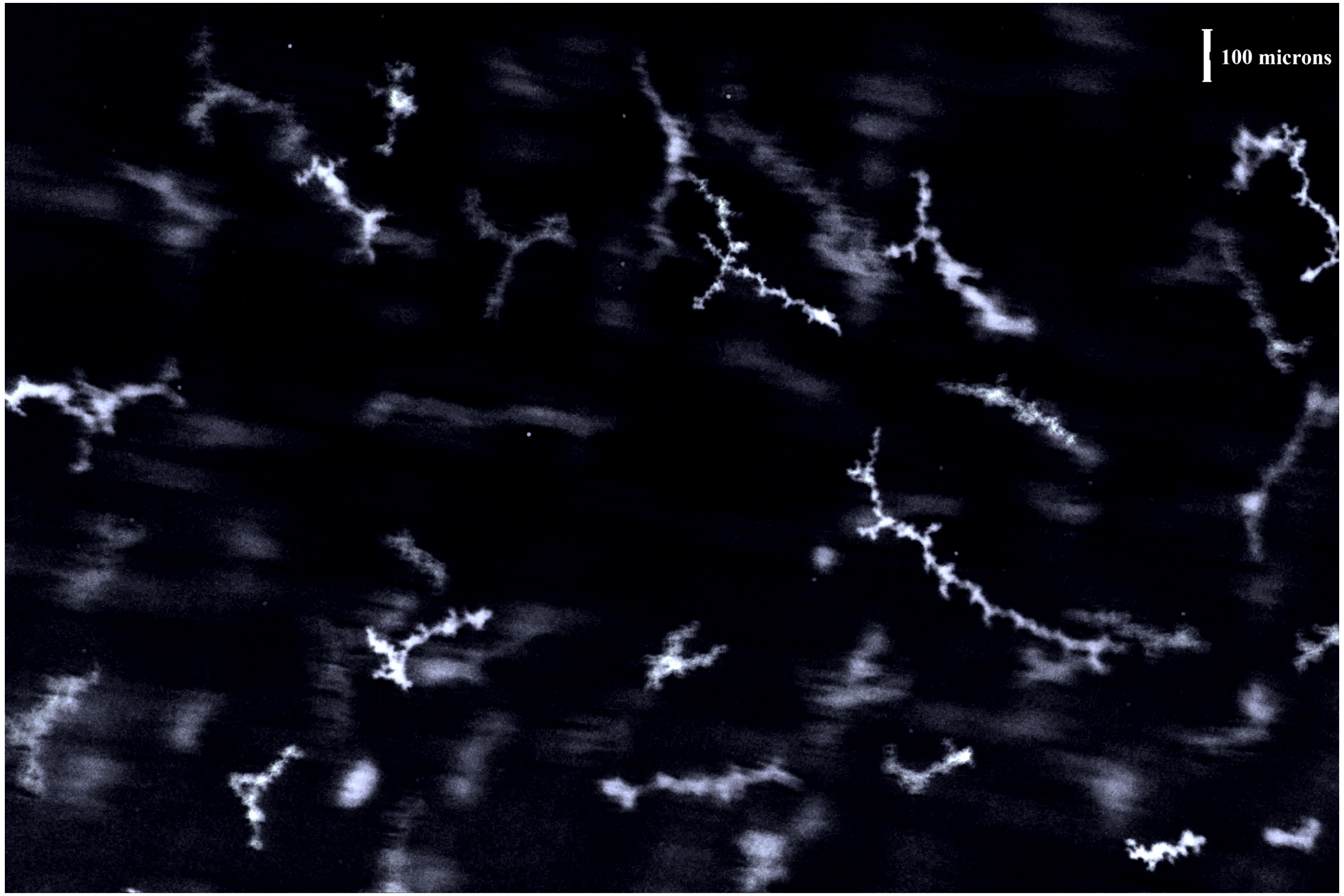

CALTECH ICE DUSTY PLASMA EXPERIMENT

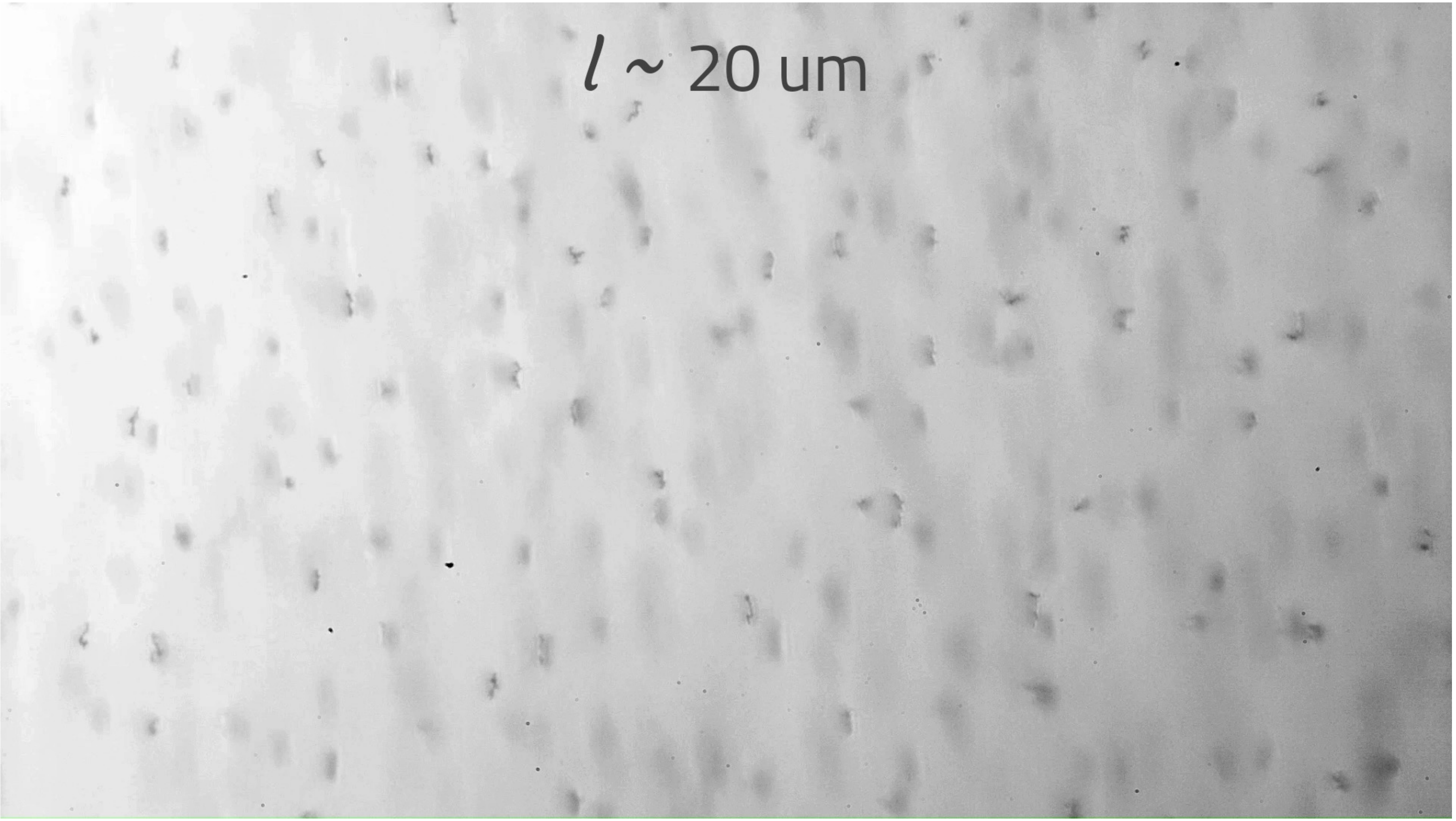

Nicolov, 2023

OTHER RELEVANT EXPERIMENTS

- Lots of other experiments out there simulate astrophysical plasmas, and astrophysically relevant fundamental plasmas!

Imperial College London

AUBURN UNIVERSITY

VET TES EN NOV TAM TVM

EMBRY-RIDDLE AERONAUTICAL UNIVERSITY 1926

Just a small selection from my limited knowledge…

OTHER JET EXPERIMENTS

- Other jet experiments exist at various universities, using different formation techniques
  - Imperial College [MAGPIE experiment]
    - Jet formed by complex wire array (16 wires!)

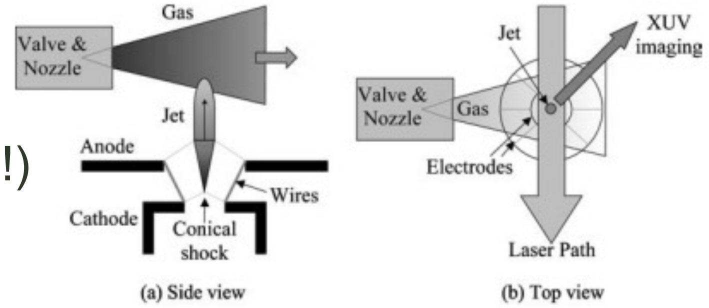

MAGPIE setup
Lebedev, 2005

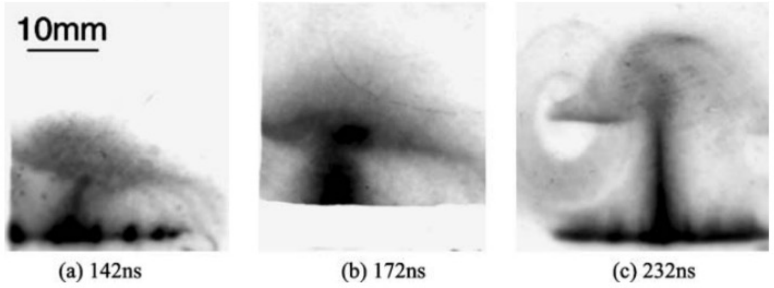

OTHER JET EXPERIMENTS

- Other jet experiments exist at various universities, using different formation techniques
  - Imperial College MAGPIE experiment
    - Jet formed by complex wire array (16 wires!)
  - Embry-Riddle EAGLE experiment
    - Jet formed with continuous circular inlet, not discrete injection points

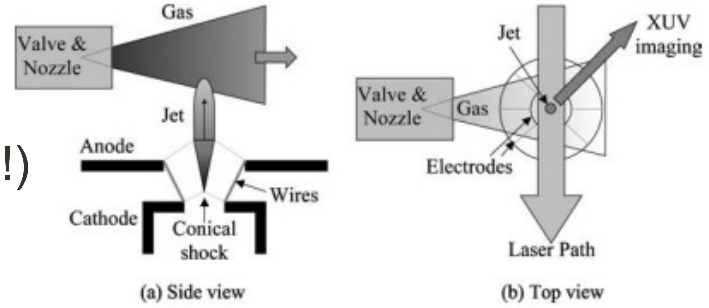

MAGPIE setup
Lebedev, 2005

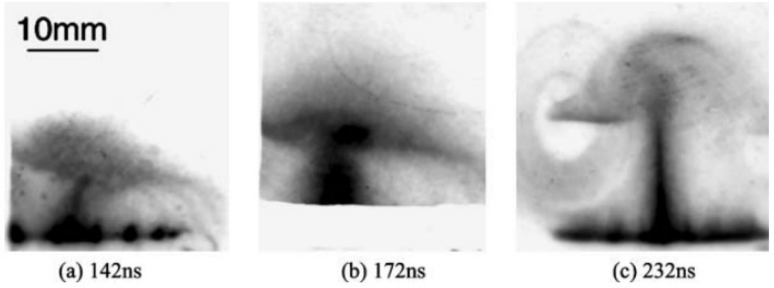

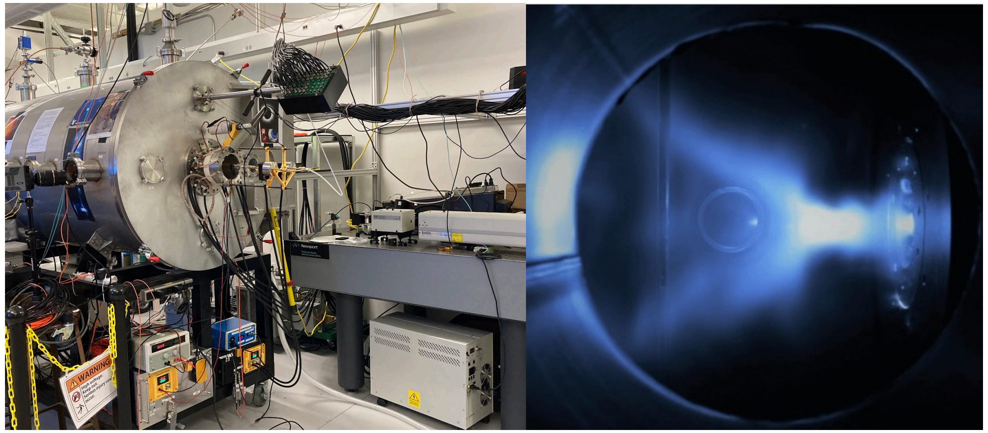

EAGLE plasma jet

PHASMA MERGING FLUX ROPE EXPERIMENT

- Angled plasma jets generate merging flux ropes in the PHASMA experiment
  - Simulates fundamental plasma processes (magnetic reconnection) that lead to the formation of large-scale structures
    - Similar to Caltech CroFT experiment, but with totally different scale & topology

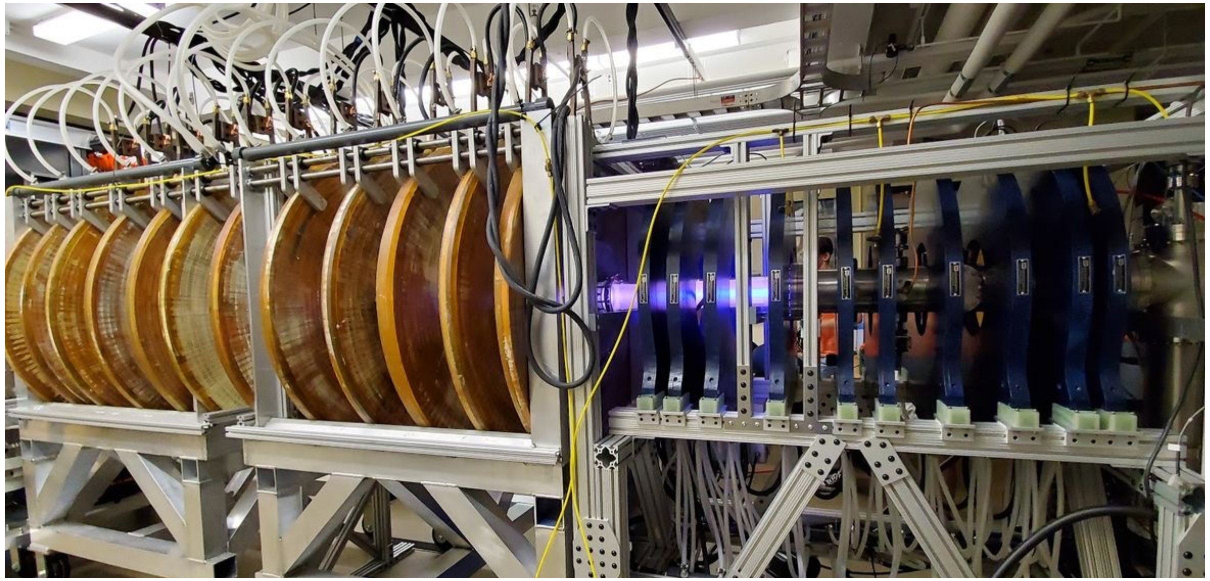

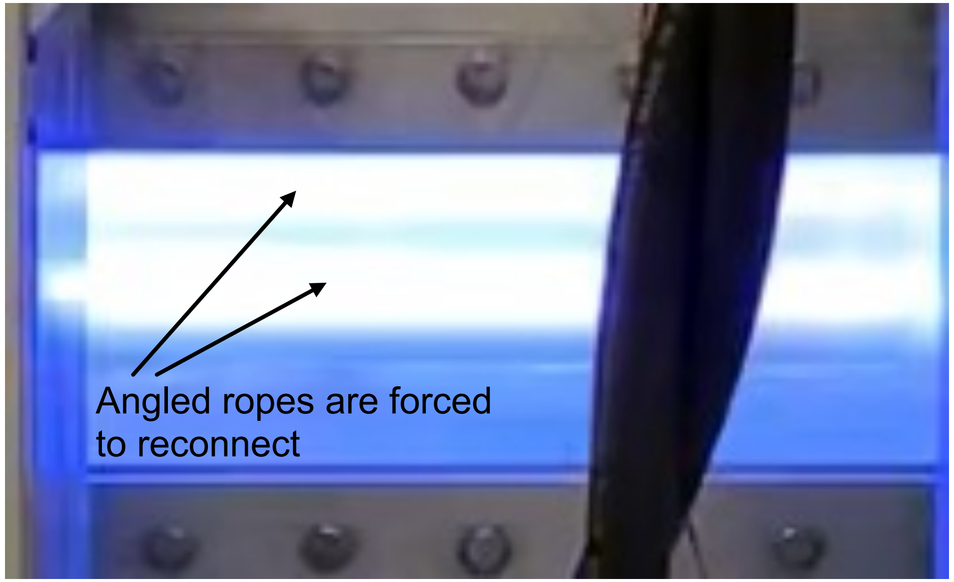

MAGNETIZED DUSTY PLASMA EXPERIMENT

- The MDPX experiment at Auburn university examines dusty plasmas which are magnetized
  - Studies dynamics with synthetic particles, like 200um silica balls injected into plasma volume

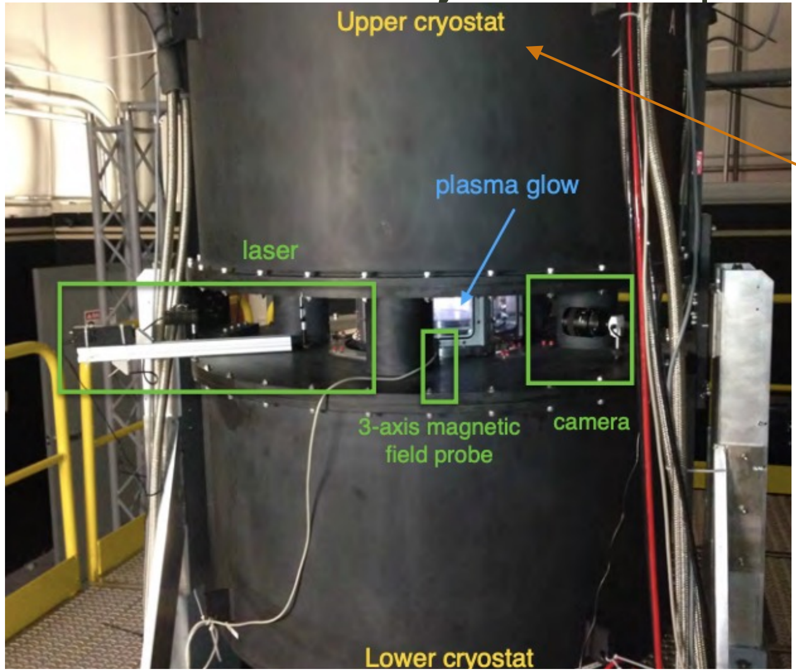

Thomas, 2018

Cryostat has central bore permitting diagnostic access

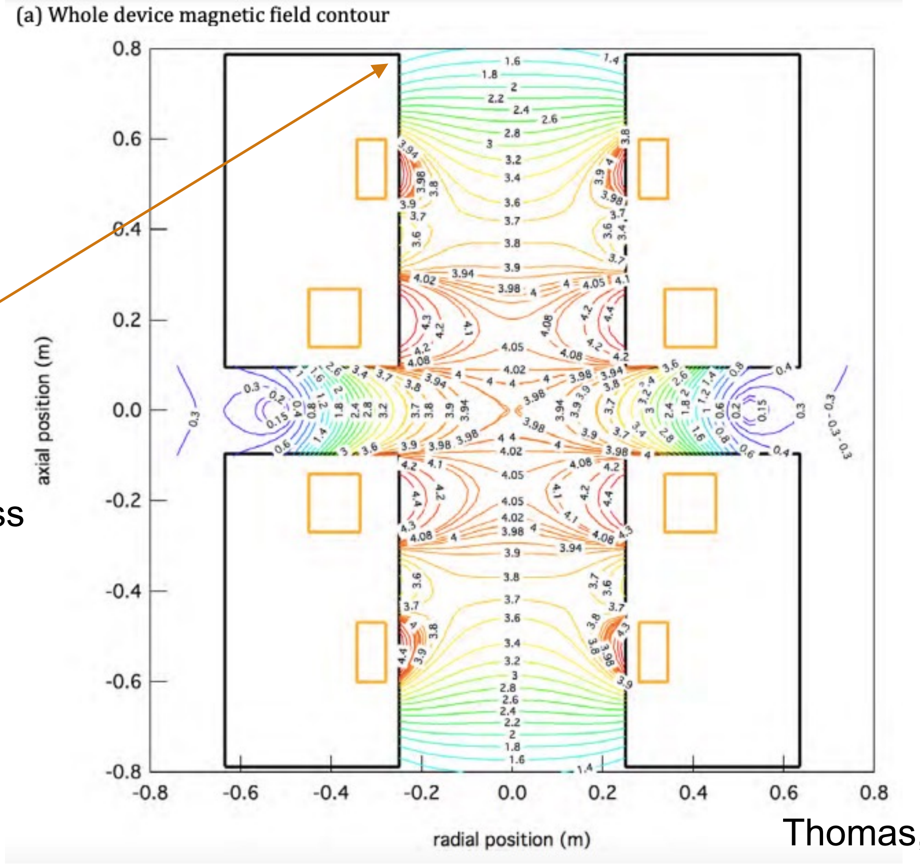

Thomas, 2018

WORKS CITED

Chaplin, Vernon. *Battery Powered RF Pre-ionization System for the Caltech Magnetohydrodynamically-Jet Experiment: RF Discharge Properties and MHD-Driven Jet Dynamics.* 2015. California Institute of Technology, PhD dissertation.

Moser, Auna. *Dynamics of magnetically driven plasma jets: An instability of an instability, gas cloud impacts, shocks, and other deformations.* 2012. California Institute of Technology, PhD dissertation.

Haw, Magnus. *Experimental and Numerical Studies of Cavities, Flows, and Waves in Arched Flux Ropes.* 2018. California Institute of Technology, PhD dissertation.

Yun, Gunsu. *Dynamics of Plasma Structures Interacting with External and Self-Generated Magnetic Fields.* 2008. California Institute of Technology, PhD dissertation.

Zhai, Xiang. *Experimental, Numerical and Analytical Studies of the MHD-driven plasma jet, instabilities and waves*. 2015. California Institute of Technology, PhD dissertation

Stensen, Eve. *Fields, Forces, and Flows: What Laboratory Experiments Reveal About the Dynamics of Arched Plasma Structures.* 2012. California Institute of Technology, PhD dissertation.

Zhang, Yang, P. Wongwaitayakornkul, and P. Bellan. "Magnetic Rayleigh-Taylor Instability in an Experiment Simulating a Solar Loop." *The Astrophysical Journal Letters,* vol. 889 no. 2, 2020, pg. L32. DOI: 10.3847/2041-8213/ab6b2d

Thomas, Edward, and Uwe Konopka. "Magnetized Dusty Plasma Experiment (MDPX) Facility Technical Summary Document." Auburn University, 2015. https://webhome.auburn.edu/~thomaed/mprl/mdpx_tech_note_v1-4_reduced.pdf

WORKS CITED

Lebedev, S.V., et. al. “Formation of Working Surfaces in Radiatively Cooled Laboratory Jets.” *Astrophysics and Space Sciences*, vol. 298, 2005, pg. 241-246. DOI: https://doi.org/10.1007/s10509-005-3941-1

Nicolov, André, and Paul Bellan. 2023, Oct. *Thermophoresis of micron-size water ice aerosols in RF-plasma afterglow.* [Poster Presentation], American Physical Society Division of Plasma Physics Annual Meeting.

Nicolov, Andre. 2023, Oct. *Growth and phase of Ice Grains Formed in a Cryogenically Cooled Plasma.* [Presentation], American Physical Society Division of Plasma Physics Annual meeting.

Tobin, Zachary. 2013, May. *Progress Update on the Crossed Flux Tube Experiment.* [Presentation], California Institute of Technology Bellan Group Meeting.

QUESTIONS?

Start

Appendix A

Appendix B

APPENDIX A

MATHEMATICAL RECITATION & COMPLETE DERIVATIONS

APPENDIX A –
PLASMA PHYSICS REFRESHER

- Major Mathematical Approaches for Examining Plasma:
  - Vlasov Theory
    - Compute dynamics of distribution function; 6-dimensional object defining particle position & momentum
  - Two-Fluid Theory
    - Treat electrons, ions, and neutrals as mixed fluid media subject to fluid & EM forces on a per-species basis
  - Magnetohydrodynamics (MHD)
    - Treat whole plasma as one fluid which is also conductive, and therefore subject to EM forces as well as fluid forces

↓ Decreasing Mathematical Complexity

APPENDIX A –
PLASMA PHYSICS REFRESHER

- Major Mathematical Approaches for Examining Plasma:
  - Vlasov Theory
    - Compute dynamics of distribution function; 6-dimensional object defining particle position & momentum
  - Two-Fluid Theory
    - Treat electrons, ions, and neutrals as mixed fluid media subject to fluid & EM forces on a per-species basis
  - Magnetohydrodynamics (MHD)
    - Treat whole plasma as one fluid which is also conductive, and therefore subject to EM forces as well as fluid forces

Decreasing Mathematical Complexity

return

APPENDIX A –
ENERGETICS OF THE KINK INSTABILITY

- Consider a cylindrical magnetofluid supporting only a surface current:

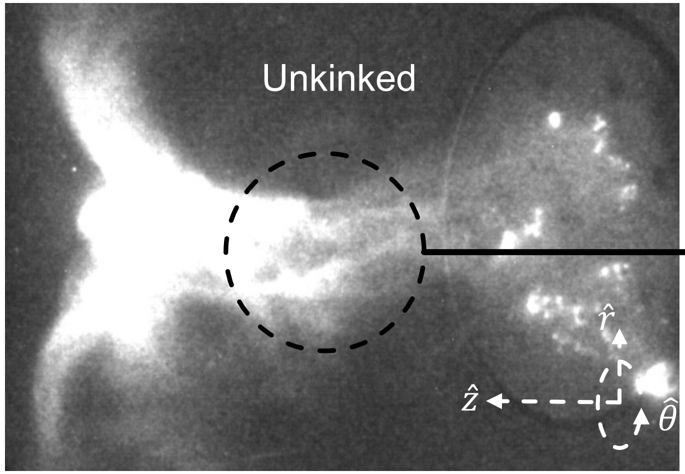

Model as azimuthally symmetric magnetofluid w/ no z-dependence

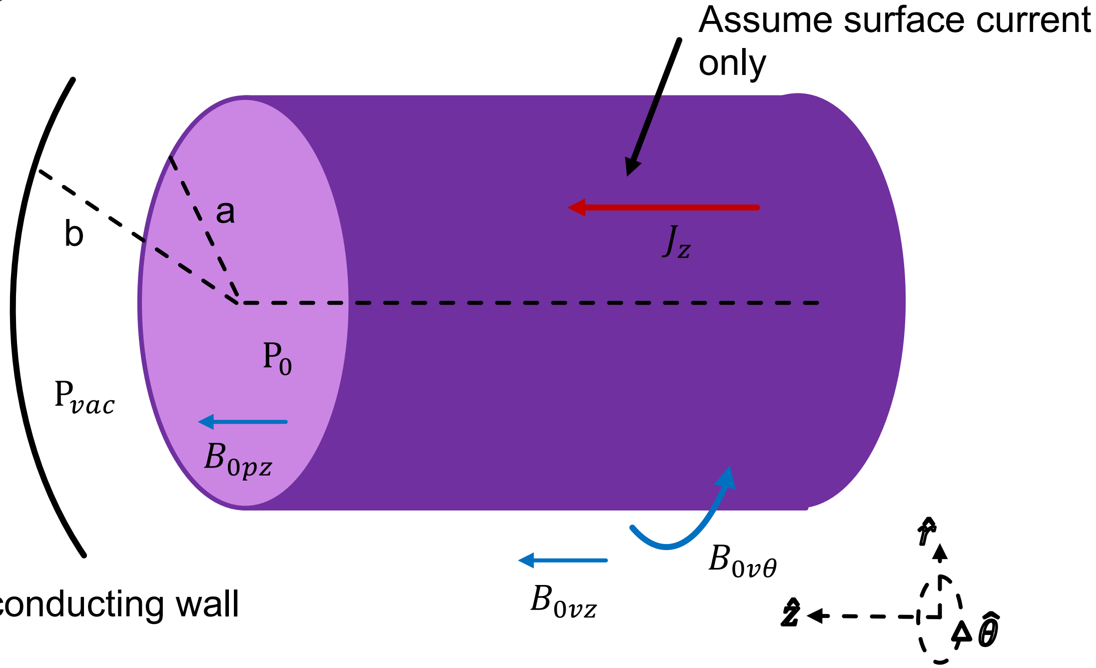

Assume MHD equilibrium state:

$$\boldsymbol{J}_0 \times \boldsymbol{B}_0 - \nabla P_0 = 0$$

return

APPENDIX A – ENERGETICS OF THE KINK INSTABILITY

- Consider a cylindrical magnetofluid supporting only a surface current:

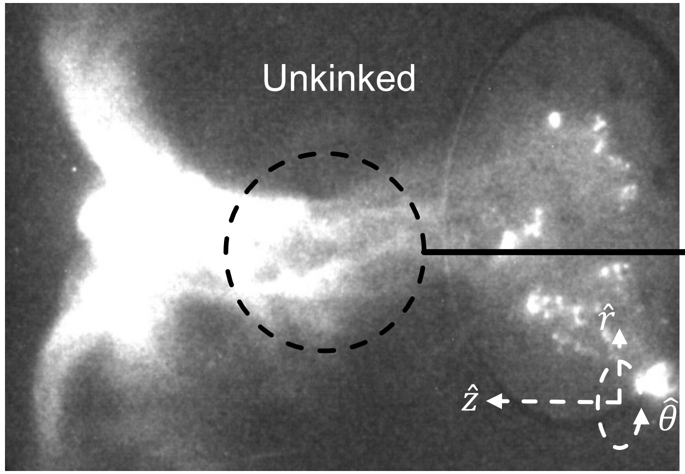

Model as azimuthally symmetric magnetofluid w/ no z-dependence

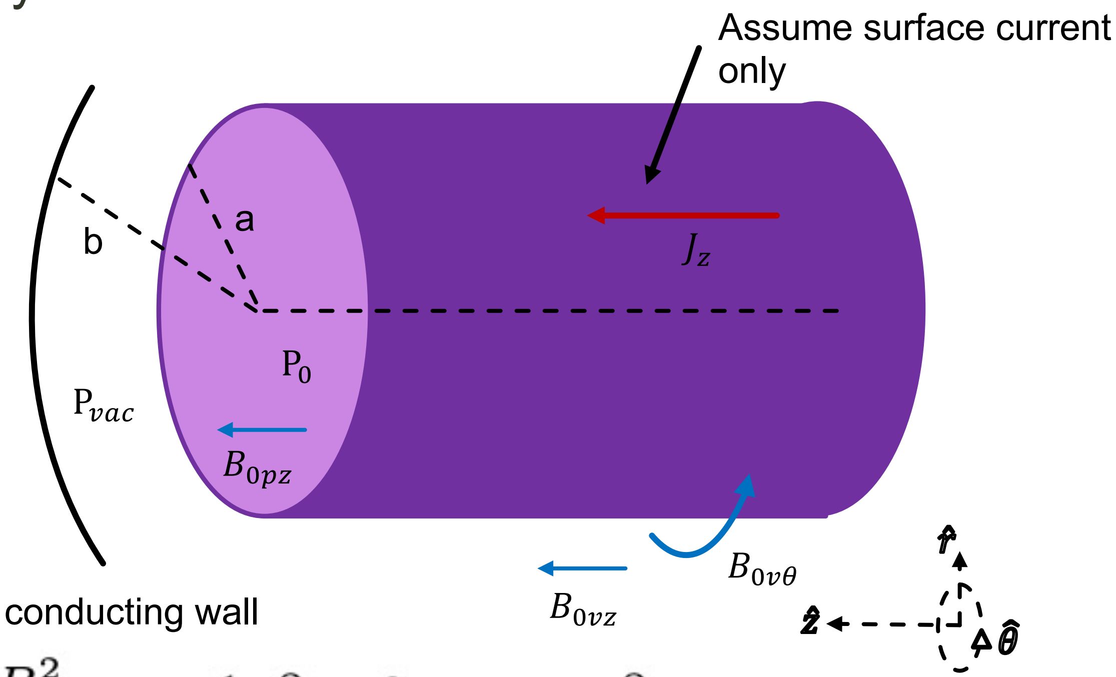

Assume MHD equilibrium state:

$$\boldsymbol{J}_0 \times \boldsymbol{B}_0 - \nabla P_0 = 0 \longrightarrow \frac{B_{0\theta}^2}{r}\hat{r} - \frac{1}{2}\frac{\partial}{\partial r}B_0^2\hat{r} - \mu_0\frac{\partial}{\partial r}P_0\hat{r} = 0$$

$$\mu_0 \boldsymbol{J}_0 \times \boldsymbol{B}_0 = (\nabla \times \boldsymbol{B}_0) \times \boldsymbol{B}_0 = -(\nabla \boldsymbol{B}_0)\cdot \boldsymbol{B}_0 + \boldsymbol{B}_0 \cdot \nabla \boldsymbol{B}_0 = -\nabla \frac{B_0^2}{2} + \boldsymbol{B}_0 \cdot \nabla \boldsymbol{B}_0$$

return

APPENDIX A – ENERGETICS OF THE KINK INSTABILITY

- Integrating EoM across surface at r=a gives stability criterion:

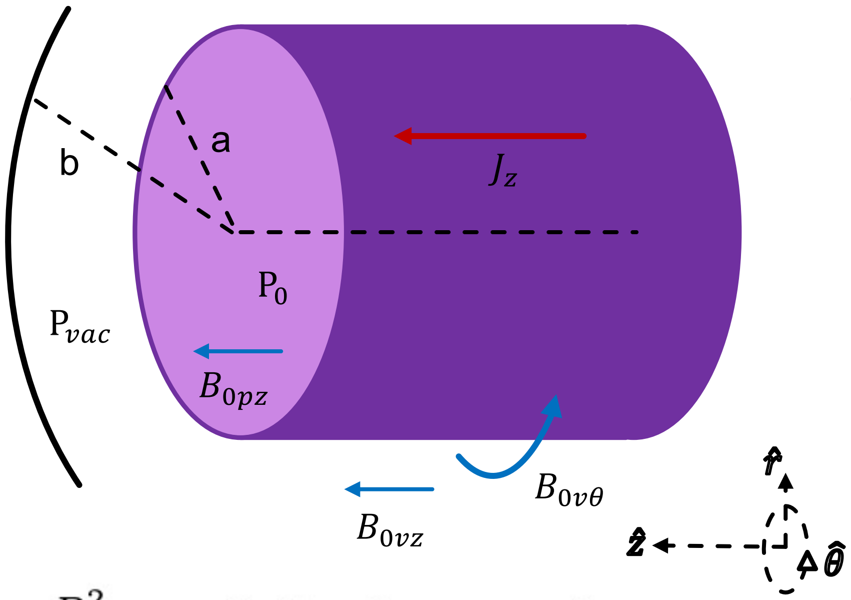

$$\frac{B_{0\theta}^2}{r}\hat{r} - \frac{1}{2}\frac{\partial}{\partial r}B_0^2\hat{r} - \mu_0\frac{\partial}{\partial r}P_0\hat{r} = 0$$

$$\int_{a^-}^{a^+}\left(\frac{B_{0\theta}^2}{r} - \frac{1}{2}\frac{\partial}{\partial r}B_0^2 - \mu_0\frac{\partial}{\partial r}P_0\right)dr = \left[\mu_0 P_0 + \frac{B_0^2}{2}\right]_{a^-}^{a^+} + \int_{a^-}^{a^+}\frac{B_{0\theta}^2}{r}dr = 0$$

0 because

$$\left(\mu_0 P_0 + \tfrac{1}{2}B_0^2\right)\Big|_{r=a^-} - \left(\mu_0 P_0 + \tfrac{1}{2}B_0^2\right)\Big|_{r=a^+} = 0$$

$$\mu_0 P_0 + \tfrac{1}{2}B_{0pz}^2 = \tfrac{1}{2}\left(B_{0vz}^2 + B_{0v\theta}^2\right)$$

Configuration only stable when magnetic pressure in vacuum = magnetic pressure + pressure in magnetofluid

return

APPENDIX A –
ENERGETICS OF THE KINK INSTABILITY

- Consider 2D positive-definite radial harmonic perturbation at magnetofluid surface:

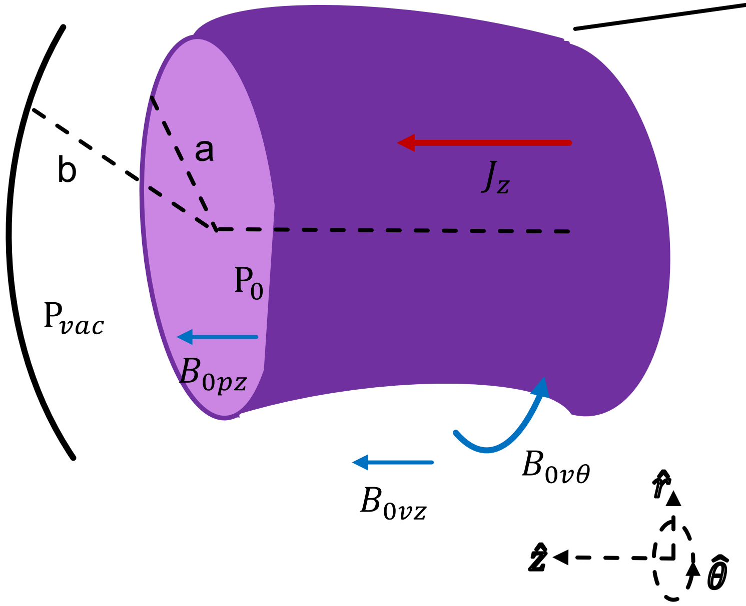

Unperturbed surface — Perturbed surface — Helical perturbation

$$S(r,\theta,z) = r - a = 0 \longrightarrow S(r,\theta,z) = r - a - \zeta e^{im\theta + ikz} = 0$$

We expect all physical fields to follow a helical perturbation as well; we linearize governing equations with this in mind

return

APPENDIX A –
ENERGETICS OF THE KINK INSTABILITY

- Consider 2D positive-definite radial harmonic perturbation at magnetofluid surface:

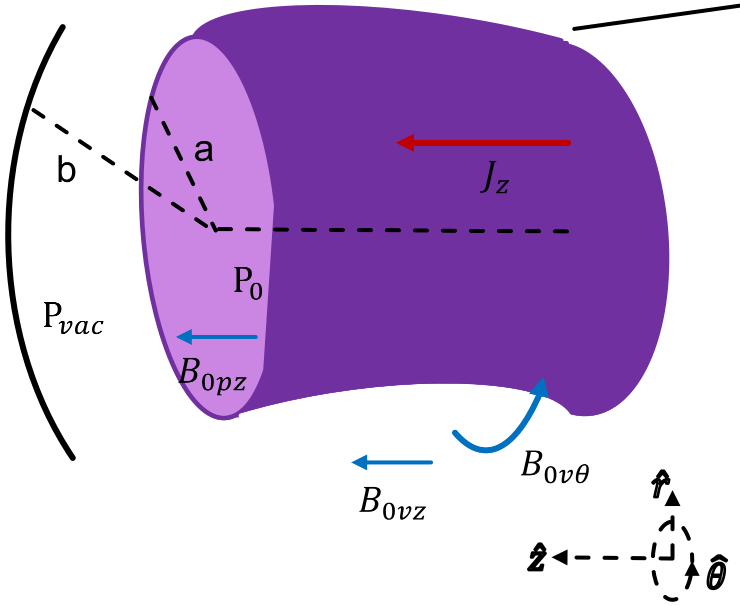

Unperturbed surface

$$S(r,\theta,z) = r - a = 0 \longrightarrow S(r,\theta,z) = r - a - \zeta e^{im\theta+ikz} = 0$$

Perturbed surface

Helical perturbation

We expect all physical fields to follow a helical perturbation as well; we linearize governing equations with this in mind

B doesn't penetrate magnetofluid surface in steady state; assume the same of perturbed B—thus, at the perturbed surface:

$$f_{ps} = f_0 + f_1 + \boldsymbol{\zeta} \cdot \nabla f_0$$

Insert pressure balance from prev. slide

$$\mu_0 P_0 + \mu_0 P_1 + \tfrac{1}{2} B_{0pz}^2 + \tfrac{1}{2} B_{0pz} B_{1pz} + \zeta \hat{r} \cdot \nabla [\mu_0 P_0 + \tfrac{1}{2} B_{0pz}^2] = \frac{B_{0v\theta}^2 + B_{0vz}^2}{2} + \frac{B_{0v\theta} B_{1v\theta} + B_{0vz} B_{1vz}}{2} + \zeta \hat{r} \cdot \nabla \frac{B_{0v}^2}{2}$$

return

APPENDIX A – ENERGETICS OF THE KINK INSTABILITY

- If external magnetic pressure exceeds internal pressure, system remains stable:

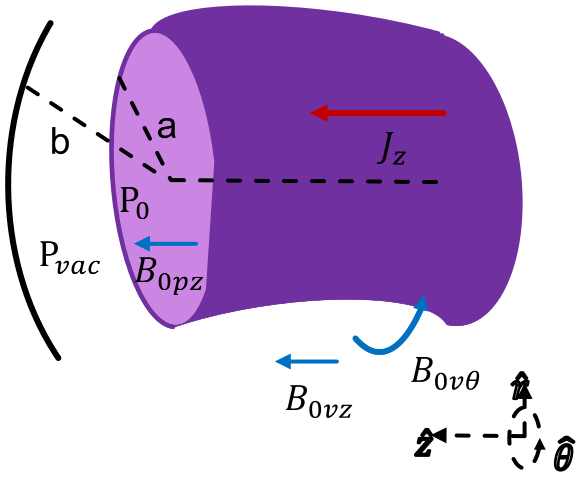

$$\mu_0 P_0 + \mu_0 P_1 + \tfrac{1}{2}B_{0pz}^2 + \tfrac{1}{2}B_{0pz}B_{1pz} + \zeta\hat{r}\cdot\nabla[\mu_0 P_0 + \tfrac{1}{2}B_{0pz}^2] = \frac{B_{0v\theta}^2 + B_{0vz}^2}{2} + \frac{B_{0v\theta}B_{1v\theta} + B_{0vz}B_{1vz}}{2} + \zeta\hat{r}\cdot\nabla\frac{B_{0v}^2}{2}$$

Equilibrium components always cancel

$$\mu_0 P_1 + \tfrac{1}{2}B_{0pz}B_{1pz} + \zeta\hat{r}\cdot\nabla[\mu_0 P_0 + \tfrac{1}{2}B_{0pz}^2] < \tfrac{1}{2}(B_{0v\theta}B_{1v\theta} + B_{0vz}B_{1vz}) + \zeta\frac{\partial}{\partial r}\frac{B_{0v}^2}{2}$$

return

APPENDIX A – ENERGETICS OF THE KINK INSTABILITY

- If external magnetic pressure exceeds internal pressure, system remains stable:

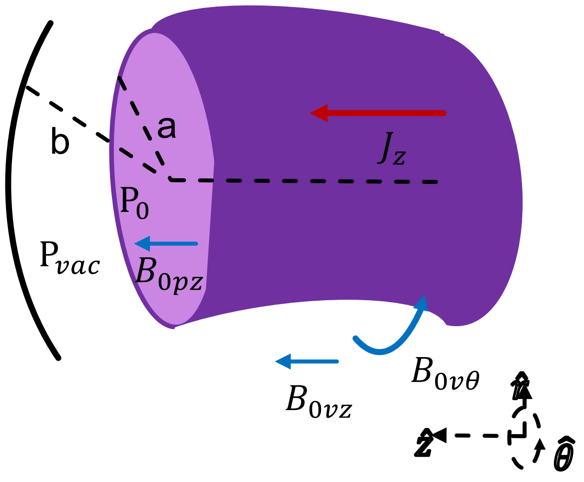

$$\mu_0 P_0 + \mu_0 P_1 + \tfrac{1}{2}B_{0pz}^2 + \tfrac{1}{2}B_{0pz}B_{1pz} + \zeta\hat{r}\cdot\nabla[\mu_0 P_0 + \tfrac{1}{2}B_{0pz}^2] = \frac{B_{0v\theta}^2 + B_{0vz}^2}{2} + \frac{B_{0v\theta}B_{1v\theta} + B_{0vz}B_{1vz}}{2} + \zeta\hat{r}\cdot\nabla\frac{B_{0v}^2}{2}$$

Equilibrium components always cancel

$$\mu_0 P_1 + \tfrac{1}{2}B_{0pz}B_{1pz} + \zeta\hat{r}\cdot\nabla[\mu_0 P_0 + \tfrac{1}{2}B_{0pz}^2] < \tfrac{1}{2}(B_{0v\theta}B_{1v\theta} + B_{0vz}B_{1vz}) + \zeta\frac{\partial}{\partial r}\frac{B_{0v}^2}{2}$$

Assume incompressibility, i.e. $\nabla\cdot\zeta = 0 \longrightarrow P_1 + \zeta\frac{\partial}{\partial r}P_0 = 0$

Further, the vacuum & plasma body carry no currents, so:

$$\frac{\partial}{\partial r}B_{0pz} = \frac{\partial}{\partial r}B_{0vz} = 0$$

$$\overline{B}_{1v\theta} + \overline{B}_{0vz}\overline{B}_{1vz} - \frac{\zeta}{r} > \overline{B}_{0pz}\overline{B}_{1pz} \longrightarrow \text{stable}$$

Where overbarred quantities are normalized to $B_{0v\theta}|_{r=a}$ and it is assumed $B_{0v\theta} \propto r^{-1}$ due to surface current J_z

return

APPENDIX A – ENERGETICS OF THE KINK INSTABILITY

- No currents exist in body of plasma or in vacuum, therefore B must be associated with a scalar potential:

$$\boldsymbol{B} = \nabla\chi$$

Laplacian yields…

From helical perturbation

$$\nabla^2\chi = \frac{\partial^2}{\partial r^2}\chi(r) + \frac{1}{r}\frac{\partial}{\partial r}\chi(r) - \left(\frac{m^2}{r} + k^2\right)\chi(r) = 0$$

2nd order elliptic PDE in cylindrical coords

For r<a:

$$\chi = \alpha \mathrm{I}_{|m|}(|k|r)$$

For a<r<b:

$$\chi = \beta_1 \mathrm{I}_{|m|}(|k|r) + \beta_2 \mathrm{K}_{|m|}(|k|r)$$

return

APPENDIX A –
ENERGETICS OF THE KINK INSTABILITY

- No currents exist in body of plasma or in vacuum, therefore B must be associated with a scalar potential:

$$\boldsymbol{B} = \nabla\chi$$

Laplacian yields…

From helical perturbation

$$\nabla^2\chi = \frac{\partial^2}{\partial r^2}\chi(r) + \frac{1}{r}\frac{\partial}{\partial r}\chi(r) - (\frac{m^2}{r} + k^2)\chi(r) = 0$$

2[nd] order elliptic PDE in cylindrical coords

For r<a:

$$\chi = \alpha \mathrm{I}_{|m|}(|k|r)$$

$$\boldsymbol{B}\cdot\nabla S \longrightarrow \boldsymbol{B}_1\cdot\nabla S_0 + \boldsymbol{B}_0\cdot\nabla S_1 = 0$$

$$\overline{B}_{1pr} - ik\overline{B}_{0pr}\zeta = 0 \;, \quad \alpha = \frac{ik\overline{B}_{0pz}\big|_{r=a}}{|k|\mathrm{I}_{|m|}(|k|a)}$$

For a<r<b:

$$\chi = \beta_1\mathrm{I}_{|m|}(|k|r) + \beta_2\mathrm{K}_{|m|}(|k|r)$$

$$\chi'\big|_{r=b} \longrightarrow 0$$

$$\beta_2 = \frac{-\beta_1\mathrm{I}'_{|m|}(|k|b)}{\mathrm{K}'_{|m|}(|k|b)}$$

return

APPENDIX A – ENERGETICS OF THE KINK INSTABILITY

For a<r<b:

$$\chi = \beta_1 \mathrm{I}_{|m|}(|k|r) + \beta_2 \mathrm{K}_{|m|}(|k|r) \xrightarrow[\boldsymbol{B}\cdot\nabla S \longrightarrow \boldsymbol{B}_1\cdot\nabla S_0 + \boldsymbol{B}_0\cdot\nabla S_1 = 0]{} \overline{\boldsymbol{B}}_{1vr} - i(\frac{m}{r} + k\overline{B}_{0vr})\zeta = 0$$

$$\overline{B}_{1vr} = \frac{|k|\beta_1}{\mathrm{K}'_{|m|}(|k|b)}[\mathrm{I}'_{|m|}\mathrm{K}'_{|m|}(|k|b) - \mathrm{I}'_{|m|}(|k|b)\mathrm{I}'_{|m|}]$$

$$\beta_1 = \frac{i(\frac{m}{a} + k\overline{B}_{0vz}\Big|_{r=a})}{|k|[\mathrm{I}'_{|m|}(|k|a)\mathrm{K}'_{|m|}(|k|b)) - \mathrm{I}'_{|m|}(|k|b)\mathrm{K}'_{|m|}(|k|a)]}$$

return

APPENDIX A – ENERGETICS OF THE KINK INSTABILITY

- Inserting potential field solutions into stability criterion results in a huge mess which we can simplify by assuming 1 free-boundary & small normalized axial wavelength:

$$|k|a[1+\overline{B}_{0vz}^{2}-P_0]\frac{\mathrm{I}_{|m|}(a)}{\mathrm{I}'_{|m|}(a)}+\frac{(m+ka\overline{B}_{0vz}\big|_{r=a})^2}{|k|a}\frac{\mathrm{I}'_{|m|}(|k|b)\mathrm{K}_{|m|}(|k|a))-\mathrm{I}_{|m|}(|k|a)\mathrm{K}'_{|m|}(|k|b)}{\mathrm{I}'_{|m|}(|k|a)\mathrm{K}'_{|m|}(|k|b))-\mathrm{I}'_{|m|}(|k|b)\mathrm{K}'_{|m|}(|k|a)} > 1 \longrightarrow \text{stable}$$

return

APPENDIX A – ENERGETICS OF THE KINK INSTABILITY

- Inserting potential field solutions into stability criterion results in a huge mess which we can simplify by assuming 1 free-boundary & small normalized axial wavelength:

$$|k|a[1+\overline{B}_{0vz}^2-P_0]\frac{\mathrm{I}_{|m|}(a)}{\mathrm{I}'_{|m|}(a)}+\frac{\left(m+ka\overline{B}_{0vz}\Big|_{r=a}\right)^2}{|k|a}\frac{\mathrm{I}'_{|m|}(|k|b)\mathrm{K}_{|m|}(|k|a))-\mathrm{I}_{|m|}(|k|a)\mathrm{K}'_{|m|}(|k|b)}{\mathrm{I}'_{|m|}(|k|a)\mathrm{K}'_{|m|}(|k|b))-\mathrm{I}'_{|m|}(|k|b)\mathrm{K}'_{|m|}(|k|a)} > 1 \longrightarrow \text{stable}$$

Let $b \to \infty$…

$$|k|a[1+\overline{B}_{0vz}^2-P_0]\frac{\mathrm{I}_{|m|}(a)}{\mathrm{I}'_{|m|}(a)}+\frac{\left(m+ka\overline{B}_{0vz}\Big|_{r=a}\right)^2}{|k|a}\frac{\mathrm{K}_{|m|}(|k|a))}{\mathrm{K}'_{|m|}(|k|a)} > 1 \longrightarrow \text{stable}$$

return

APPENDIX A –
ENERGETICS OF THE KINK INSTABILITY

- Inserting potential field solutions into stability criterion results in a huge mess which we can simplify by assuming 1 free-boundary & small normalized axial wavelength:

$$|k|a[1+\overline{B}_{0vz}^2-P_0]\frac{\mathrm{I}_{|m|}(a)}{\mathrm{I}'_{|m|}(a)}+\frac{(m+ka\overline{B}_{0vz}\big|_{r=a})^2}{|k|a}\frac{\mathrm{I}'_{|m|}(|k|b)\mathrm{K}_{|m|}(|k|a))-\mathrm{I}_{|m|}(|k|a)\mathrm{K}'_{|m|}(|k|b)}{\mathrm{I}'_{|m|}(|k|a)\mathrm{K}'_{|m|}(|k|b))-\mathrm{I}'_{|m|}(|k|b)\mathrm{K}'_{|m|}(|k|a)} > 1 \longrightarrow \text{stable}$$

↓ Let $b \to \infty$…

$$|k|a[1+\overline{B}_{0vz}^2-P_0]\frac{\mathrm{I}_{|m|}(a)}{\mathrm{I}'_{|m|}(a)}+\frac{(m+ka\overline{B}_{0vz}\big|_{r=a})^2}{|k|a}\frac{\mathrm{K}_{|m|}(|k|a))}{\mathrm{K}'_{|m|}(|k|a)} > 1 \longrightarrow \text{stable}$$

↓ Assume $|k|a \ll 1$

$$\begin{cases} \mathrm{I}_m(s) \approx \frac{1}{|m|!}(\frac{s}{2})^{|m|} & \text{for small s} \\ \mathrm{K}_m(s) \approx \frac{|m-1|!}{2}(\frac{s}{2})^{-|m|} & \text{for small s} \end{cases}$$

$$|k|a[1+\overline{B}_{0vz}^2-P_0]+\frac{(m+ka\overline{B}_{0vz})^2}{|k|a} > |m|$$

return

APPENDIX A –
ENERGETICS OF THE KINK INSTABILITY

- We now find the general form of the Kruskal-Shafranov condition:

$$|k|a[1+\overline{B}_{0vz}^2 - P_0] + \frac{(m+ka\overline{B}_{0vz})^2}{|k|a} > |m|$$

$$x^2 + (m+x)^2 > |m| \quad \text{where } x = ka\overline{B}_{0vz}$$

Unstable if $\begin{cases} x > \frac{1}{2}(|m| + \sqrt{2|m| - m^2}) \\ x < \frac{1}{2}(|m| - \sqrt{2|m| - m^2}) \end{cases}$

Two roots for $m = -1 \rightarrow x > 1$ stable region
One root for $m = -2 \rightarrow x > 1$ stable region
no roots for $m \leq -3 \rightarrow$ no unstable region

return

APPENDIX A – ENERGETICS OF THE KINK INSTABILITY

- With m=-1, we arrive at the same condition from before!
  - If not satisfied, plasma is susceptible to helical surface instability → kinking

$$x^2 + (m+x)^2 > |m| \quad \text{where } x = ka\overline{B}_{0vz}$$

$$\downarrow \; m = -1$$

$$x > 1$$

$$\boxed{\frac{2\pi a}{L}\frac{B_{0z}}{B_{0\theta}} > 1}$$

For an axial wavelength spanning the length of the magnetofluid column

m=-1 mode induces kink

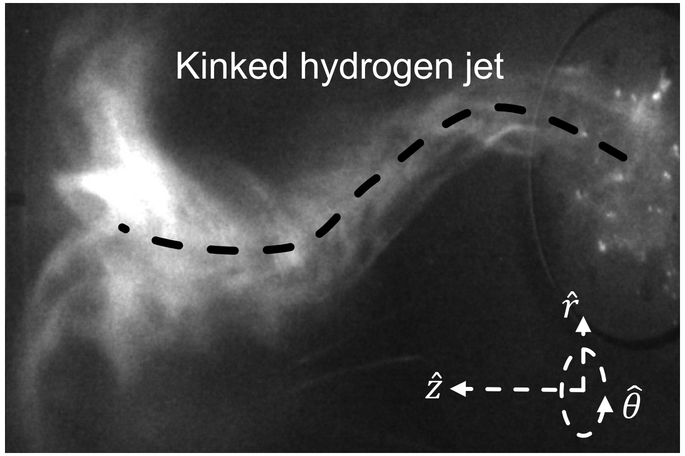

$$S(r,\theta,z) = r - a - \zeta e^{im\theta + ikz} = 0$$

return

APPENDIX A –
ENERGETICS OF THE KINK INSTABILITY

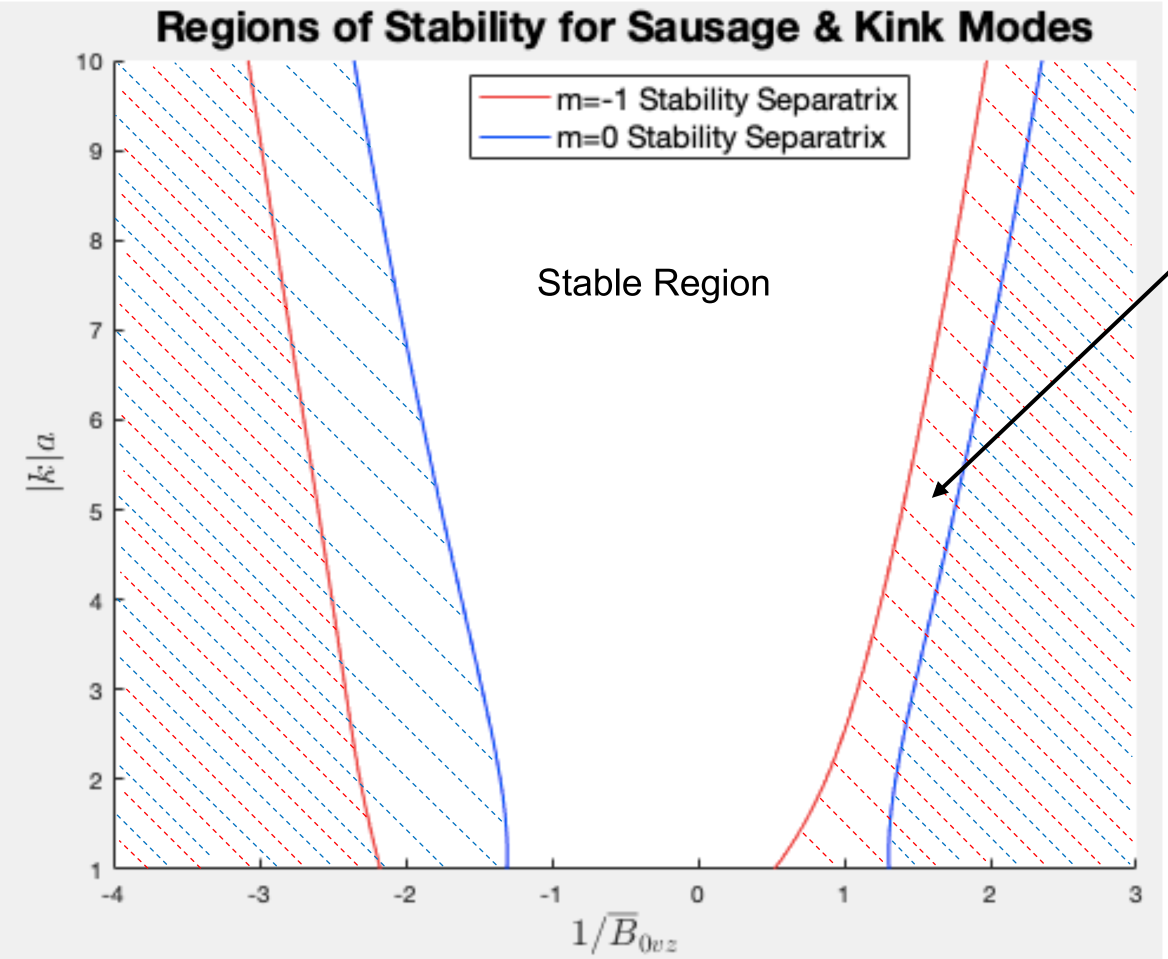

Easier to excite m=-1 mode because it has a larger unstable region for positive B_z; kink more probable than sausage

return

APPENDIX A – ENERGETICS OF THE KINK INSTABILITY

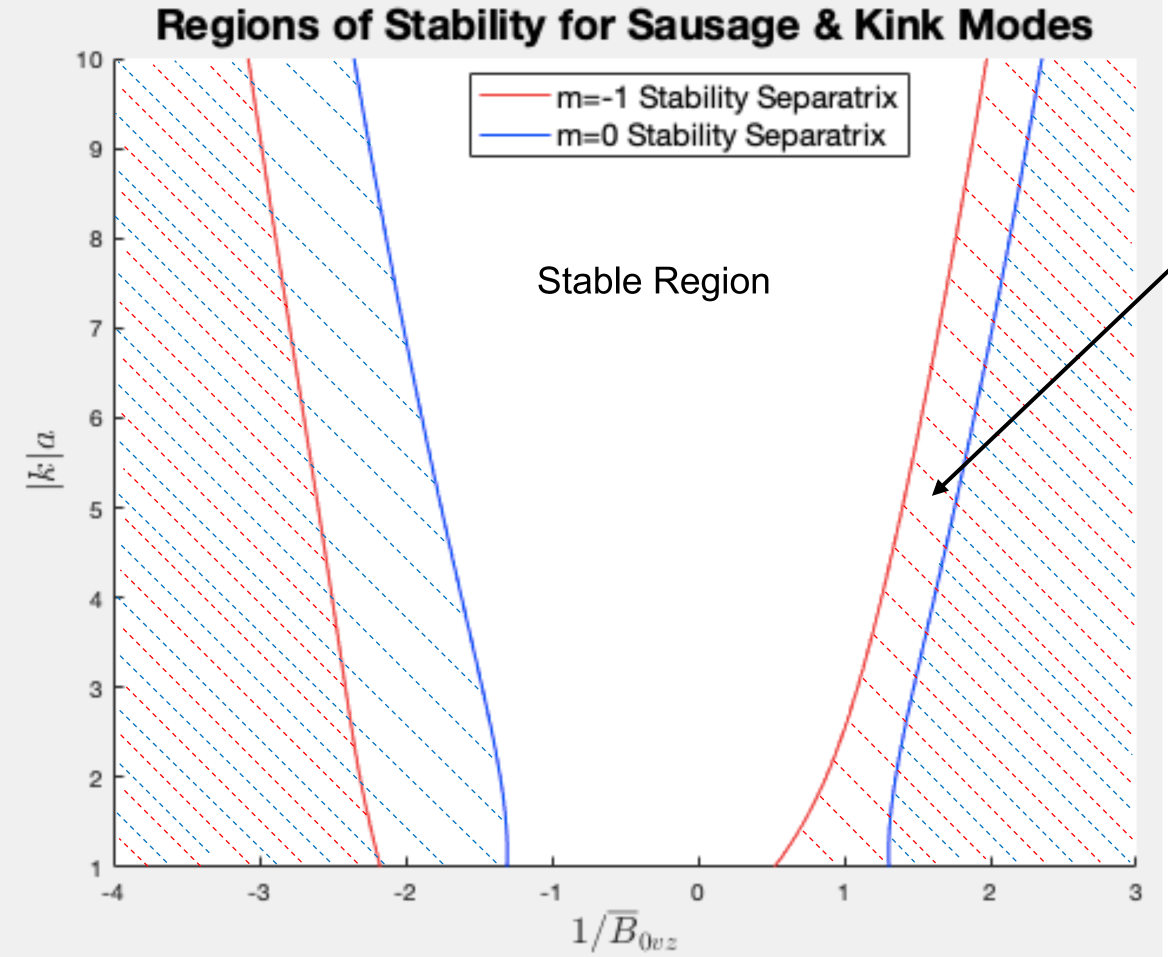

Easier to excite m=-1 mode because it has a larger unstable region for positive B_z; kink more probable than sausage

m=-2 modes have also been previously observed in the jet

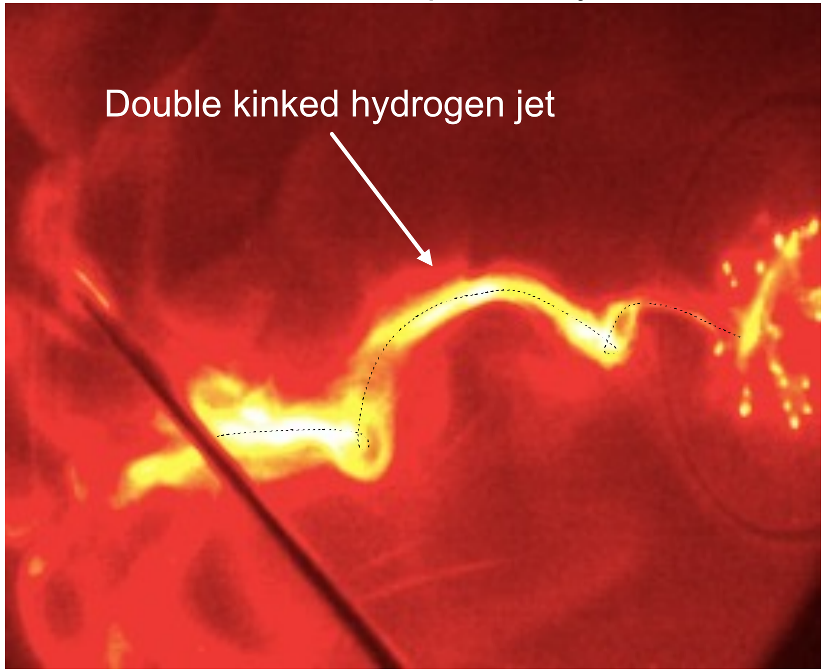

Moser, 2012

return

APPENDIX A – SIMPLE MODEL OF THE RAYLEIGH-TAYLOR INSTABILITY

- The Rayleigh-Taylor Instability is most easily assessed in incompressible, inviscid fluid atop low-density fluid or vacuum:

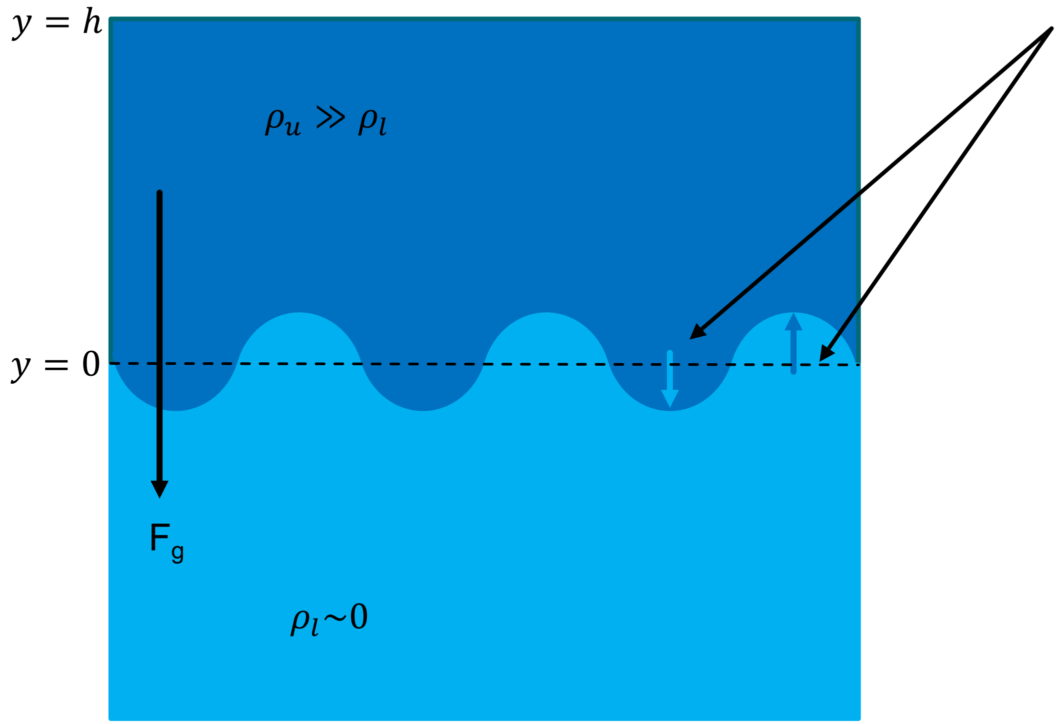

Small perturbations in fluid interface result in $\frac{\delta W_u}{V} = -2\rho_u g \Delta h$ for upper fluid, $\frac{\delta W_l}{V} = 2\rho_l g \Delta h$ for upper fluid

$\therefore$ total energy change is $\frac{\delta W}{V} = 2(\rho_l - \rho_u) g \Delta h < 0$, thus interchange is energetically favorable

return

APPENDIX A – SIMPLE MODEL OF THE RAYLEIGH-TAYLOR INSTABILITY

- The Rayleigh-Taylor Instability is most easily assessed in incompressible, inviscid fluid atop low-density fluid or vacuum:

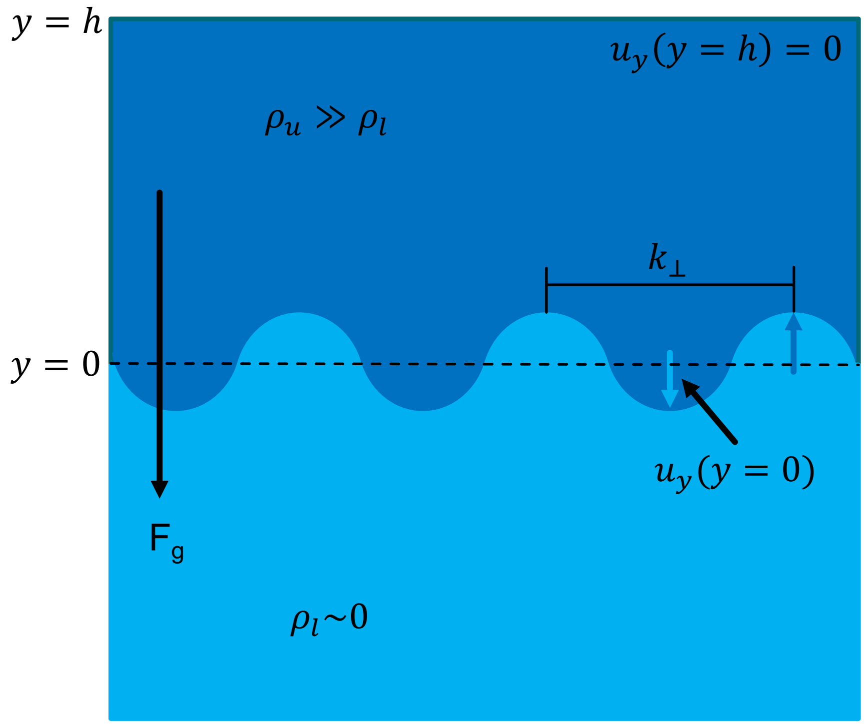

Assume a perturbation of the form:

$$\boldsymbol{u}_1 = \boldsymbol{u}_1(y)e^{\gamma t + i\boldsymbol{k}\cdot\boldsymbol{x}}$$

return

APPENDIX A – SIMPLE MODEL OF THE RAYLEIGH-TAYLOR INSTABILITY

- The Rayleigh-Taylor Instability is most easily assessed in incompressible, inviscid fluid atop low-density fluid or vacuum:

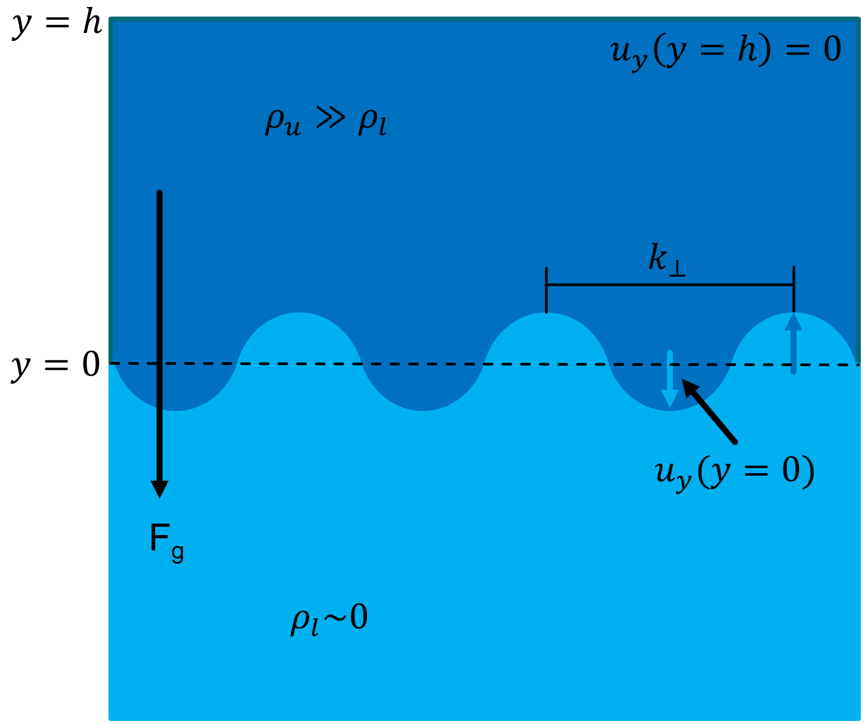

Assume a perturbation of the form:

$$\boldsymbol{u}_1 = \boldsymbol{u}_1(y) e^{\gamma t + i\boldsymbol{k}\cdot\boldsymbol{x}}$$

Linearized equation of motion & continuity equation become:

$$\frac{\partial \rho}{\partial t} + \nabla \cdot (\rho \boldsymbol{u}) \longrightarrow \frac{\partial \rho_1}{\partial t} + \boldsymbol{u}_1 \cdot \nabla \rho_0 = 0$$

$$\rho(\frac{\partial}{\partial t}\boldsymbol{u} + \boldsymbol{u} \cdot \nabla \boldsymbol{u}) = -\nabla P - \rho g \hat{y} \longrightarrow \rho_0 \frac{\partial}{\partial t}\boldsymbol{u}_1 = -\nabla P_1 - \rho_1 g \hat{y}$$

return

APPENDIX A – SIMPLE MODEL OF THE RAYLEIGH-TAYLOR INSTABILITY

- The Rayleigh-Taylor Instability is most easily assessed in incompressible, inviscid fluid atop low-density fluid or vacuum:

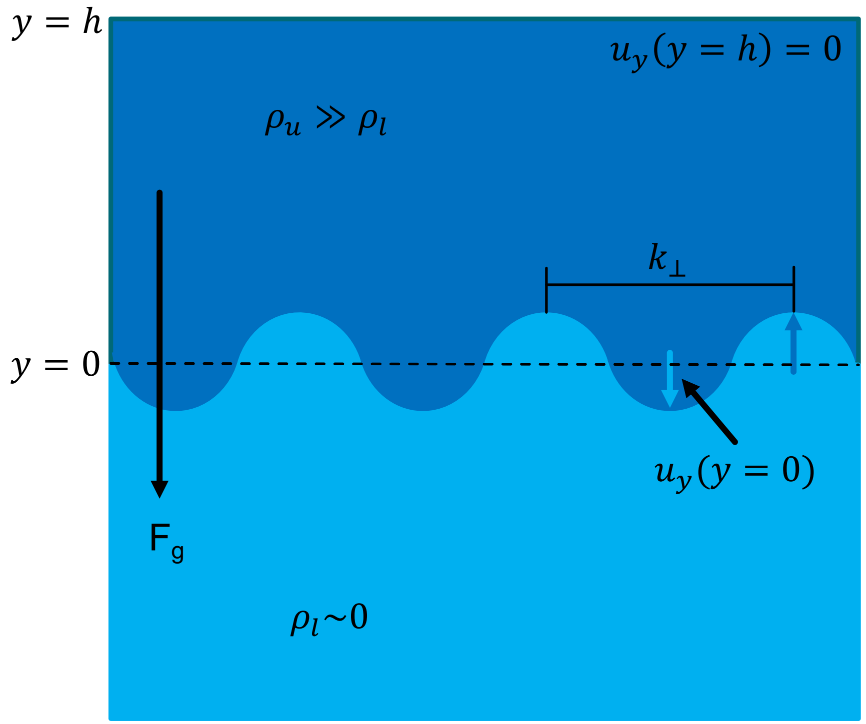

Assume a perturbation of the form:

$$\boldsymbol{u}_1 = \boldsymbol{u}_1(y) e^{\gamma t + i\boldsymbol{k}\cdot\boldsymbol{x}}$$

Linearized equation of motion & continuity equation become:

$$\frac{\partial \rho}{\partial t} + \nabla \cdot (\rho \boldsymbol{u}) \longrightarrow \frac{\partial \rho_1}{\partial t} + \boldsymbol{u}_1 \cdot \nabla \rho_0 = 0$$

$$\rho(\frac{\partial}{\partial t}\boldsymbol{u} + \boldsymbol{u} \cdot \nabla \boldsymbol{u}) = -\nabla P - \rho g \hat{y} \longrightarrow \rho_0 \frac{\partial}{\partial t}\boldsymbol{u}_1 = -\nabla P_1 - \rho_1 g \hat{y}$$

$$\nabla \cdot \boldsymbol{u}_1 = \frac{\partial u_{1y}}{\partial y} + i\boldsymbol{k} \cdot \boldsymbol{u}_{1\perp} = 0$$

Incompressibility condition

return

APPENDIX A – SIMPLE MODEL OF THE RAYLEIGH-TAYLOR INSTABILITY

- Governing equations of wavelike perturbation come from linearized EoM:

$$\rho_0 \frac{\partial}{\partial t} \boldsymbol{u}_1 = -\nabla P_1 - \rho_1 g \hat{y}$$

Insert $\boldsymbol{u}_1 = \boldsymbol{u}_1(y) e^{\gamma t + i\boldsymbol{k}\cdot\boldsymbol{x}}$

$$\gamma \rho_0 (u_{1y}\hat{y} + \boldsymbol{u}_{1\perp}) = -\frac{\partial}{\partial y} P_1 \hat{y} - i\boldsymbol{k} P_1 - \rho_1 g \hat{y}$$

return

APPENDIX A – SIMPLE MODEL OF THE RAYLEIGH-TAYLOR INSTABILITY

- Governing equations of wavelike perturbation come from linearized EoM:

$$\rho_0 \frac{\partial}{\partial t} \boldsymbol{u}_1 = -\nabla P_1 - \rho_1 g \hat{y}$$

Insert $\boldsymbol{u}_1 = \boldsymbol{u}_1(y) e^{\gamma t + i\boldsymbol{k}\cdot\boldsymbol{x}}$

$$\gamma \rho_0 (u_{1y} \hat{y} + \boldsymbol{u}_{1\perp}) = -\frac{\partial}{\partial y} P_1 \hat{y} - i\boldsymbol{k} P_1 - \rho_1 g \hat{y}$$

Perpendicular direction:

$$\gamma \rho_0 \boldsymbol{u}_{1\perp} = -i\boldsymbol{k} P_1 \xrightarrow[\text{incompressibility cond.}]{\text{Dot with } ik\text{, assert}} \gamma \rho_0 \frac{\partial}{\partial y} u_{1y} = -k^2 P_1$$

Parallel direction:

Assume density also goes as as $e^{\gamma t + i\boldsymbol{k}\cdot\boldsymbol{x}}$: $\frac{\partial \rho_1}{\partial t} + \boldsymbol{u}_1 \cdot \nabla \rho_0 = 0 \longrightarrow \gamma \rho_1 = -u_{1y} \frac{\partial}{\partial y} \rho_0$

return

APPENDIX A – SIMPLE MODEL OF THE RAYLEIGH-TAYLOR INSTABILITY

- Definitions of ρ_1 and P_1 allows us to pull an ODE out of the EoM:

$$\gamma\rho_0 u_{1y} = -\frac{\partial}{\partial y}P_1 - \rho_1 g \longrightarrow \frac{\partial}{\partial y}[\gamma^2\rho_0\frac{\partial u_{1y}}{\partial y}] = [\gamma^2\rho_0 - g\frac{\partial rho_0}{\partial y}]k^2 u_{1y}$$

Inside the upper fluid $\frac{\partial\rho_0}{\partial y} = 0, \rho_0 = const$:

$$\frac{\partial^2}{\partial y^2}u_{1y} = k^2 u_{1y} \longrightarrow u_{1y} = A\sinh(k(y-h))$$

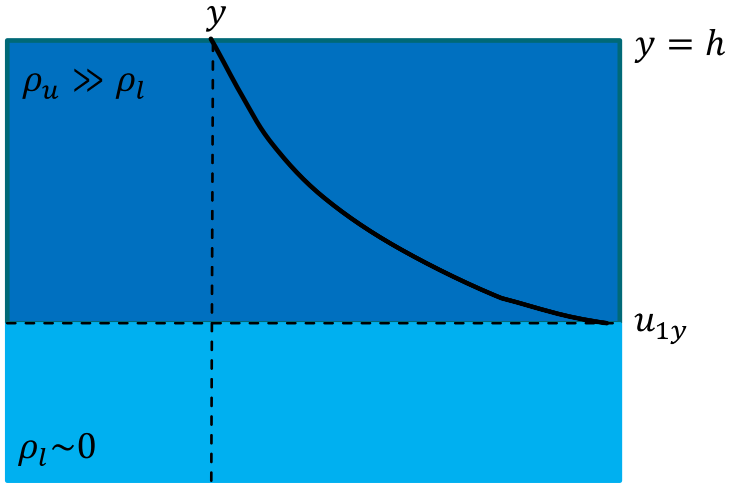

return

APPENDIX A – SIMPLE MODEL OF THE RAYLEIGH-TAYLOR INSTABILITY

At fluid interface:

$$\int_{0_-}^{0_+} \frac{\partial}{\partial y}[\gamma^2 \rho_0 \frac{\partial u_{1y}}{\partial y}]dy = \int_{0_-}^{0_+} [\gamma^2 \rho_0 - g\frac{\partial \rho_0}{\partial y}]k^2 u_{1y} dy$$

Integration by parts

$$\gamma^2 \rho_0 \frac{\partial u_{1y}}{\partial y}\Big|_{0_-}^{0_+} = -gk^2 \rho_0 u_{1y}\Big|_{0_-}^{0_+} + \int_{0_-}^{0_+} [\gamma^2 k^2 \rho_0 u_{1y} - gk^2 \rho_0 \frac{\partial u_{1y}}{\partial y}]dy$$

return

APPENDIX A – SIMPLE MODEL OF THE RAYLEIGH-TAYLOR INSTABILITY

At fluid interface:

$$\int_{0_-}^{0_+} \frac{\partial}{\partial y}[\gamma^2 \rho_0 \frac{\partial u_{1y}}{\partial y}]dy = \int_{0_-}^{0_+} [\gamma^2 \rho_0 - g\frac{\partial \rho_0}{\partial y}]k^2 u_{1y} dy$$

Integration by parts

$$\gamma^2 \rho_0 \frac{\partial u_{1y}}{\partial y}\Big|_{0_-}^{0_+} = -gk^2 \rho_0 u_{1y}\Big|_{0_-}^{0_+} + \int_{0_-}^{0_+} [\gamma^2 k^2 \rho_0 u_{1y} - gk^2 \rho_0 \frac{\partial u_{1y}}{\partial y}]dy$$

0 because u_{1y} continuous at $y = 0$

return

APPENDIX A – SIMPLE MODEL OF THE RAYLEIGH-TAYLOR INSTABILITY

At fluid interface:

$$\int_{0_-}^{0_+} \frac{\partial}{\partial y}[\gamma^2 \rho_0 \frac{\partial u_{1y}}{\partial y}]dy = \int_{0_-}^{0_+} [\gamma^2 \rho_0 - g\frac{\partial \rho_0}{\partial y}]k^2 u_{1y} dy$$

Integration by parts

$$\gamma^2 \rho_0 \frac{\partial u_{1y}}{\partial y}\Big|_{0_-}^{0_+} = -gk^2 \rho_0 u_{1y}\Big|_{0_-}^{0_+} + \int_{0_-}^{0_+} [\gamma^2 k^2 \rho_0 u_{1y} - gk^2 \rho_0 \frac{\partial u_{1y}}{\partial y}]dy$$

0 because u_{1y} continuous at $y = 0$

Insert $u_{1y} = A\sinh(k(y-h))$

$$\gamma^2 \frac{\partial u_{1y}}{\partial y} = -gk^2 u_{1y}$$

$$\gamma^2 k\cosh(k(y-h)) = -gk^2 \sinh(k(y-h))$$

return

APPENDIX A – SIMPLE MODEL OF THE RAYLEIGH-TAYLOR INSTABILITY

- With a functional description, a growth rate can be established!

$$\gamma^2 = -kg\tanh(k(y-h)) \longrightarrow \boxed{\gamma^2 = -kg\tanh(kh)}$$

return

APPENDIX A – SIMPLE MODEL OF THE RAYLEIGH-TAYLOR INSTABILITY

- With a functional description, a growth rate can be established!

$$\gamma^2 = -kg\tanh(k(y-h)) \longrightarrow \boxed{\gamma^2 = -kg\tanh(kh)}$$

- In a real fluid, surface tension opposes the force of gravity:

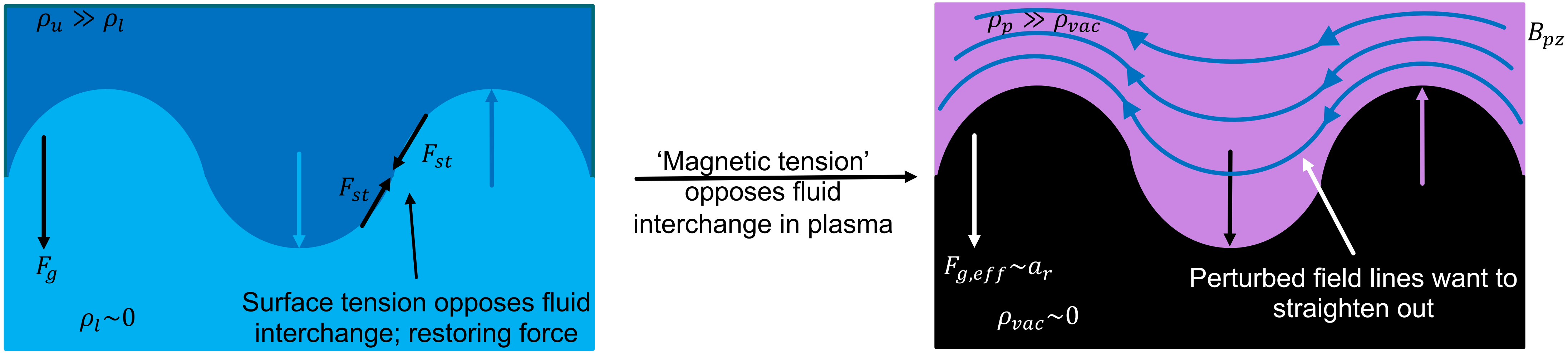

In frame of moving plasma, radial acceleration becomes an effective gravity

return

APPENDIX A – SIMPLE MODEL OF THE RAYLEIGH-TAYLOR INSTABILITY

- Pretty picture of the RTI at cosmic scales:

NASA image of the crab nebula

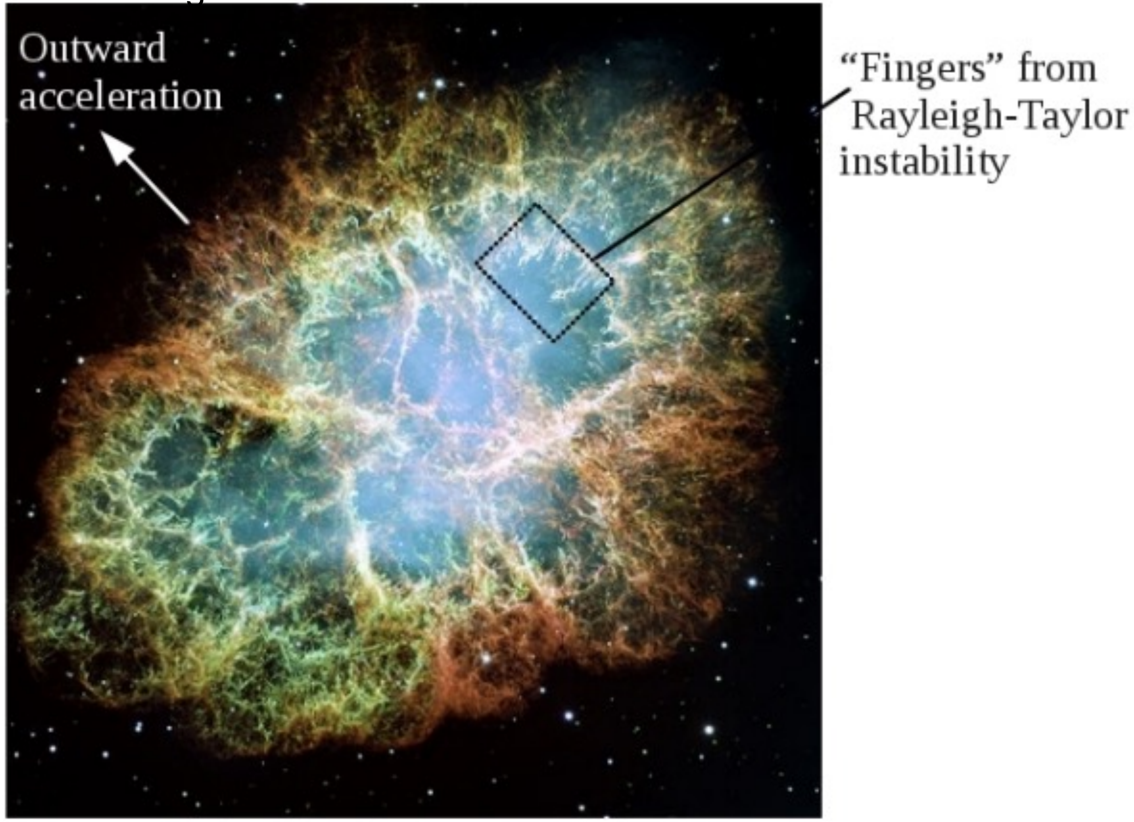

Moser, 2012

return

APPENDIX B

EXPERIMENTAL DESIGN & PREVIOUS WORK

APPENDIX B –
JET EXPERIMENT SEQUENCE

- Neutral gas is injected via injection ports
  - Background magnetic field is applied by energizing circular field coil, ~1mWb typ.
  - Gas breaks down when voltage is applied across electrodes, ~5kV typ.

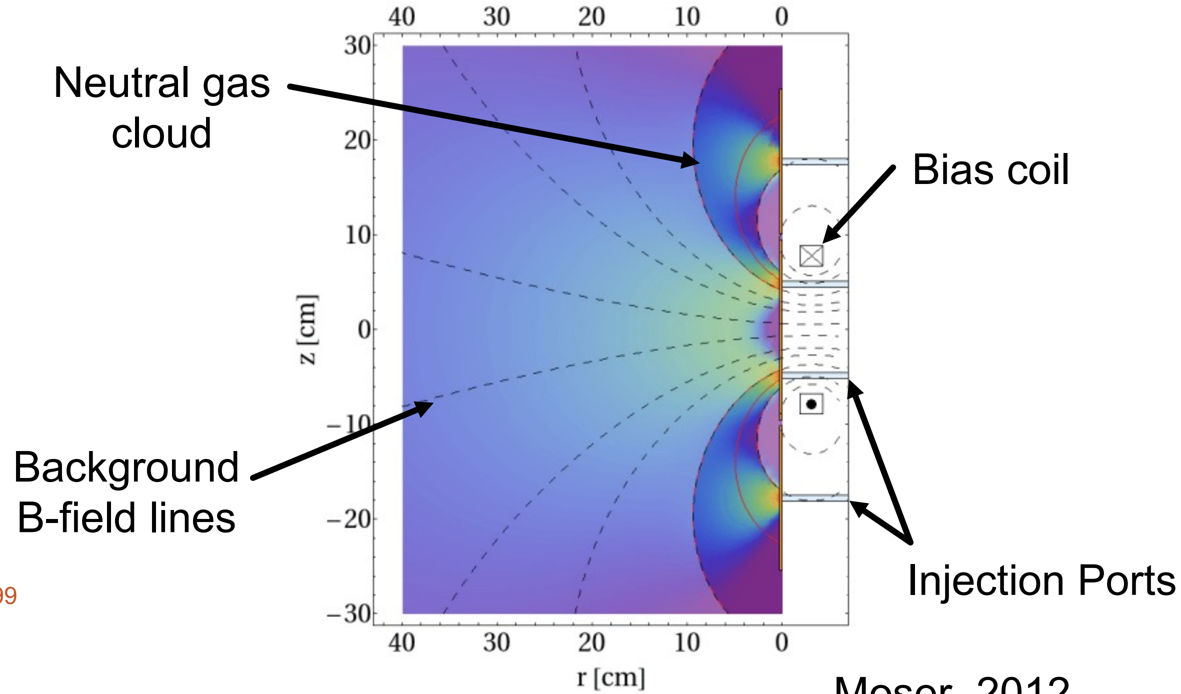

Moser, 2012

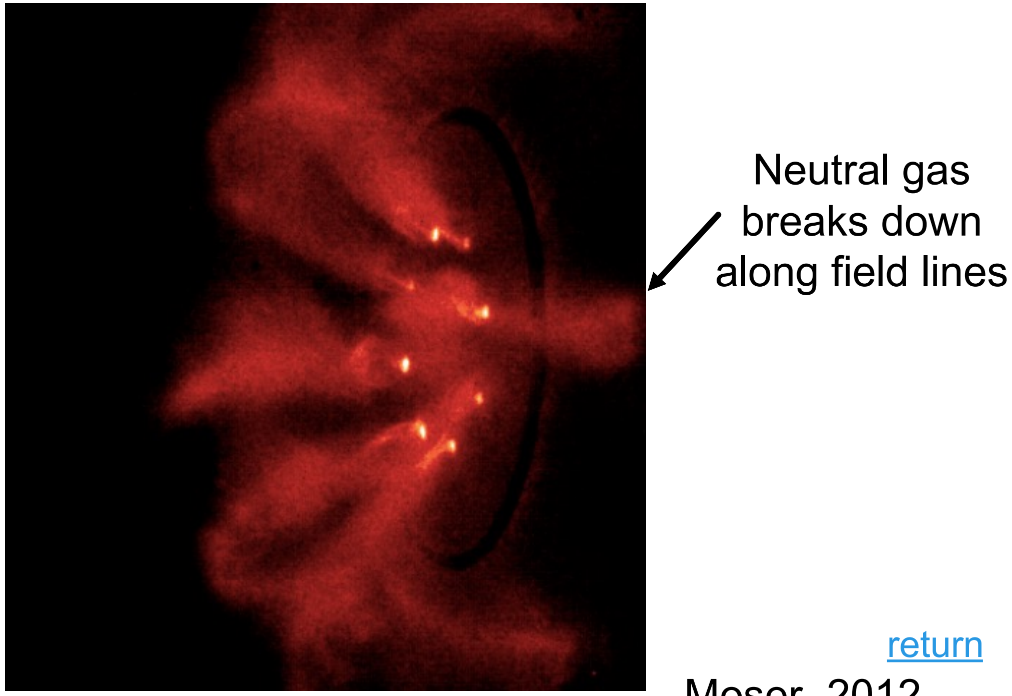

Moser, 2012

[return](#)

APPENDIX B – JET EXPERIMENT SEQUENCE

- How do particles get energized enough to produce suprathermal X-rays?
  - The Caltech Jet Experiment produces *X-rays exceeding the average thermal energy of particles by ~3000 times,* averaging ~6-7keV
  - Indicates transition from MHD-driven behavior to non-MHD-driven behavior

A. Create Plasma

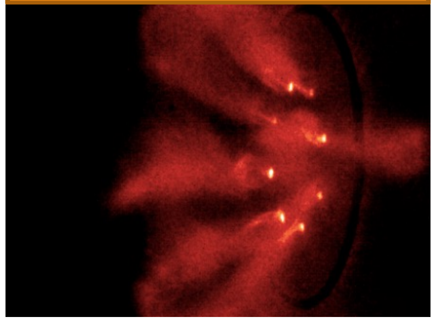

Moser, 2012

return

APPENDIX B –
JET EXPERIMENT SEQUENCE

- <u>How do particles get energized enough to produce suprathermal X-rays?</u>
  - The Caltech Jet Experiment produces *X-rays exceeding the average thermal energy of particles by ~3000 times,* averaging ~6-7keV
  - Indicates transition from MHD-driven behavior to non-MHD-driven behavior

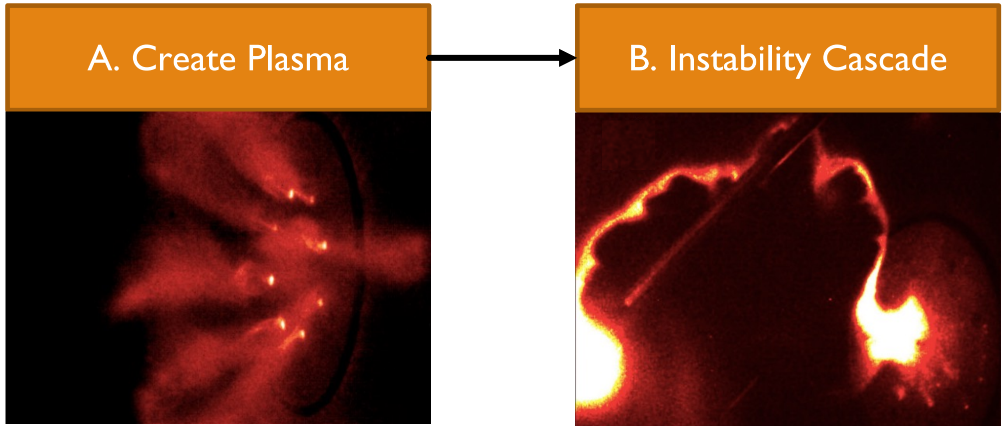

Moser, 2012

Moser, 2012

return

APPENDIX B – JET EXPERIMENT SEQUENCE

- How do particles get energized enough to produce suprathermal X-rays?
  - The Caltech Jet Experiment produces *X-rays exceeding the average thermal energy of particles by ~3000 times,* averaging ~6-7keV
  - Indicates transition from MHD-driven behavior to non-MHD-driven behavior

A. Create Plasma → B. Instability Cascade → C. Plasma Particles are heated

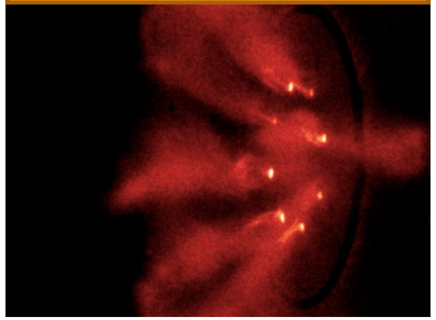

Moser, 2012

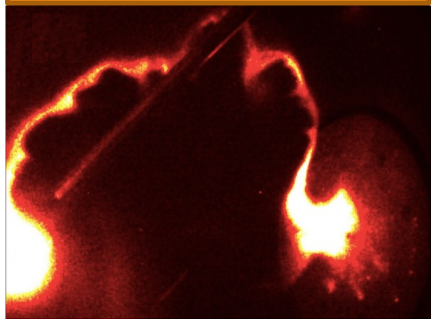

Moser, 2012

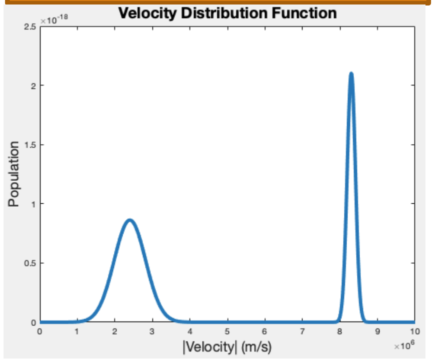

return

APPENDIX B –
JET EXPERIMENT SEQUENCE

- <u>How do particles get energized enough to produce suprathermal X-rays?</u>
  - The Caltech Jet Experiment produces *X-rays exceeding the average thermal energy of particles by ~3000 times,* averaging ~6-7keV
  - Indicates transition from MHD-driven behavior to non-MHD-driven behavior

A. Create Plasma → B. Instability Cascade → C. Plasma Particles are heated → D. Heated Particles create X-rays

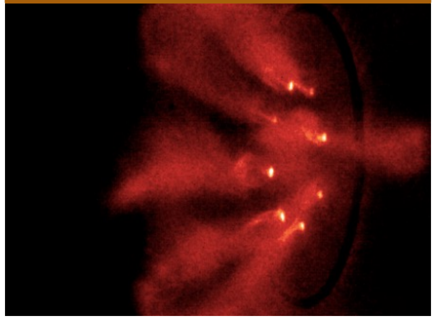

Moser, 2012

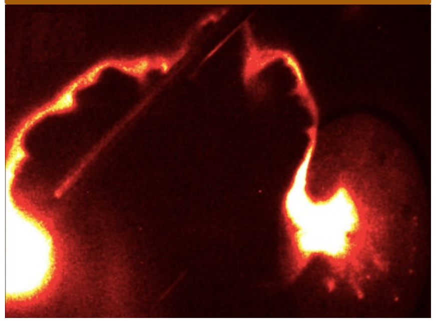

Moser, 2012

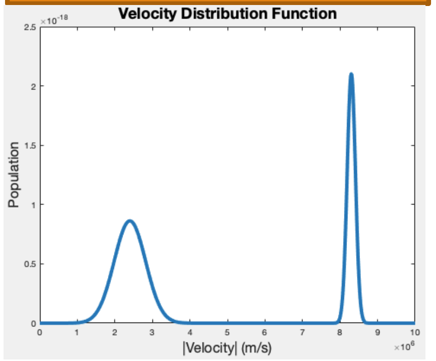

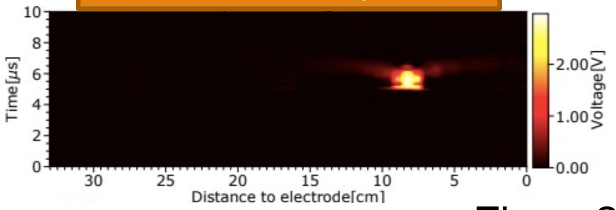

Zhou, 2023

return

APPENDIX B –
JET EXPERIMENT SEQUENCE

- <u>How do particles get energized enough to produce suprathermal X-rays?</u>
  - The Caltech Jet Experiment produces *X-rays exceeding the average thermal energy of particles by ~3000 times,* averaging ~6-7keV
  - Indicates transition from MHD-driven behavior to non-MHD-driven behavior

A. Create Plasma → B. Instability Cascade → C. Plasma Particles are heated → D. Heated Particles create X-rays

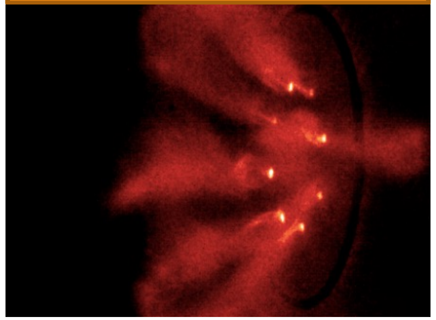

Moser, 2012

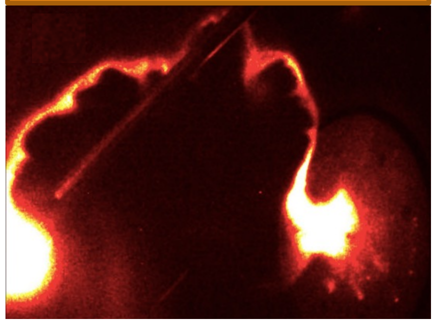

Moser, 2012

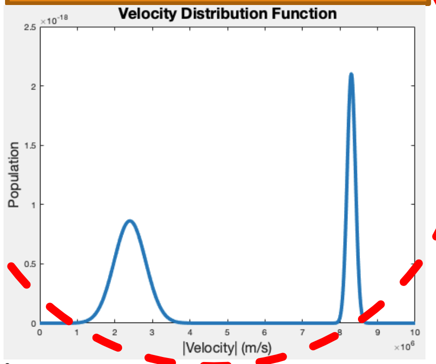

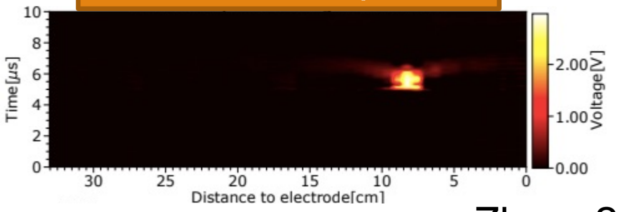

Zhou, 2023

Where and how does this happen?

MHD-driven

Non MHD-driven; multi-scale effects

return

APPENDIX B –
CALTECH JET EVOLUTION

- Neutral gas is injected via injection ports
  - Background magnetic field is applied by energizing circular field coil, ~1mWb typ.
  - Gas breaks down when voltage is applied across electrodes, ~5kV typ.

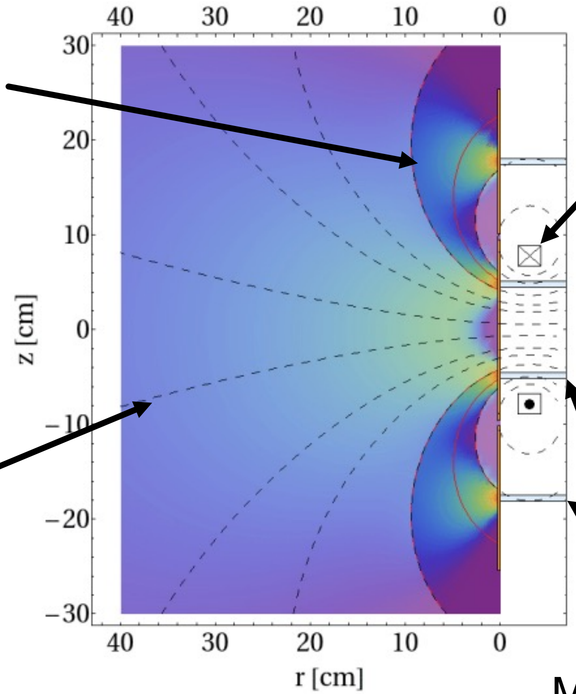

Moser, 2012

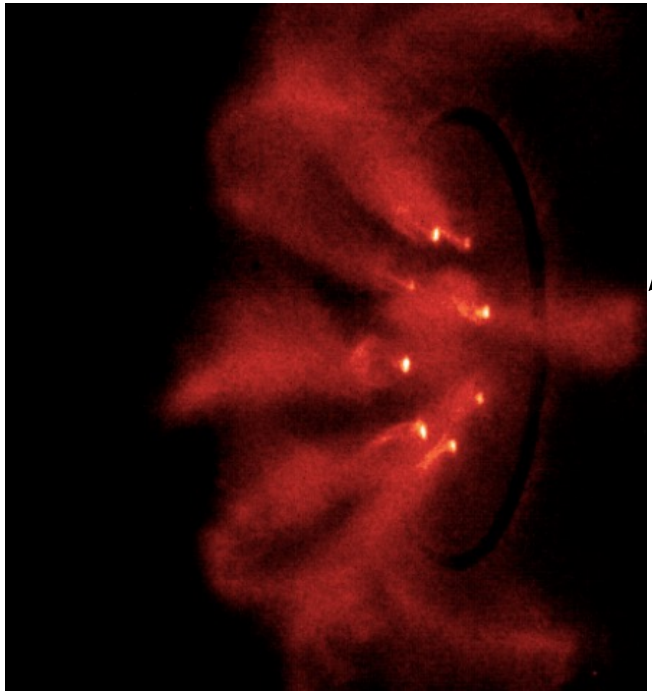

Neutral gas breaks down along field lines

Moser, 2012

return

APPENDIX B – CALTECH JET EVOLUTION

- Plasma jets coil up due to the kink instability when the Kruskal-Shafranov condition is violated:

$$q = \frac{2\pi a}{L}\frac{B_{0z}}{B_{0\theta}}$$

Where L is the plasma length (~0.4m at typical kink onset), a is the cylindrical jet radius (~4cm or less)

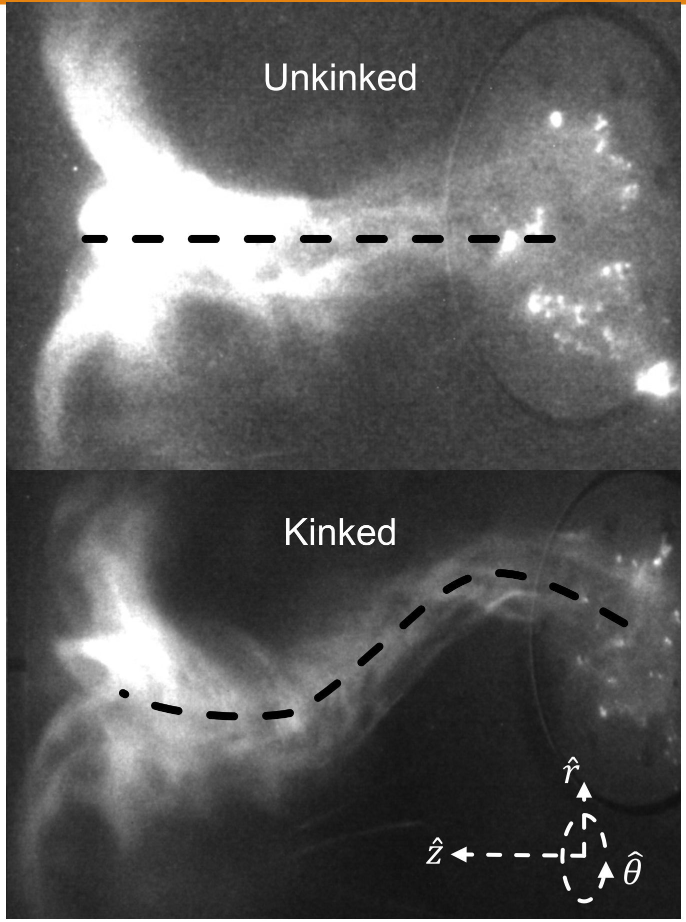

return

APPENDIX B – CALTECH JET EVOLUTION

- Plasma jets coil up due to the kink instability when the Kruskal-Shafranov condition is violated:

$$q = \frac{2\pi a}{L} \frac{B_{0z}}{B_{0\theta}}$$

$$q > 1 \longrightarrow \text{stable structure, no kink}$$

$$q < 1 \longrightarrow \text{unstable structure, kink develops}$$

Where L is the plasma length (~0.4m at typical kink onset), a is the cylindrical jet radius (~4cm or less)

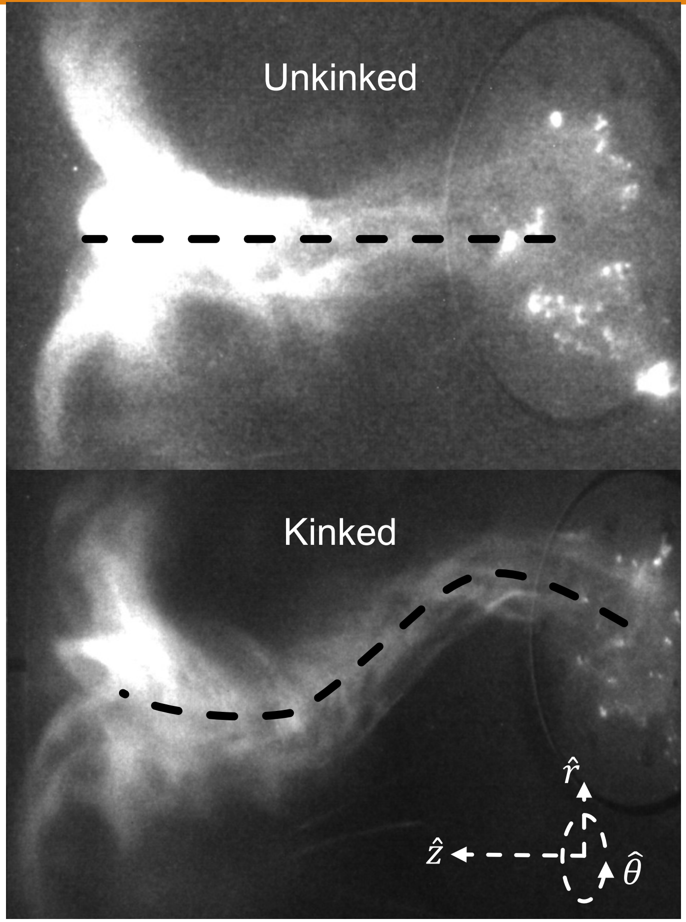

return

APPENDIX B – CALTECH JET EVOLUTION

- Radial acceleration from kink instability induces the Rayleigh-Taylor instability (RTI)
  - Vacuum ‘bubbles’ into plasma, causing surface ripples

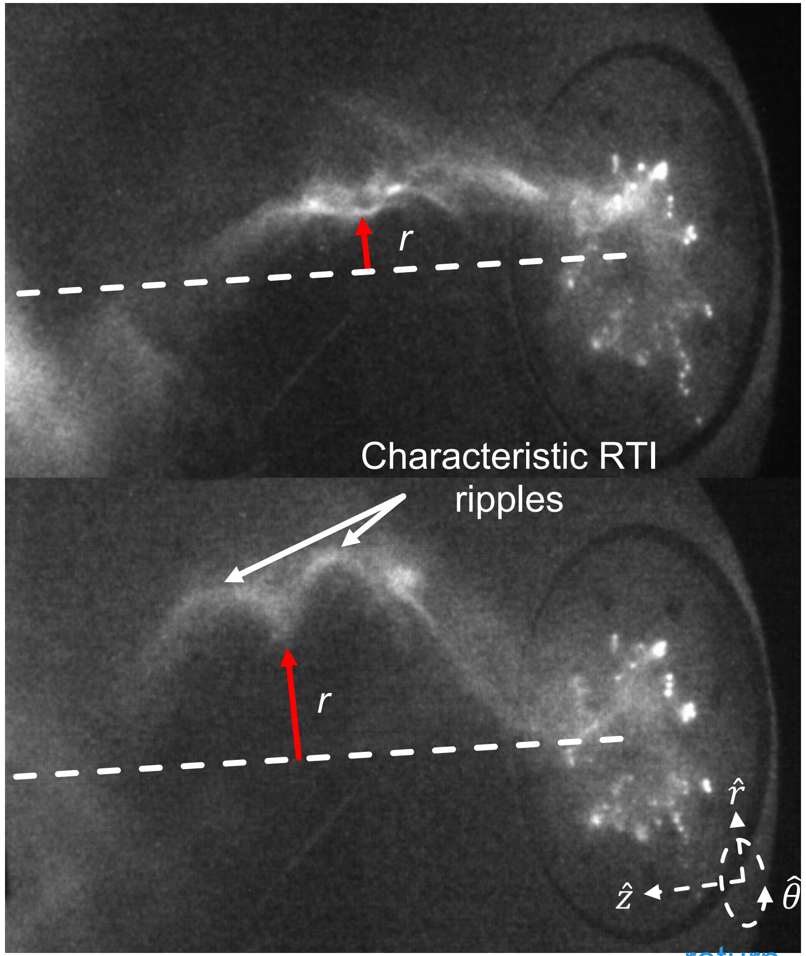

return

APPENDIX B – CALTECH JET EXPERIMENTAL SEQUENCE

- Radial acceleration from kink instability induces the Rayleigh-Taylor instability (RTI)
  - Vacuum ‘bubbles’ into plasma, causing surface ripples

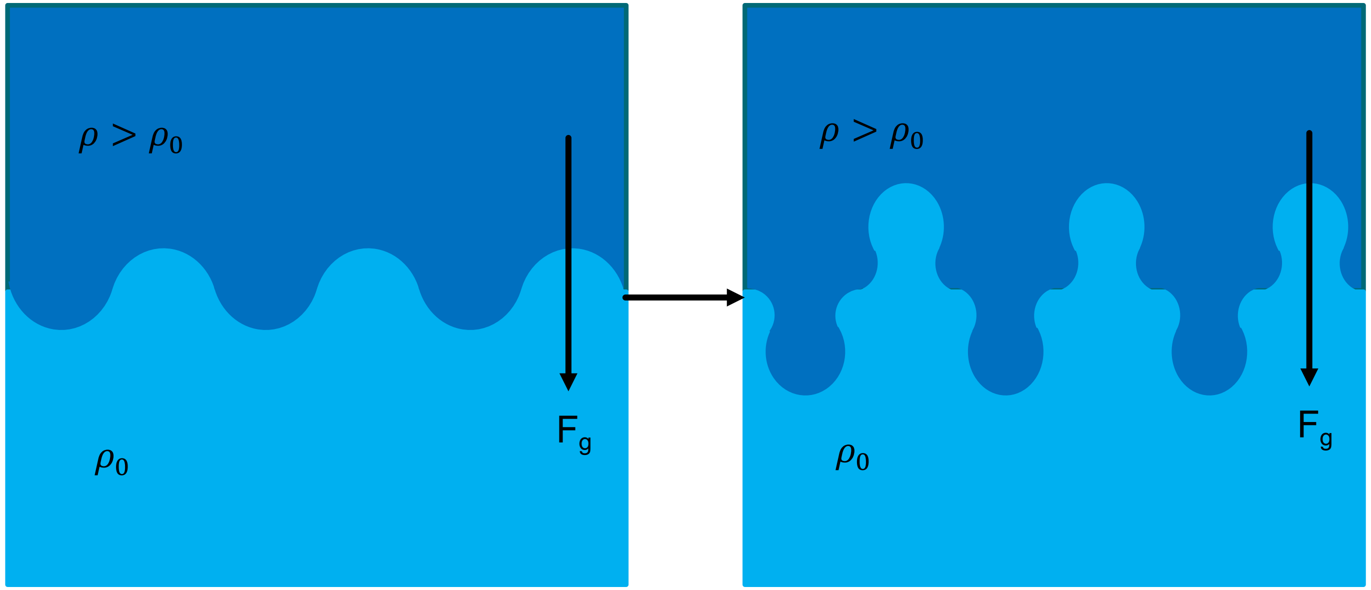

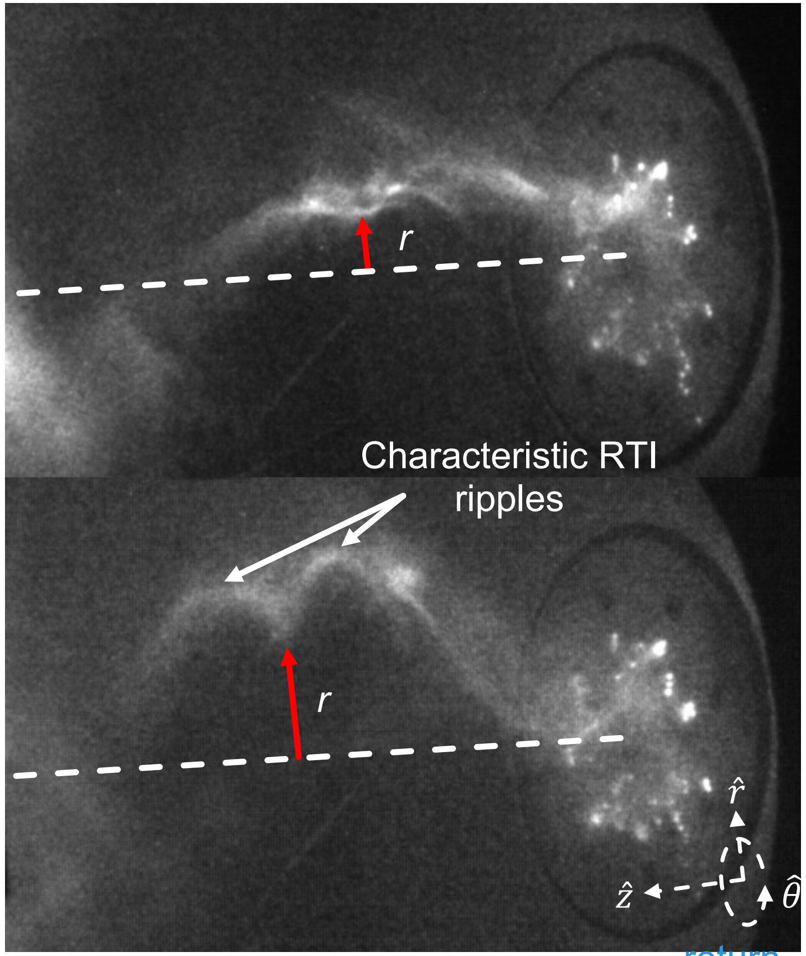

return

APPENDIX B – CALTECH JET EVOLUTION

- RTI can choke plasma filament down to ion skin-depth, order of < ~1cm
  - MHD can no longer apply; kinetic physics or multi-scale physics dominate
  - Induces kinetic instabilities

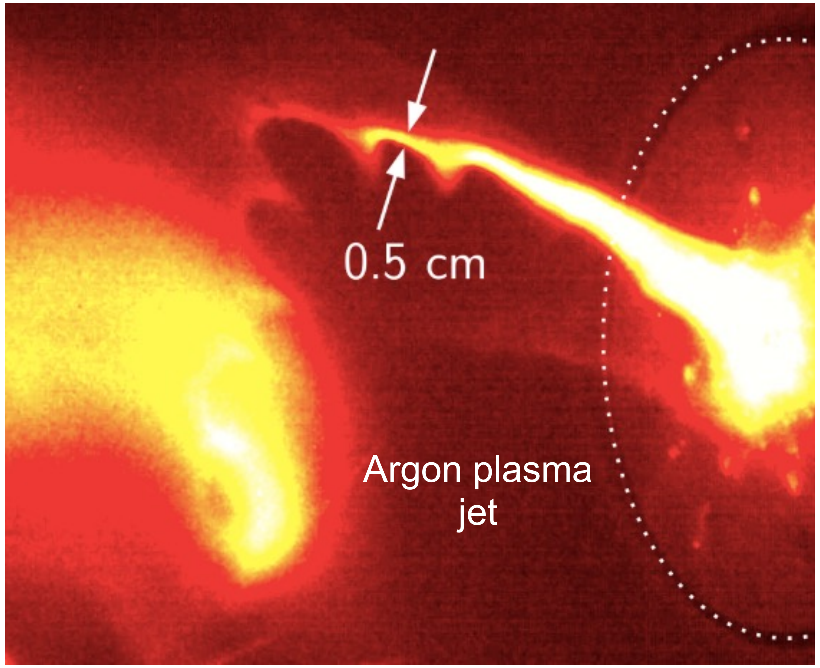

Moser, 2012

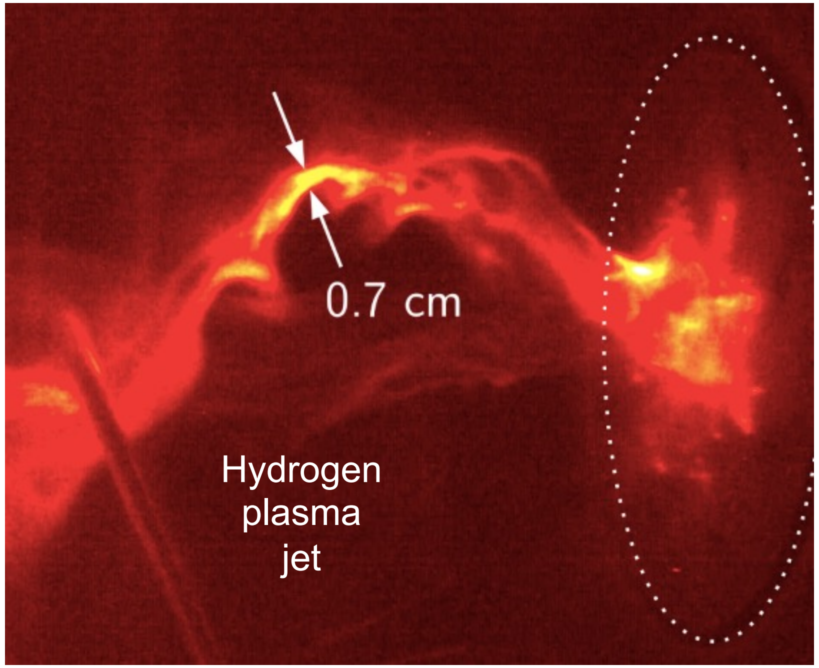

Moser, 2012

return

APPENDIX B –
DETAILED OVERVIEW OF JET EXPERIMENT

- Caltech Jet Experiment ignition diagram:

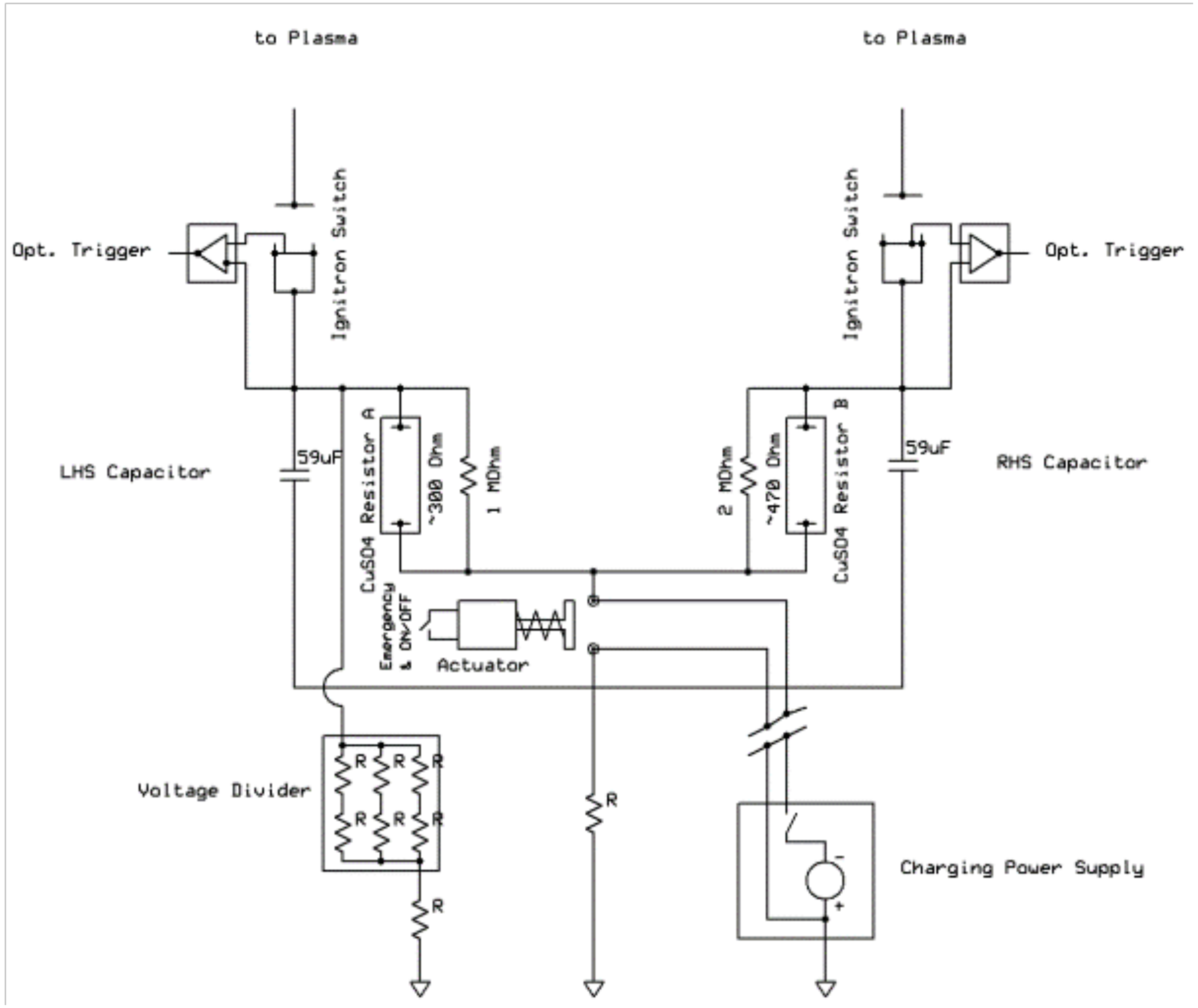

return

APPENDIX B – DETAILED OVERVIEW OF JET EXPERIMENT

- Caltech Jet Experiment ignition diagram:

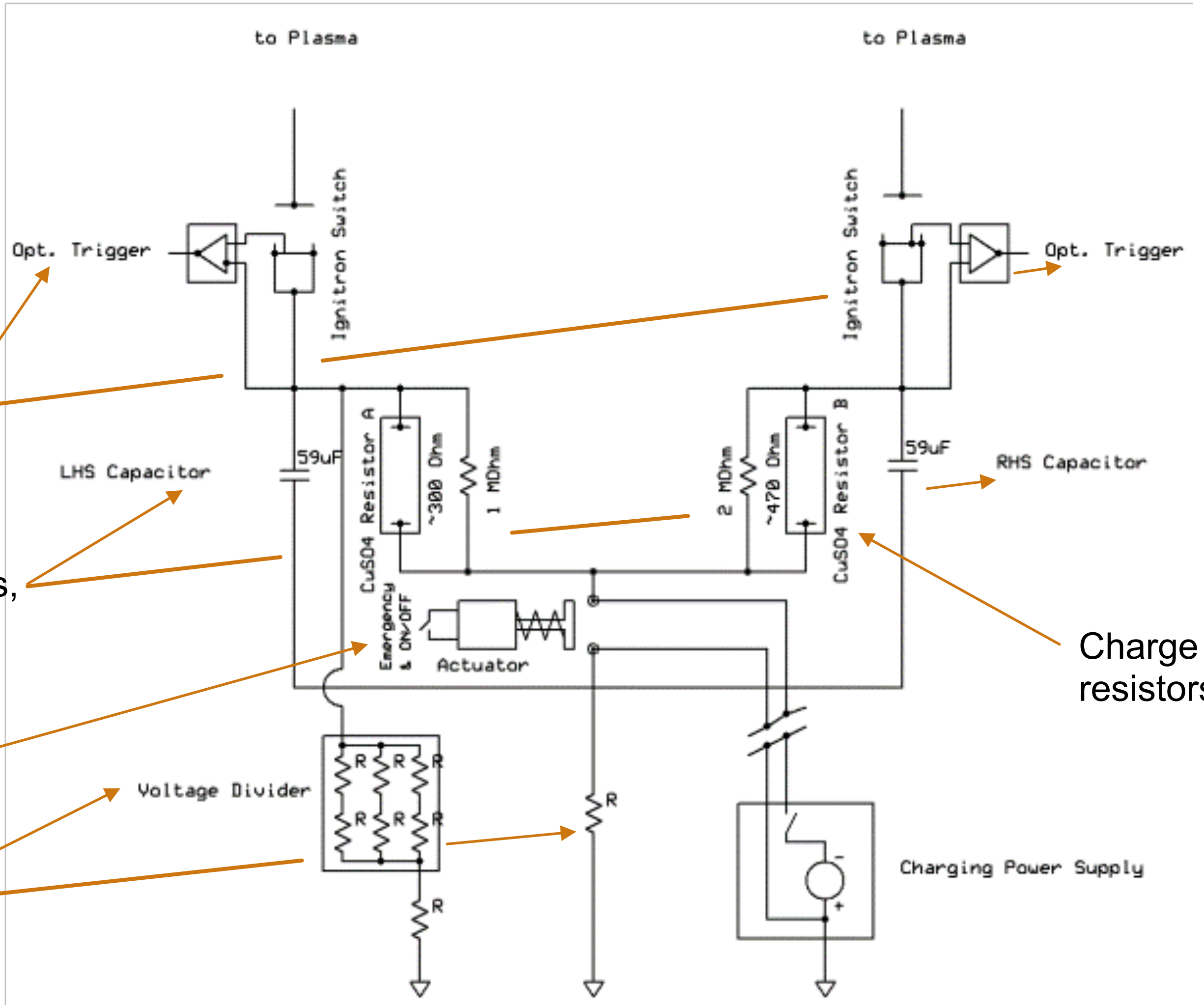

Ignition trigger input closes ignitron

Primary discharge capacitors, ~10kV rated

Emergency shutoff relay

Bleed resistors

Charge limiting resistors

return

APPENDIX B – DETAILED OVERVIEW OF JET EXPERIMENT

- Caltech Jet Experiment ignition diagram:

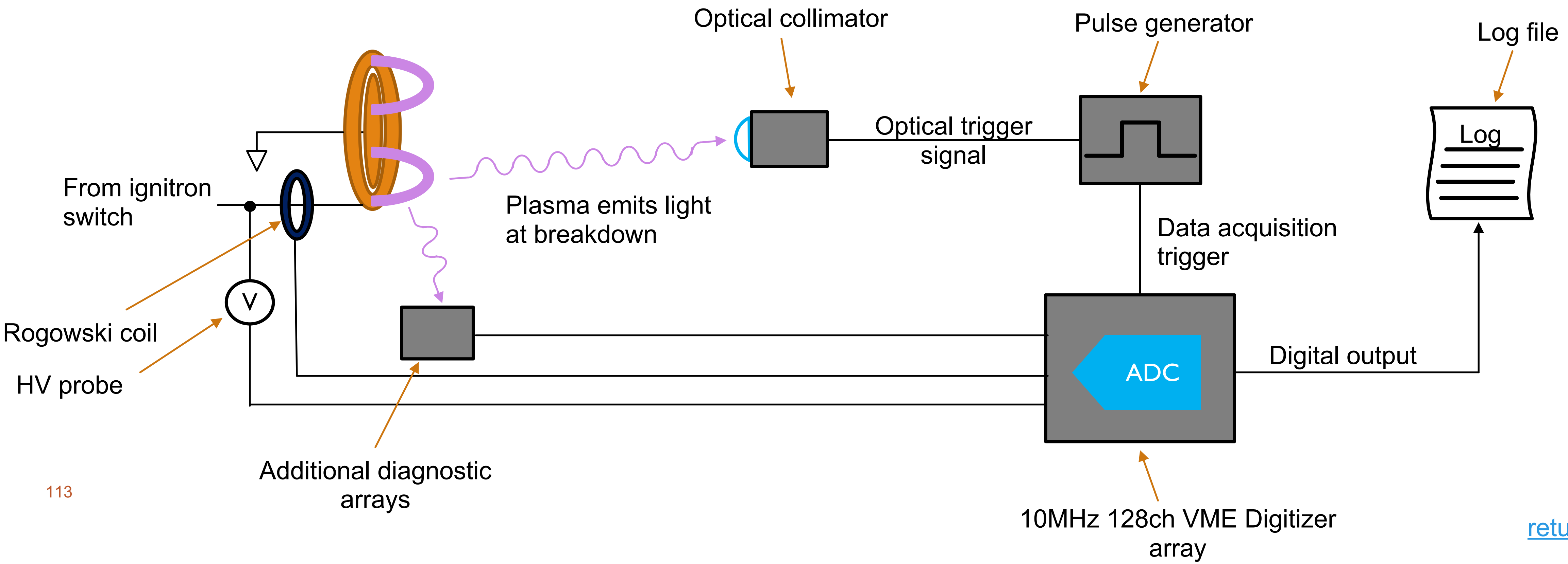

return

APPENDIX B – DETAILED OVERVIEW OF JET EXPERIMENT

- Caltech Jet Experiment gas injection system:

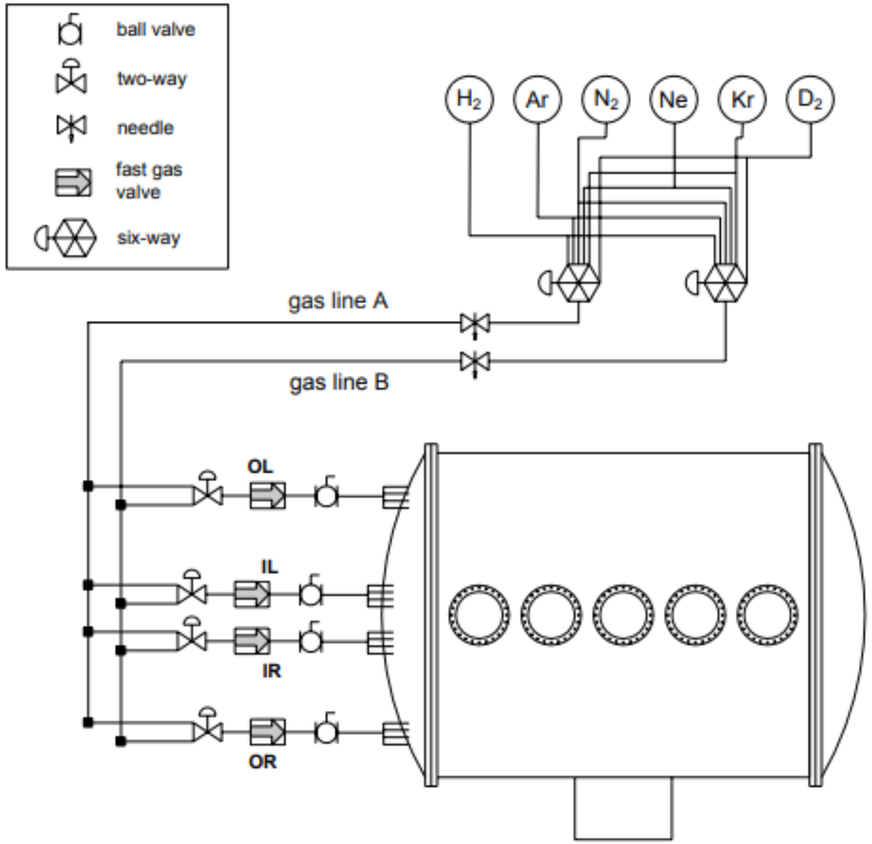

Yun, 2008

return

APPENDIX B –
DETAILED OVERVIEW OF JET EXPERIMENT

- Caltech Jet Experiment gas injection system:

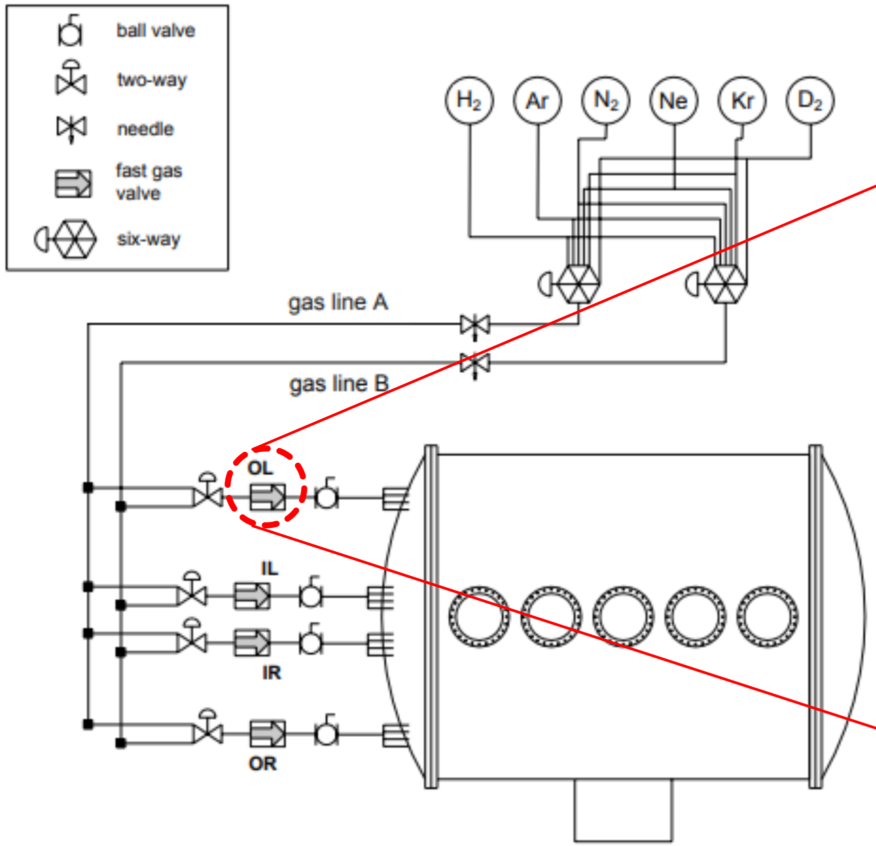

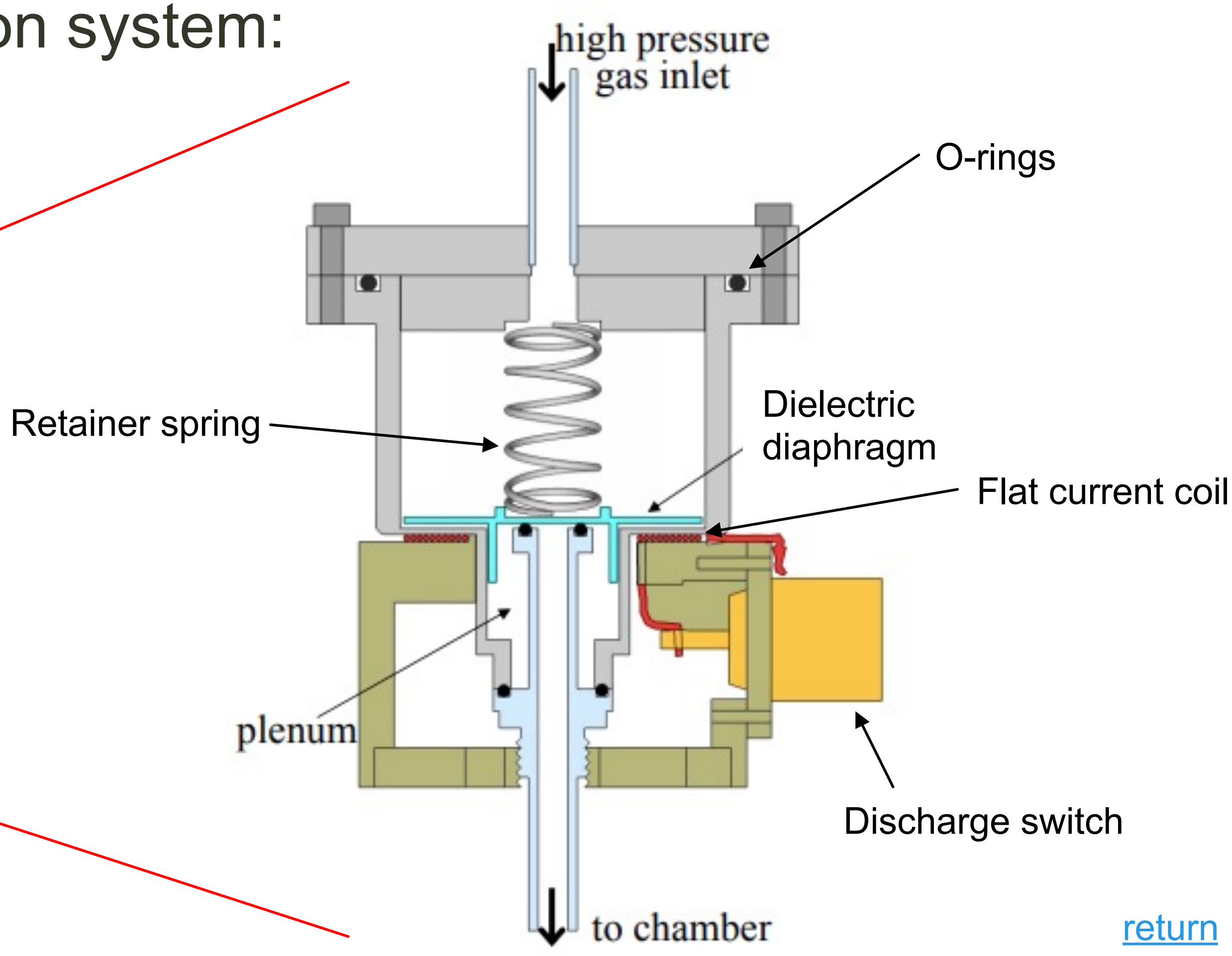

Yun, 2008

return

APPENDIX B – THE PROBLEM THAT MADE ME LOSE MY MIND THE MOST

- What is it?

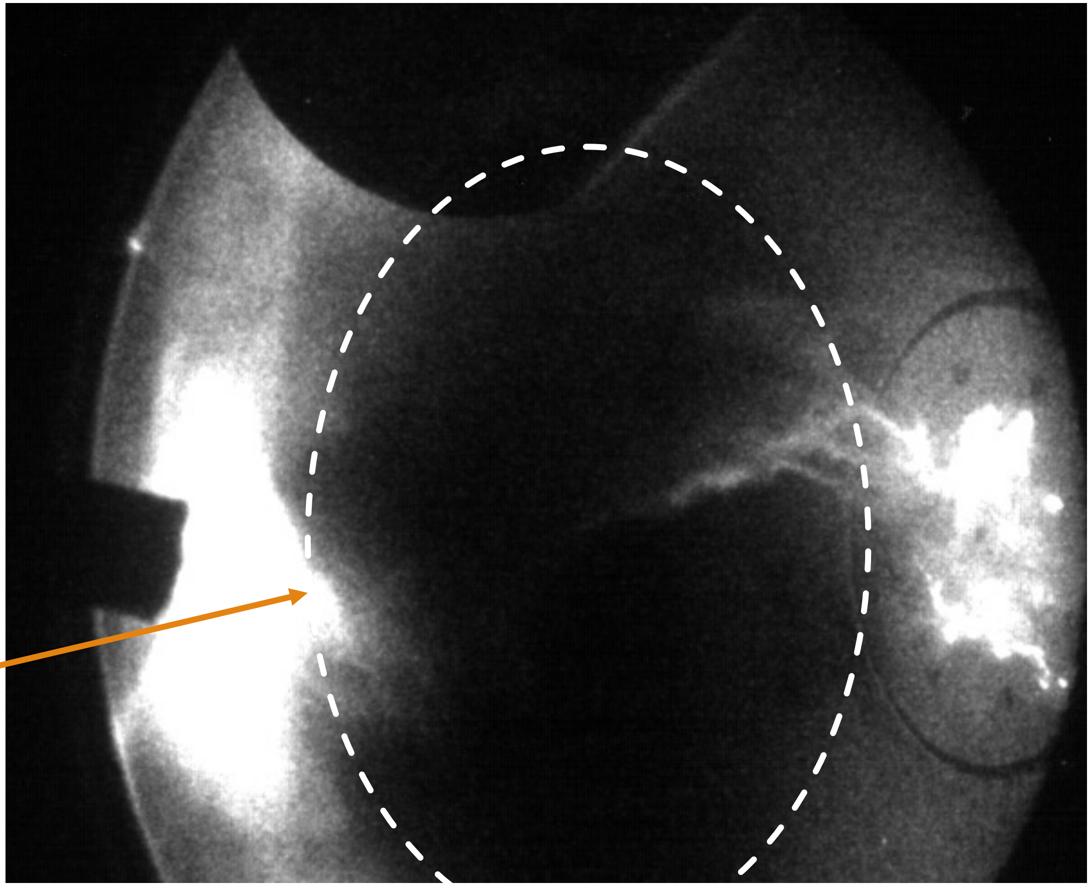

Large deposits on window were obscuring visible information

Fig. XX: Hydrogen jet 32764, exhibiting kink and possible RTI, obscured by optically opaque deposits on window

APPENDIX B – THE PROBLEM THAT MADE ME LOSE MY MIND THE MOST

- What is it?
  - Copper deposits from plasma impingement on electrodes!

Large deposits on window were obscuring visible information

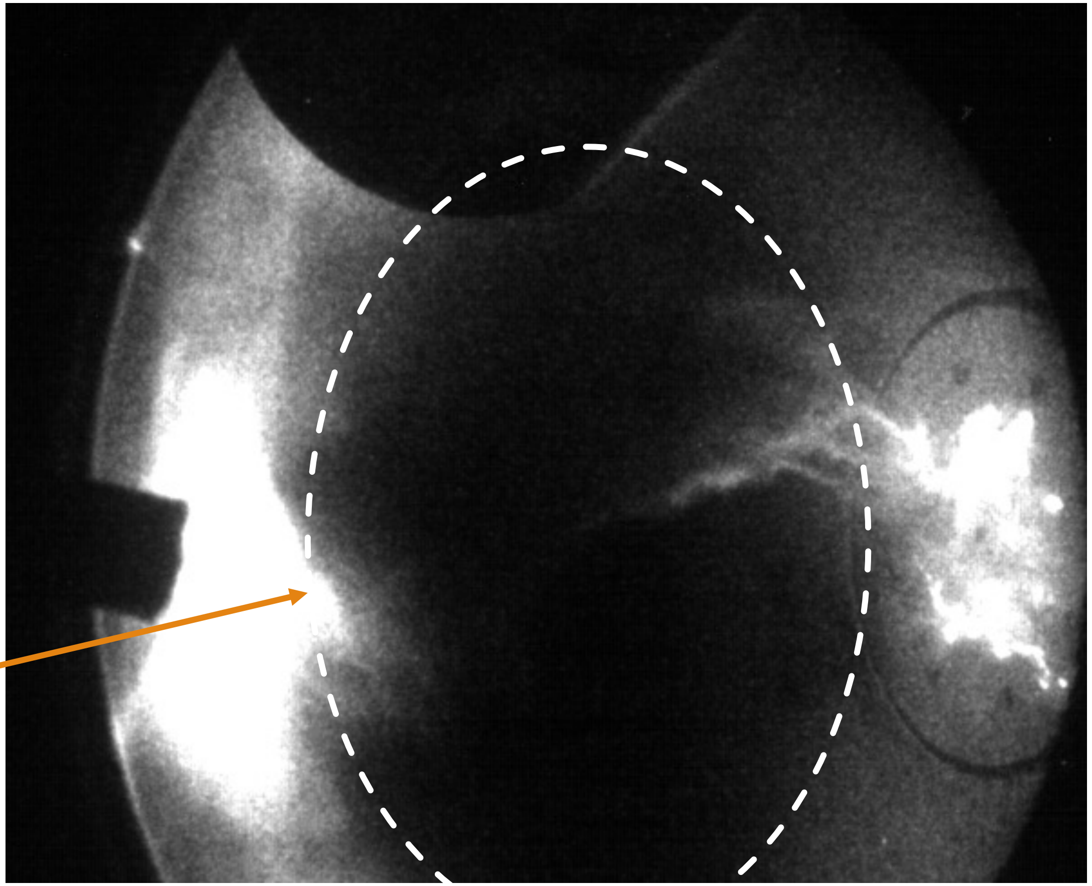

Fig. XX: Hydrogen jet 32764, exhibiting kink and possible RTI, obscured by optically opaque deposits on window

APPENDIX B – THE PROBLEM THAT MADE ME LOSE MY MIND THE MOST

- What is it?
  - Copper deposits from plasma impingement on electrodes!
  - Solved by removing windows from chamber and bathing them in H_2O_2 for ~6hrs

Large deposits on window were obscuring visible information

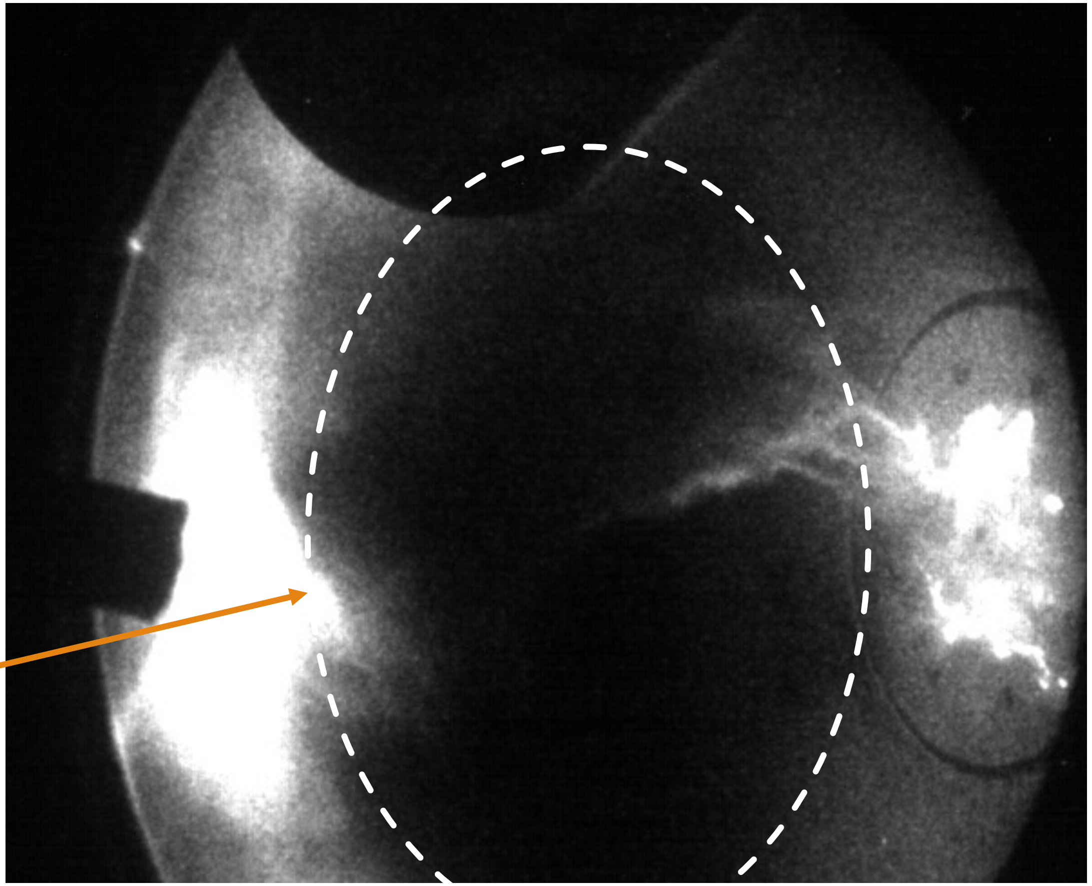

Fig. XX: Hydrogen jet 32764, exhibiting kink and possible RTI, obscured by optically opaque deposits on window